



<https://theses.gla.ac.uk/>

Theses Digitisation:

<https://www.gla.ac.uk/myglasgow/research/enlighten/theses/digitisation/>

This is a digitised version of the original print thesis.

Copyright and moral rights for this work are retained by the author

A copy can be downloaded for personal non-commercial research or study, without prior permission or charge

This work cannot be reproduced or quoted extensively from without first obtaining permission in writing from the author

The content must not be changed in any way or sold commercially in any format or medium without the formal permission of the author

When referring to this work, full bibliographic details including the author, title, awarding institution and date of the thesis must be given

Enlighten: Theses

<https://theses.gla.ac.uk/>
research-enlighten@glasgow.ac.uk

THE BEHAVIOUR OF FLEXIBLE SLABS
ON IDEALISED AND ACTUAL FOUNDATIONS.

A Thesis presented to the University of
Glasgow for the Degree of Doctor of Philosophy

by

Ian Moffat Smith, B.Sc., M.S.

Department of Civil Engineering,
University of Glasgow.

June, 1967.

ProQuest Number: 10646172

All rights reserved

INFORMATION TO ALL USERS

The quality of this reproduction is dependent upon the quality of the copy submitted.

In the unlikely event that the author did not send a complete manuscript and there are missing pages, these will be noted. Also, if material had to be removed, a note will indicate the deletion.



ProQuest 10646172

Published by ProQuest LLC (2017). Copyright of the Dissertation is held by the Author.

All rights reserved.

This work is protected against unauthorized copying under Title 17, United States Code
Microform Edition © ProQuest LLC.

ProQuest LLC.
789 East Eisenhower Parkway
P.O. Box 1346
Ann Arbor, MI 48106 – 1346

The Behaviour of Flexible Slabs on Idealised and Actual Foundations.

SUMMARY

Ph.D. Thesis.

Ian M. Smith.

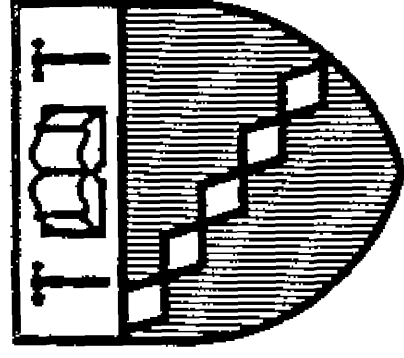
University of Glasgow,
Department of Civil Engineering
1967.

Due to a lack of contact between the disciplines of soil mechanics and structural engineering there is a tendency for flexible structures to be analysed under grossly simplified assumptions regarding the interaction between the structure and its soil foundation. For example, it is often assumed that the contact pressure on the base of a structure is uniform, or linearly varying. In the thesis it is proposed that the use of a digital computer enables a structure and its foundation to be analysed as a complete entity. The computer is essential because of the complexity of the mathematical formulation of the problem and because of the scale of the analysis involved.

Most of the theoretical work concerns the finite element method for the analysis of structure and foundation, although some work on the finite difference method is also presented. The former method allows a more realistic approximation to be made to the inhomogeneity of soil deposits.

An evaluation of current methods and some advances in the theory of the finite element method as applied to plate or slab structures are presented, culminating in an analysis incorporating the effect of transverse shear deformations on the bending of elastic plates.

The theories are then applied to the evaluation of a set of experimental results obtained for circular plates bearing on a sand foundation and loaded with concentrated central loads. The classical idealisations of foundations are found to be inadequate and more realistic models are proposed for the particular plate structure and loading case examined.



With the Librarian's Compliments

The University of Aston in Birmingham
Gosta Green
Birmingham B4 7ET

C O N T E N T S

ACKNOWLEDGEMENTS

CHAPTER 1 Review of the Analysis of Flexible Structures Bearing on Deformable Foundations.

1.1	Introduction	p 1
1.2	The Winkler Foundation	p 2
1.3	Coupled Spring Foundations	p 4
1.4	Elastic Solid Foundations	p 5
1.5	Comparison of Foundation Models	p 6
1.6	The Stress-Strain Characteristics of Soils	p 7
1.7	Some Other Procedures for the Design of Flexible Structures Bearing on Deformable Foundations	p 10
1.8	Conclusions	p 12

CHAPTER	2	Finite Element Methods for the Analysis of Elastic Plates in Bending.	
2.1		Introduction	p 13
2.2		Antecedents of Modern Finite Element Methods	p 13
2.3		Force Method and Displacement Method	p 15
2.4		Derivation of Discrete Element Stiffness (Flexibility) Properties	p 17
2.5		Rectangular Element Stiffness Matrices for Plates in Bending 1959 - 1964	p 18
2.6		Matrix Formulation of Consistent Displacement Approaches	p 21
2.6		Three New Element Stiffness Matrices	p 25
2.7		Parallel Work 1964 - 1967	p 31
2.8		Evaluation of Rectangular Finite Elements for the Analysis of Thin Elastic Plates in Bending	p 34
2.9		Analysis of "Moderately Thick Plates" by Means of Rectangular Finite Elements	p 39
2.10		Finite Element Method for Axisymmetric Plates in Bending	p 42
2.11		Computation	p 44

CHAPTER	3	Elastic Solid Foundations Analysed by Finite Element Methods	
3.1		Introduction	p 45
3.2		Previous Work	p 45
3.3		Evaluation of the Element	p 46
3.4		Circular Plate Bearing on a Semi- Infinite Elastic Medium	p 46
3.5		Conclusions	p 47
CHAPTER	4	Finite Difference Method for the Solution of Plate Flexure Problems	
4.1		Introduction	p 48
4.2		Solutions by Fourth Order Finite Differences	p 48

CHAPTER	5	Experimental Work	
5.1		Introduction: Previous Work	p 52
5.2		Determination of Contact Pressures	p 53
5.3		Calibration of Pressure Cells and Determination of the Flexural Rigidities of the Test Plates	p 56
5.4		Determination of the Required Size of Sand Container	p 57
5.5		Classification of the Sand Used for the Full Scale Tests	p 59
5.6		Placement of the Sand in the Full Scale Tests	p 59
5.7		Plates Bearing on Sand and Subjected to Uniformly Distributed Loads	p 60
5.8		Circular Plates Bearing on Sand and Subjected to Concentrated Central Loadings	p 61
5.9		Apparatus and Test Procedure	p 62
5.10		Analysis and Discussion of the Experimental Results	p 64
5.11		Conclusions	p 67

REFERENCES

APPENDIX	1	Fifth Order Stiffness Matrix	
APPENDIX	2	Seventh Order Stiffness Matrix	
APPENDIX	3	A Stiffness Matrix for Axisymmetrically Loaded Circular Plates	
APPENDIX	4	Computer Programs	

ACKNOWLEDGEMENTS.

The work described in this thesis was carried out in the Department of Civil Engineering at the University of Glasgow under the direction of Professor Hugh B. Sutherland whose help and interest throughout the project are gratefully acknowledged.

The Author's thanks are also due to the staff of the Engineering Department Workshops and in particular to Messrs. J. Coleman and J. Thomson, without whose help the experimental work could not have been conducted.

In conclusion the Author is grateful for the facilities provided by the University Computing Department. Miss D. Geddes was a constant source of assistance in the running of the Author's programs.

CHAPTER 1.

REVIEW OF THE ANALYSIS OF FLEXIBLE STRUCTURES BEARING ON DEFORMABLE FOUNDATIONS

1.1 Introduction

In the Author's experience there tends to be a rather rigid division between engineers concerned with the analysis and design of structures, and those concerned with the soil mechanics and foundation aspects. This leads to sweeping assumptions on the part of designers about the nature of the interaction between a structure and its foundation; for example it is often assumed that the contact pressure on the base of a structure is uniform, or at best linearly varying across the structure.

In the case of flexible foundations, a further difficulty is introduced by the complexity of the mathematical formulation, which generally involves fourth order ordinary or partial differential equations. This leads to a further division, since the solutions to these governing equations have generally been obtained by mathematicians who may have no idea of how the solutions are to be used in engineering practice.

The intention of this thesis is to reconcile the three way division by means of computer-oriented analysis techniques. The Author believes that the development of digital computers on a large scale renders obsolete Terzaghi's statement (1), that "the solution of fourth order equations is beyond the capacity of the average practising engineer", and further that the ease with which computers can handle very large problems should encourage the integrated analysis of structures and their foundations as complete entities.

Chapter 1 of the thesis consists of a review of previous work on the analysis of flexible structures bearing on deformable foundations, with emphasis on the "three-dimensional" (plate or slab) rather than the "two-dimensional" (beam) problem.

In Chapters 2, 3 and 4 the theoretical basis is developed for the analysis of three-dimensional structures bearing on deformable foundations by computer oriented techniques, while in Chapter 5 these techniques are applied to the evaluation of the results of a series of tests carried out on plates bearing on a uniform sand foundation artificially created in the laboratory.

1.2 The Winkler Foundation

The Winkler model (sometimes called Winkler-Zimmerman, especially in the U.S.S.R., or even Hertzian, since Hertz was the first to consider plates on this type of foundation as distinct from beams) is the simplest elastic foundation model it is possible to use. It was first suggested by Winkler in 1867. One assumes that the foundation can be represented by a bed of infinitely closely spaced, but discrete springs which have a stiffness, k , transverse to the plane of the plate (or beam) resting on them but zero stiffness against any other displacement or rotation. k is called the "foundation modulus" or "modulus of subgrade reaction" and typically has dimensions lb/in^3 . A large proportion of the literature dealing with structures bearing on this model concerns beams, and often the methods described cannot be extrapolated to the more complex plate problem.

Hetenyi (2) presents a number of exact solutions to the governing differential equation of a beam on a Winkler foundation:

$$EI \frac{d^4 y}{dx^4} = q - ky \quad \text{eq(1.1)}$$

and in a recent contribution (3) has traced the history of developments in the study of the Winkler foundation, and of other foundation types, up to the present day. It might be pointed out that the study of eq(1.1) has been given added impetus because of its applicability to other problems, for example thin shells. Barden (4) has catalogued the various approximate procedures available for the solution of eq(1.1) and concludes that the

approach due to Hendry (5) is the most effective.

For a summary of contributions to the study of plates bearing on various types of foundation, reference should be made to the standard work of Timoshenko and Woinowsky-Krieger (6), Chapter 8. The extension to the consideration of the simplest plate problem, that of the radially symmetric plate on a Winkler foundation was first discussed by Hertz in 1884. The governing equation becomes

$$\left(\frac{d^2}{dr^2} + \frac{1}{r} \frac{d}{dr}\right) \left(\frac{d^2 w}{dr^2} + \frac{1}{r} \frac{dw}{dr}\right) = \frac{q - kw}{D} \quad \text{eq(1.2)}$$

and was solved by Hertz for the special case of a plate with a concentrated central load. By using Bessel functions, Schleicher (7) was able to obtain solutions to a wider variety of axisymmetric plate problems.

The general case of a finite rectangular plate bearing on a Winkler foundation, governed by the equation:

$$D \left(\frac{\partial^4 w}{\partial x^4} + 2 \frac{\partial^4 w}{\partial x^2 \partial y^2} + \frac{\partial^4 w}{\partial y^4} \right) = q - kw \quad \text{eq(1.3)}$$

seems first to have been analysed, about 1920, by H. Happel, using the approximate Rayleigh-Ritz procedure. Further applications of the same method are due to Vint and Elgood (8) who also conducted experiments on a steel plate bearing on springs and to Murphy (9) who compared the theoretical results from the Ritz procedure with the experimental values for a steel plate bearing on a hard rubber subgrade. Pickett, Ravel, Janes and McCormick (10) used Fourier series for the solution of the same problem, but considered their solution inferior to Murphy's. In a series of papers (11), Allen and Severn used the method of finite difference approximations to eq(1.3) to obtain solutions for the more complicated boundary conditions pertaining at exterior walls, re-entrant corners etc. of flexible foundation rafts. This work will be discussed more fully in a later section (4.2) together with the Author's own contributions to the finite difference method.

A solid plate can be approximated by a grid framework, by a suitable choice of the stiffnesses of the members of the grid, and this approach has been used by Sawko (12) for the solution of some problems involving Winkler foundations (including Allen and Severn's problem). Sawko was able to modify a computer program, originally written for the analysis of plane frameworks, to incorporate the effect of the foundation stiffness. Gridwork analogies are the forerunners of the more sophisticated finite element analyses presented later in this thesis (Chapters 2 and 3). Their merits will be discussed more fully there.

1.3 Coupled Spring Foundations

Winkler's hypothesis of an "uncoupled" medium is untenable for a beam or plate structure bearing on a continuous, highly interconnected medium. The degree of error will be shown to be dependent on such variables as the flexibility of the structure and the distribution of loading. Due to the difficulty of analysing flexible structures bearing on semi-infinite media (see Section 1.4), foundation models of intermediate complexity have been sought. Those are called "coupled" or "generalised" spring foundations. Work in this field is reviewed by Hetenyi (3) and in a comprehensive paper by Kerr (13). If time dependent properties in the foundation can be ignored, three "coupled spring" models have been proposed:

- (i) Governed by a fourth order equation. The mathematical model for this type is either,
 - (a) a spring bed, where the tops of the springs are connected to a thin stretched elastic membrane,
 - (b) a spring bed where there is shear interaction between the springs,
 - (c) a spring bed where the springs resist moments applied to them as well as transverse forces.The same differential equation governs (a), (b) and (c).
- (ii) Governed by a sixth order equation, obtained by making simplifying assumptions about the behaviour of an elastic solid.

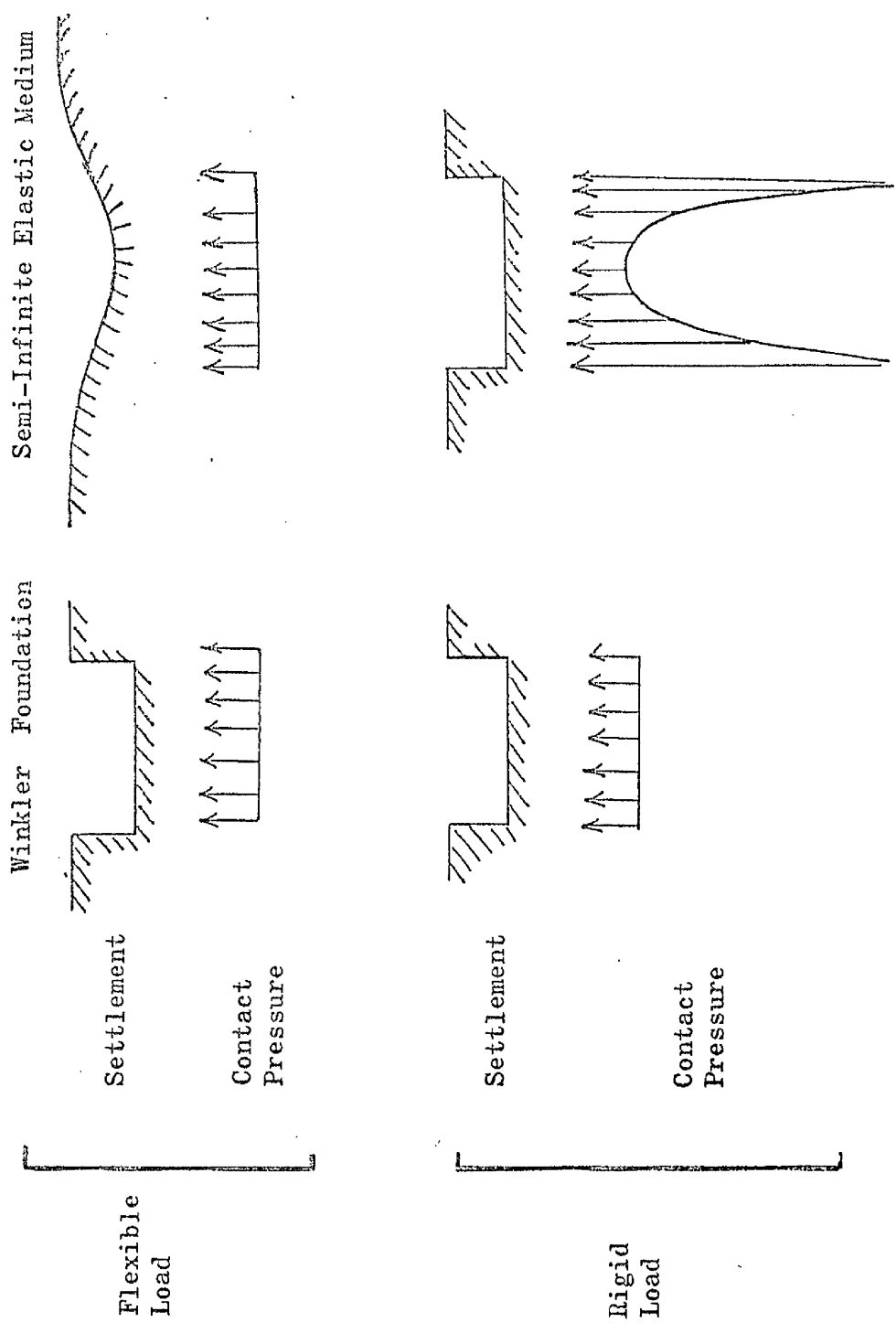


Fig. 1.1 Comparison of Winkler and Semi-Infinite Elastic Medium Models

(iii) Governed by an eighth order equation. The mathematical model for this type is a two-layer spring bed, the layers separated by a flexible beam or plate.

Since it will be shown that elastic solid foundations can be conveniently analysed using digital computers, the usefulness of these "intermediate" models is open to question.

While this thesis was being prepared, Severn (14) published an analysis of rectangular plates, bearing both on Winkler and on coupled spring foundations, using the finite element method. This work parallels the main contributions of this thesis and will be discussed later in conjunction with the Author's own work. In the same category is a paper by Cheung and Zienkiewicz (15) dealing with plates on Winkler and on semi-infinite, isotropic, homogeneous elastic solid foundations by the finite element method.

1.4 Elastic Solid Foundations

Treating a foundation as an elastic solid involves, with the exception of the special case of axisymmetry, the solution of a problem in three dimensional elasticity. Due to the complexity of the theory of elasticity in three dimensions, nearly all of the problems in this class which have been solved have concerned the semi-infinite, homogeneous isotropic, elastic medium although in principle the class contains media of finite dimensions and more arbitrary elastic properties, for example anisotropy or variability of the elastic properties with location in the medium. Holl (16) solved the problem of an infinitely large plate in a state of axisymmetry (using Bessel functions). For finite plates, two approximate methods have been used. Borowicka (17) solved the problem of the finite circular plate by matching the plate and foundation deflections when each was expressed as an infinite series. The solution involves solving a set of linear equations, the number depending on how many terms of the infinite series are retained. Gorbunov-Posadov and Serebrjanyi (18) used the same method for rectangular slabs. As an alternative, finite difference approximations have been used, circular plates being tackled by

Habel (19) and rectangular plates by Pickett, Ravel, James and McCormick (10) and by Pickett and McCormick (20). In all of the above analyses, an isotropic elastic half-space was assumed, but an approximate method published by Barden (21) considers a circular plate on an anisotropic elastic half space. Barden matched the displacements of plate and foundation at a finite number of points, n , and had to solve n simultaneous equations after the fashion of Borowicka. An interesting feature of Barden's work is his discovery that the surface deflections of a special type of anisotropic medium can be obtained from those of an isotropic medium simply by multiplying by a dimensionless factor which can be tabulated for varying degrees of anisotropy (22). Sommer (23) has recently described a computer-dependent method for analysing a complete structure bearing on an elastic solid medium, thereby enabling the influence of the flexural rigidity of the superstructure on the settlements and contact pressures to be assessed. Only the two dimensional problem was considered by Sommer.

1.5 Comparison of Foundation Models

Engineering practice in the design of flexible structures is often to assume that the distribution of contact pressure between structure and soil is uniform, or linearly varying whatever the flexibility of the structure or distribution of loading. Where a foundation model is used, it is most common in the U.K. and U.S.A. to use the Winkler model, whereas, according to Tsyтович (24), U.S.S.R. practice is to use the elastic half-space model. As far as the Author is aware, the use of coupled spring foundations is not common practice for the design of flexible structures bearing on soil. Fig.1.1 shows the implications of the two main assumptions. On the Winkler foundation, a uniformly loaded structure will experience a uniform uplift pressure (and uniform settlement) whatever the flexibility of the structure. On the other hand, on the elastic half space, a rigid structure will be subjected to an "inverse parabolic" contact pressure distribution while settling uniformly, whereas a flexible structure, uniformly loaded, will be subjected to a uniform contact pressure distribution while undergoing

a "parabolic" displacement form. Therefore the assumption of uniform contact pressure for any foundation condition is unlikely to be acceptable. Similarly, the Winkler model and the elastic half-space cannot both represent the behaviour of a foundation under all circumstances of structure flexibility and loading. Vesic (25) and Barden (4) have tried to show that the two foundation models correspond, but have chosen the ideal case of flexible beams subjected to concentrated loads. In reference (24) Tsytovich called for a discussion of the limits of applicability of the theories of the linear elastic half-space and the Winkler model. Such a discussion is one of the aims of this thesis.

1.6 The Stress-Strain Characteristics of Soils

Having considered the foundation models which can be conveniently analysed by existing mathematical methods, it is pertinent to question to what extent these models duplicate the known stress-deformation properties of naturally occurring foundation materials. (This leaves aside completely for the moment questions regarding the correctness of the idealisations of the structures being analysed. For example is it reasonable to assume that a massive, heavily reinforced concrete raft can be represented by a perfectly isotropic, elastic Kirchhoff plate?)

Detailed study of the stress-deformation relationships of soils is a fairly recent development in soil mechanics, a subject which has been primarily concerned with the failure of soil masses, with the exception of the special case of consolidation of cohesive soils. At first sight a comparison of the assumed and observed properties is discouraging. The assumptions in the previous sections have typically involved:

- (i) time independent stress-strain behaviour
- (ii) linear, recoverable stress-strain behaviour
- (iii) homogeneity
- (iv) (quite often) isotropy
- (v) "stability" in the sense that for an increment of stress applied to a soil element, no work is done by the soil

against the imposed stress system. These assumptions are examined in turn, for a particular soil in a particular condition before stressing. (i.e. no extrapolation to the behaviour of the soil under different initial conditions or to the behaviour of any other soil is assumed.)

(i) A large proportion of naturally occurring soils exhibit time-dependent stress-strain behaviour. Assumption (i) can therefore only apply to soils which are predominantly cohesionless, although the time dependence exhibited by heavily overconsolidated cohesive materials at stress levels below the preconsolidation pressure may be insignificant.

(ii) The stress-strain relationships of cohesionless soils are markedly non-linear and deformations are usually irrecoverable at least to some extent. The latter property means that the behaviour of a structure on a cohesionless sub-soil on first loading may differ considerably from the behaviour on subsequent loadings. Although the non-linearity of the stress-strain relation is not catered for directly by the theories so far advanced, these theories, allied with the use of iterative methods employing a computer, can account for non-linearity. For a variety of stress states, cohesionless soils have been found to follow a strain-stress law of the form:

$$\epsilon = a \sigma^K$$

where a and K are pure numbers. A selection of observations is given below:

Jakobsen (26)	$e_u = 0.608 \times 10^{-3} \sigma^{0.612}$	
Chaplin (27)	$e_v = a \sigma^{0.5}$	
Schultze and Moussa (28)	$e_u = 0.0106 \sigma^{0.206}$) limiting values
	$e_u = 0.0037 \sigma^{0.680}$	
Brinch Hansen (29)	$e_v = 0.58 e^{1.8} \sigma^{0.53}$	
	$e_u = 2.6 e^{2.25} \sigma^{0.46}$	

In the above, u = uniaxial, v = volumetric, e = initial void ratio. The coefficient a varies widely, while the exponent K seems to be of the order of 0.5 for most soils. (The value of 0.2 reported by Schultze and Moussa refers to a relative density of zero.)

(iii) Cohesionless soils can be inhomogeneous to varying degrees and this is not catered for in any of the analyses considered so far. Finite element methods given later in this thesis will be found to be capable of dealing with arbitrary inhomogeneity.

(iv) If anisotropy exists in a cohesionless soil the difficulties presented are not too great. Barden (22) has already dealt with one special case of anisotropy and, in principle, arbitrary anisotropy can be accounted for by the methods described later.

(v) The property which makes the analysis of the stress-strain behaviour of particulate materials throughout the stress range up to failure so difficult is the property of dilatency which makes such materials "unstable" in the terms of the theory of plasticity. That is, under a small increment of stress, work may be done by the material against the applied stress increment. Rowe (30) has begun to tackle this problem which the Author considers to be the key to the advancement of soil mechanics in the field of stress-strain relationships. However, the deformations beneath flexible structures at working loads are usually small, and the soil is certainly nowhere near failure. The majority of sands will not dilate at such low strains, but for very dense sands, which dilate throughout the strain range, the elasticity theories are inadequate. Nor is there any attempt in this thesis to create mathematical models of that type of behaviour.

Considerable restrictions have therefore been placed on the types of foundation, and sequences of load application which can be described in terms of the classical elastic models (even although these are generalised for non-linearity, inhomogeneity and anisotropy). Nevertheless of all problems in soil mechanics, the analysis of the flexible structure resting on a cohesionless (but not exceptionally dense) medium holds out the best hope for a solution in terms of elasticity. This is because:

- (a) Deformations are predominantly time independent.
- (b) The loading is applied once only. The problems of flexible road or airfield pavements are correspondingly more difficult.

- (c) The deformations are so small that they tend to produce a compression of the soil without mobilising high shear stresses which result in a tendency towards dilatent behaviour.

1.7 Some Other Procedures for the Design of Flexible Structures Bearing on Deformable Foundations

(i) Beam-Strip Methods

These are the earliest, and simplest, methods of analysis available for foundation rafts although they involve, correspondingly the greatest number of assumptions. The raft is divided into a series of continuous beams crossing one another at right angles. The reactions of these main beams on each other at the intersection points are assumed as are the reactions on the main beams of the slabs filling the spaces in the beam gridwork. In the context of these sweeping assumptions regarding the structural behaviour, it has been usual to assume a uniformly distributed pressure between soil and raft. Recent recommendations for the design of foundation rafts (31) permit the use of this method for "flexible rafts where the variation in adjacent column loads and spans is not greater than 20%", but advocate approaches based on plate theories for general raft design.

(ii) Baker's Soil Line Method (32)

This method is a generalisation of the beam-strip method which allows for the variation in soil pressure across the raft and for its relation to deflection (Winkler Hypothesis). The simplification is introduced that the soil pressure is assumed to vary linearly along any of the main beams. In order to cover the worst possible case, limits between which the coefficient of subgrade reaction, k , must lie are based on the results of tests at the site. Baker concedes that the method, despite its approximate nature, is lengthy, a feature which does not commend it to practising engineers. Baker has demonstrated (32) that, for a beam, his method gives results in close agreement with the Hetenyi analysis of the elastic line. At the very outset of this thesis, access to high speed

computing capability was assumed and in this light, Baker's method introduces superfluous assumptions. In the absence of a computer it might take equivalent times for skilled operators to employ the soil line method or the Allen and Severn relaxation method for a "one off" solution, but the former can deal more quickly with the effects of the factors mentioned by Baker in his discussion of Allen and Severn's work (33):

- (i) Variation of k values over the site.
- (ii) Errors in assessing k values.
- (iii) Restraint of the building frame to bending of the raft.
- (iv) Reduction of flexural rigidity of the raft due to cracking and creep with time.
- (v) Variation in the distribution of live load in the building.

The methods proposed in the next three chapters can cope with all of the five points listed above.

(iii) Yield Line Method

Thus far, only elastic methods of analysis have been considered. In recent years increasing attention has been paid to ultimate load methods of analysis (U.L.M.) involving, in the case of reinforced concrete slabs, the yield line theory first developed by Johansen (34). Some protagonists of the U.L.M. imply that it should supersede the elastic methods altogether, but the Author prefers to think of the two approaches as complementary. A major advantage claimed for the U.L.M. is its simplicity compared with elastic methods but approximate procedures such as finite differences and finite elements, allied with the use of computers, are rendering tractable an ever increasing number of problems by elasticity techniques. Further, Wood (35) has shown that elastic solutions give exceedingly good results, in terms of economic designs, for reinforced concrete slabs as long as the distribution of the reinforcement is varied. Despite the simplicity of the U.L.M. once a lower bound yield pattern has been found, the discovery of this pattern does not seem to be trivial for complex structures.

Davies (36) has solved the problem of a circular tank foundation slab subjected to parabolic and inverse parabolic contact pressure distributions, but this is the only solution of a foundation problem by the yield line method known to the Author. Further consideration of the method is outwith the scope of this thesis, although its merits as an alternative to the elastic analyses presented in the succeeding chapters are conceded.

1.8 Conclusions

A study of available methods of analysing flexible structures bearing on deformable soil foundations indicates that these methods are limited in their scope. Many are restricted to two-dimensional problems, and most are only capable of dealing with uniform structures bearing on uniform foundations such as the pure Winkler and the semi-infinite, homogeneous, elastic models. In this thesis, methods are developed whereby beams, circular, rectangular or irregular plates with arbitrarily variable elastic or sectional properties and bearing on non-uniform Winkler, or Coupled, or semi-infinite elastic foundations with arbitrary anisotropy and inhomogeneity can be analysed with equal facility. Non-linear elastic properties in any of the foundation types can be tackled by the same principles using iterative procedures. The methods are entirely dependent on the use of electronic digital computers, and have been used in turn for the evaluation of a limited series of experimental results for plates on a sand foundation. A fuller experimental study, together with an examination of case histories could lead to the compilation of a set of charts which would adequately describe the majority of foundation types. Further, the methods proposed, and particularly the finite element method, might be extended to include truer models of soil behaviour than the classical elastic models, by the inclusion of such features as dilatency and time dependence.

CHAPTER 2.

FINITE ELEMENT METHODS FOR THE ANALYSIS OF ELASTIC PLATES IN BENDING

2.1 Introduction

It has already been pointed out in Section 1.1 that computers can be of considerable use in the solution of problems involving flexible structures bearing on elastic foundations for two reasons. Firstly for the solution of the differential equations by numerical methods, and secondly because of the scale of the problems involved, thus taking advantage both of the speed of computation and of the large storage capacity of modern machines. At the beginning of this research, the potentialities both of the finite difference and of the finite element method were investigated, and it was felt that the latter offered the best prospects for solutions to the originally envisaged problem of rectangular plates bearing on elastic foundations and subjected to restraint from a superstructure. The finite element analyses for plates in bending reported in the literature as of 1964 were studied, and some apparent discrepancies which were found led to the development of new analyses, using rectangular plate elements, which are described in this Chapter. A little work was also done using the finite difference method, and this is described in Chapter 4.

2.2 Antecedents of Modern Finite Element Methods

The thin elastic plate subjected to bending actions is such a common structural element that considerable effort has been expended in the past on its analysis. The governing differential equation of flexure is

$$D \left(\frac{\partial^4 w}{\partial x^4} + 2 \frac{\partial^4 w}{\partial x^2 \partial y^2} + \frac{\partial^4 w}{\partial y^4} \right) = q$$

$$\text{or} \quad DV^4 w = q \quad \text{eq(2.1)}$$

Analytical solutions exist for certain rather restricted examples of plate geometry, loading and boundary conditions, a good selection being given in the standard work of Timoshenko and Woinowsky-Krieger (6). However if there is any complexity in the geometry, loading distribution

or support conditions, recourse has to be made to an approximate analysis. Of these, the most widely used are the finite difference and finite element methods. The method of finite difference approximations to the biharmonic equation, eq(2.1), is considered in some detail in Chapter 4.

Alternatively there is the method of finite elements which is referred to here in its broadest sense as any idealisation of a continuum by a finite number of discrete elements connected at points called "nodes". The salient feature of the use of either the finite difference or the finite element method is the necessity of solving large numbers of linear algebraic equations and while some solutions by the former method were obtained some years ago using the relaxation techniques of Southwell (37) the introduction of the high speed electronic digital computer has vastly increased the scope of approximate analysis procedures.

The first steps in finite element analysis of structures were taken by Hrennikoff (38) and by McHenry (39) in the early 1940's, when plates subjected to in-plane or bending actions were idealised as frameworks of bars whose elastic properties were varied so that the behaviour of the framework under load approximated closely to the behaviour of the solid plate. Analyses of plates using such "one-dimensional" elements are still being reported (40) but the Author agrees with Hrennikoff (41) that the more sophisticated "two-dimensional" elements which have been developed are more likely to come into general use. Two-dimensional elements can represent a more general state of stress than one dimensional elements, and with certain configurations of the latter, Poisson's ratio cannot assume an arbitrary value. The only point in favour of one-dimensional elements is that a standard plane framework computer program can be used to analyse plates subjected to in-plane stress or flexure; the analysis is not less complicated or less time consuming.

Ten years after the early work using one-dimensional elements the availability of electronic digital computers gave a great boost to structural analysis by matrix methods in general and by the

finite element method in particular. The complexity of aircraft fuselages and wings was a powerful incentive for the adoption of automated analysis procedures in the aviation industry, and the outstanding contributions of Argyris (42) and of Turner, Clough, Martin and Topp (43) describe the early work in this field. Comprehensive bibliographies are given in references (43) and (44).

2.3 Force Method and Displacement Method

Two different (although complementary and highly interrelated) methods are most commonly employed in the analysis of structures employing finite element techniques. These methods are the force (or flexibility or compatibility) method where the unknowns are taken to be forces in the structure and the displacement (or stiffness or equilibrium) method where the unknowns are displacements at the nodes of the structure. A third method, which is part force method and part displacement method is sometimes used. The term "displacements" includes quantities which may not be readily recognised as such. For example in what follows, $\partial^3 w / \partial x^2 \partial y$ is treated as an unknown in the displacement method although its physical significance is obscure. For this reason these displacements are called "generalised" displacements, and the forces which correspond to them "generalised" forces. It must be emphasised that the difference in methods arises in the analysis of the total structure after the force-deformation relationships of the individual elements have been obtained.

At the primary level of the isolated element, flexibility and stiffness are directly related and means of deriving the element flexibility matrix corresponding to an element stiffness matrix and vice versa are given by Gallagher (45).

At the secondary level of the interconnection of elements it is necessary to introduce the concepts of a pure compatible approach and a pure equilibrium approach, a terminology proposed by Fraeijs de Veubeke (46). By "pure" one implies that either compatibility or equilibrium must be satisfied throughout the group of interconnected elements, that is in the interior of the elements and along the boundaries between the elements. These pure approaches

are of considerable importance firstly if monotonic convergence to a correct solution is sought as the number of finite elements comprising a structure is increased, and secondly if an upper or lower bound to the energy of the structure is desired. Melosh (47) provides the proof that a pure approach is a necessary (though not sufficient) condition for monotonic convergence of a solution as the number of elements per structure is increased, while Fraeijs de Veubeke (46) shows that a purely compatible approach provides a ~~upper~~ ^{lower} bound, and a purely equilibrium approach an ~~upper~~ ^{upper} bound to the influence coefficients for a structure where, if a single force F produces a displacement d in its line of action, the influence coefficient c is defined by

$$d = cF.$$

This implies that a pure compatible analysis of a structure should result in a displacement under a single load which is less than the true value. Unfortunately bounds on the displacements of a structure with a ~~more~~ general loading, i.e. distributed loads etc. cannot be inferred, nor can bounds be placed upon the stresses calculated by a pure approach. All that is known is that the potential energy of the finite element idealisation of the structure is less than the potential energy of the true structure. Nevertheless, stronger bound theorems may eventually be formulated and perhaps experience will show that the pure compatible and pure equilibrium approaches always produce results which bracket the true ones, although the bounds are in some cases reversed. For these reasons, the pure approaches are considered to be highly important and the new work in this chapter is completely devoted to pure compatible methods. The results obtained are compared with those obtained using methods which violate both compatibility and equilibrium.

At the tertiary level of actual analysis of a given structure subject to certain boundary conditions, the topology of the structure is the governing factor in the selection between force and displacement methods of analysis. Structures with predominant chain topologies are more amenable to analysis by the force method, the

number of unknowns frequently being considerably less than if the displacement method were used. On the other hand structures with more complicated topologies are more easily handled by the displacement technique. Structures with interconnected two-dimensional elements fall into the second class. The selection of redundants or groups of redundants for the analysis of this second class by the force method presents some difficulty although mention should be made of an automated method devised by Denke (48) for this selection process. Practice in the aviation industry is to use the force method for the analysis of fuselages, and the displacement method for the analysis of wings (49). Analogies in civil engineering practice would be the use of the force method for analysis of building frameworks and the displacement method for shear walls and floor slabs. The plate structures considered in this thesis fall into this second class and the displacement method has been used throughout for the analysis of these structures.

2.4 Derivation of Discrete Element Stiffness (Flexibility) Properties

In the previous section, Section 2.3, it was pointed out that, apart from possible computational inaccuracies, the results obtained from the analysis of a structure by the force method and by the displacement method will be identical once the stiffnesses (and hence the flexibilities) of the elements constituting the structure have been derived. Therefore the prime interest in the comparison of the various finite element analyses described in the literature and of the new analyses given in this chapter lies in a comparison of the (generalised) force-displacement relationships of similar elements. Several means of deriving these relationships are used in the literature, for example the use of the principle of virtual work, or the use of a strain energy formulation together with Castigliano's theorem. Gallagher (45) has catalogued various matrix methods of analysis with particular reference to plane stress problems. This chapter attempts to fulfil one of Gallagher's suggestions for future work, namely an evaluation of matrix methods of analysis for plates in bending (with special reference to rectangular finite elements).

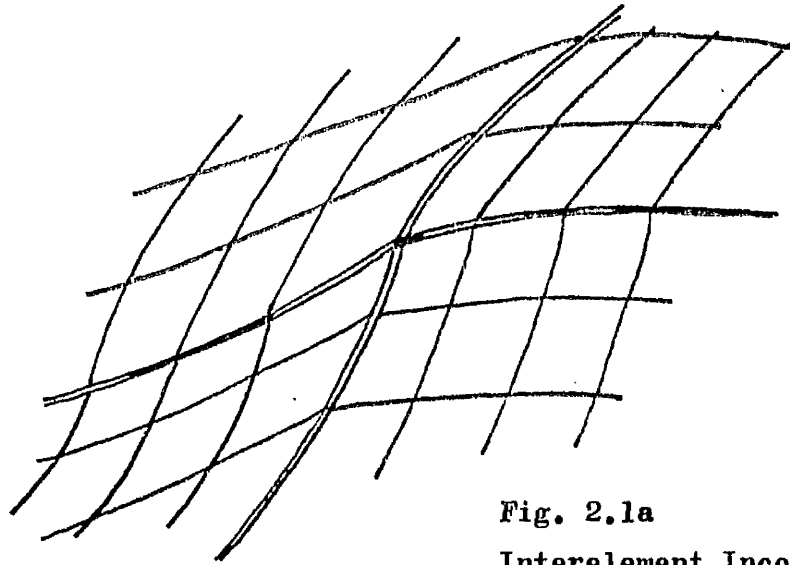


Fig. 2.1a
Interelement Incompatibility

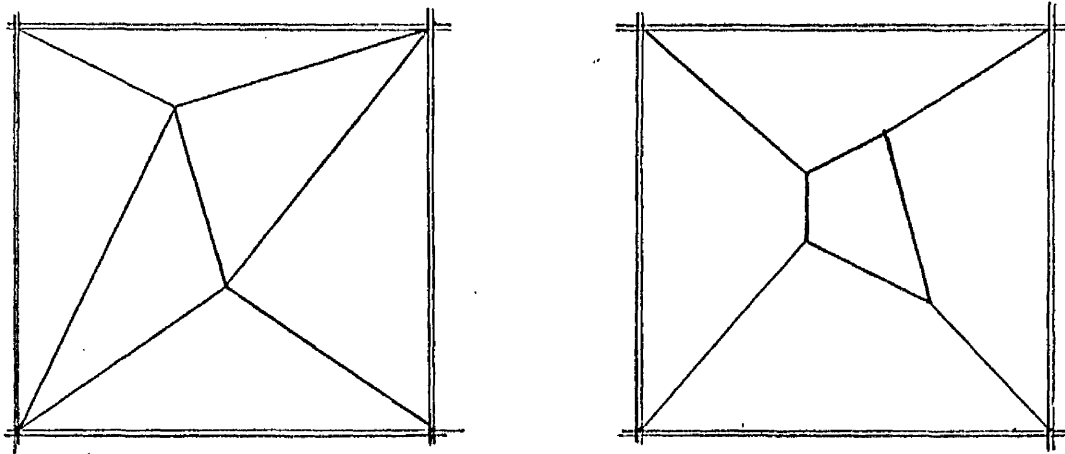


Fig.2.1b Mesh Refinement using Triangles or Quadrilaterals

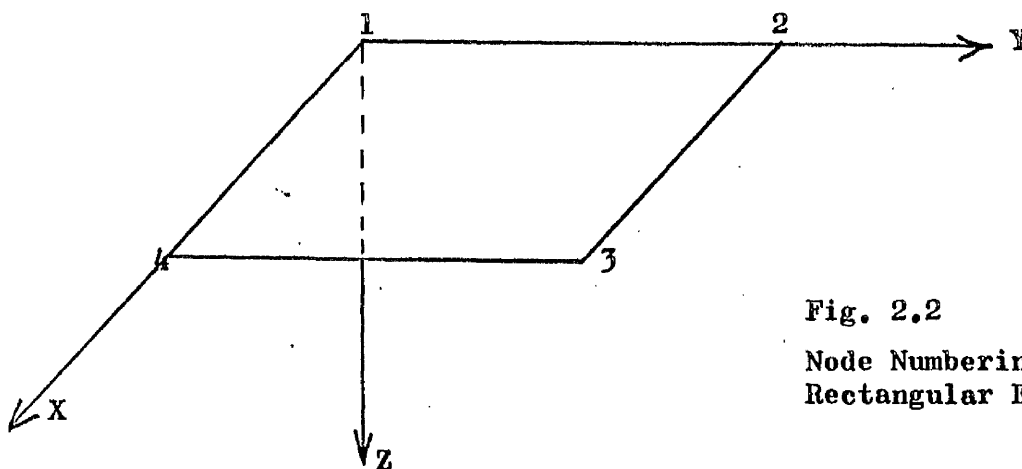


Fig. 2.2
Node Numbering System For
Rectangular Elements

2.5 Rectangular Element Stiffness Matrices for Plates in Bending 1959-1964

Whereas the early work on two-dimensional finite elements by Argyris and others, described in Section 2.2, had been restricted to plates subjected to in-plane stresses, in 1959 the finite element method was first applied to the analysis of thin plates in bending by Adini (50) and by Papanfuss (51). Neither of these analyses was published, and it has only been possible to consult the former. The main interest in Adini's work centres on his assumption of the displacement function for a rectangular element in terms of twelve undetermined coefficients as follows:

$$\begin{aligned}
 w = & a_1x + a_2x^2 + a_3x^3 \\
 & + a_4y + a_5y^2 + a_6y^3 \\
 & + a_7xy + a_8x^2y + a_9x^3y + a_{10}xy^2 + a_{11}xy^3 + a_{12} \quad \text{eq(2.2)}
 \end{aligned}$$

This assumption has been extensively used by subsequent workers and it is important to examine its implications as far as interelement compatibility is concerned. Differentiating eq(2.2) one obtains:

$$\begin{aligned}
 \frac{\partial w}{\partial x} = & a_1 + 2a_2x + 3a_3x^2 \\
 & + a_7y + 2a_8xy + 3a_9x^2y + a_{10}y^2 + a_{11}y^3 \\
 \text{and } \frac{\partial w}{\partial y} = & a_4 + 2a_5y + 3a_6y^2 \\
 & + a_7x + a_8x^2 + a_9x^3 + 2a_{10}xy + 3a_{11}xy^2
 \end{aligned}$$

Hence along any line $x = \text{constant}$ the displacement w and the slope along that line are uniquely defined by a cubic equation with four undetermined coefficients. These coefficients are defined by the displacements and slopes at the ends of the line, i.e. the edges of the element. However $\frac{\partial w}{\partial x}$ is characterised by an equation of the form

$$\frac{\partial w}{\partial x} = A_1x^2 + A_2x + A_3$$

so that the two values of $\frac{\partial w}{\partial x}$ at the ends of the line do not fully define the cross slope $\frac{\partial w}{\partial x}$. Therefore in general a discontinuity in the cross-slope between elements will arise when

this displacement assumption is used, as shown in Fig.2.1a. Adini assumed a distribution of stress resultants along the edges of the element and computed the stiffness matrix by the principle of virtual work. The matrix operations leading to the formation of a stiffness matrix are given in Section 2.6 in conjunction with the description of other element analyses.

Dill and Ortega (52) derived another early plate stiffness matrix; but since their approach does not maintain inter-element compatibility and is not readily available in the literature it has not been consulted.

Another matrix which does not maintain interelement compatibility was derived by Melosh (53). Melosh set up the expression for the bending strain energy of the plate element in terms of the nodal degrees of freedom and applied Castigliano's theorem to obtain the element force-displacement relationships. This approach has been programmed by the Author in order that the results obtained by it may be compared with subsequent methods, and it is referred to hereafter as "Melosh 1961".

The first published attempt to maintain complete inter-element compatibility was made by Melosh in a subsequent paper (47) but the attempt was unsuccessful because Melosh used Lagrangian interpolation in order to obtain his displacement function. Pearson (54) shows that the equation of the bivariate Lagrangian interpolation surface over a rectangular region is given by eq(2.2), which has already been shown to violate interelement compatibility. The stiffness matrix obtained by this second approach of Melosh (termed hereafter "Fitted Lagrange") is not identical with Adini's because Melosh used a "consistent" displacement formulation (see Section 2.7) whereas, by assuming stress distributions as well as displacement distributions, Adini was using what will be termed a "mixed" approach. That is, a consistent approach involves the assumption of displacements or stresses, but not both. Melosh's approach is however identical to an approach proposed by Zienkiewicz and Cheung (55). The identity between

these two methods was masked for a time by misprints in Melosh's paper subsequently pointed out by Tocher and Kapur (56) and the Author's first task on commencing work in this field was to establish this identity.

As far as the Author is aware the first successful derivation of an element displacement function satisfying complete interelement compatibility is due to Papenfuss (51) in an unpublished thesis (quoted by Clough and Tocher (57)). This derivation involves the use of Hermitian cubic polynomials:

Boundary Conditions		Polynomial
$x = 0$	$x = a$	
$w = 1 \frac{\partial w}{\partial x} = 0$	$w = \frac{\partial w}{\partial x} = 0$	$p_1(x) = \frac{1}{a^3}(a^3 - 3ax^2 + 2x^3)$
$w = 0 \frac{\partial w}{\partial x} = 1$	$w = \frac{\partial w}{\partial x} = 0$	$p_2(x) = \frac{1}{a^2}(a^2x - 2ax^2 + x^3)$
$w = \frac{\partial w}{\partial x} = 0$	$w = 1 \frac{\partial w}{\partial x} = 0$	$p_3(x) = \frac{1}{a^3}(3ax^2 - 2x^3)$
$w = \frac{\partial w}{\partial x} = 0$	$w = 0 \frac{\partial w}{\partial x} = 1$	$p_4(x) = \frac{1}{a^2}(x^3 - ax^2)$

which had by 1964 been derived independently by other workers including Schmit (58) and the Author. By using combinations of these polynomials a displacement function completely satisfying interelement compatibility can be written in terms of the conventional twelve generalised displacements for a rectangular element (transverse displacement and two rotations at each node) as follows:

$$\{w\} = [D] \{v\}$$

If, with reference to Fig.2.2 the generalised displacements are written in the order:

$$\{v\} = \left[w_i \quad \left(\frac{\partial w}{\partial x}\right)_i \quad \left(\frac{\partial w}{\partial y}\right)_i \right]_{i=1,2,3,4}$$

the $[D]$ vector is:

$$\{D\} = \begin{Bmatrix} p_1(x) & p_1(y) \\ p_2(x) & p_1(y) \\ p_1(x) & p_2(y) \\ p_1(x) & p_3(y) \\ p_2(x) & p_3(y) \\ p_1(x) & p_4(y) \\ p_3(x) & p_3(y) \\ p_4(x) & p_3(y) \\ p_3(x) & p_4(y) \\ p_3(x) & p_1(y) \\ p_4(x) & p_1(y) \\ p_3(x) & p_2(y) \end{Bmatrix}$$

This method is referred to from now on as "Lagrange Hermite" and the method of deriving the appropriate stiffness matrix is described in the next section.

Note. The following matrix notation is used throughout this thesis:

$$\begin{aligned} \{v\} & \equiv \text{column vector } v. \\ [r] & \equiv \text{row vector } r \equiv \{r\}^T \\ [M] & \equiv \text{rectangular matrix } M \\ [M]^T & \equiv \text{transpose of } M \\ [M^{-1}] & \equiv \text{inverse of } M \end{aligned}$$

2.6 Matrix Formulation of Consistent Displacement Approaches

Although the procedures used by Melosh (47) and by Zienkiewicz and Cheung (55) lead to identical stiffness matrices, the methods of derivation are different, and the Author's view is that Melosh's approach is superior. The steps in the two methods are now examined.

(a) Direct method - due to Melosh (47)

- (i) The displacement function is written in terms of the generalised displacements

$$\{w\} = [D_M] \{v\}$$

(The symbols are written in full in Table 2.1)

(ii) The stress resultants (or stresses) are written in terms of the generalised displacements

$$\{M\} = [A] \{B\} \{w\}$$

(iii) The strain energy is written in terms of the stress resultants

$$\begin{aligned} dU &= \frac{1}{2} [S] \{M\} \\ \text{where } \{S\} &= [Q]^T \{B\} \{w\} \\ \text{i.e. } [S] &= [w] [B] [Q] \end{aligned}$$

$$\begin{aligned} \text{Hence } dU &= \frac{1}{2} [w] [B] [Q] [A] \{B\} \{w\} \\ &= \frac{1}{2} [v] [D_M] [B] [Q] [A] \{B\} [D_M] \{v\} \\ \text{or } U &= \frac{1}{2} \int_A [v] [D_M] [B] [Q] [A] \{B\} [D_M] \{v\} dA \end{aligned}$$

(iv) Let $[K] = \int_A \{D_M\} [B] [Q] [A] \{B\} [D_M] dA$

= the element stiffness matrix

Thus $U = \frac{1}{2} [v] [K] \{v\}$

(v) The potential energy in the absence of body forces can be written

$$\pi = U - \int_{S_t} [w] [T] dS_t$$

where S_t is the area of the element surface over which surface tractions T are prescribed.

Hence $\pi = \frac{1}{2} [v] [K] \{v\} - \int_{S_t} [v] \{D_M\} [T] dS_t$

Minimising the potential with respect to the generalised displacements yields for the equilibrium condition

$$\frac{\partial \pi}{\partial v} = [K] \{v\} - \int_{S_t} \{D_M\} [T] dS_t$$

Hence $\int_{S_t} \{D_M\} [T] dS_t = [K] \{v\}$

where the left hand side represents the generalised forces, related to the generalised displacements $\{v\}$ through the stiffness matrix $[K]$. The only examples of surface tractions considered in this chapter are, a uniform load $q = \text{constant}$ over the whole element, and concentrated loads applied at the nodal points. In the first case the generalised forces are given by $q \int_0^a \int_0^b \{D_M\} dx dy$, and the result of this

$$\begin{aligned}
 [D_M] &= \text{Melosh displacement assumption. See (47), (56).} \\
 [v] &= \left[w_1 \left(\frac{\partial w}{\partial x} \right)_1 \left(\frac{\partial w}{\partial y} \right)_1 \dots \dots \dots w_4 \left(\frac{\partial w}{\partial x} \right)_4 \left(\frac{\partial w}{\partial y} \right)_4 \right] \\
 &\quad \text{with reference to Fig. 2.2.}
 \end{aligned}$$

$$[M] = \begin{bmatrix} M_x & M_y & M_{xy} \end{bmatrix}$$

$$[A] = \begin{bmatrix} -D & -\nu D & 0 \\ -\nu D & -D & 0 \\ 0 & 0 & -(1-\nu)D \end{bmatrix}$$

$$[B] = \begin{bmatrix} \frac{\partial^2}{\partial x^2} & \frac{\partial^2}{\partial y^2} & \frac{\partial^2}{\partial x \partial y} \end{bmatrix}$$

$$[Q] = \begin{bmatrix} -1 & 0 & 0 \\ 0 & -1 & 0 \\ 0 & 0 & -2 \end{bmatrix}.$$

Table 2.1.

$$[D_Z] = \left[1 \quad x \quad y \quad x^2 \quad xy \quad y^2 \quad x^3 \quad x^2y \quad xy^2 \quad y^3 \quad x^3y \quad xy^3 \right]$$

$$[c] =$$

1	0	0	0	0	0	0	0	0	0	0	0
0	1	0	0	0	0	0	0	0	0	0	0
0	0	1	0	0	0	0	0	0	0	0	0
1	0	b	0	0	b ²	0	0	0	b ³	0	0
0	1	0	0	b	0	0	0	b ²	0	0	b ³
0	0	1	0	0	2b	0	0	0	3b ²	0	0
1	a	b	a ²	ab	b ²	a ³	a ² b	ab ²	b ³	a ³ b	ab ³
0	1	0	2a	b	0	3a ²	2ab	b ²	0	3a ² b	b ³
0	0	1	0	a	2b	0	a ²	2ab	3b ²	a ³	3ab ²
1	a	0	a ²	0	0	a ³	0	0	0	0	0
0	1	0	2a	0	0	3a ²	0	0	0	0	0
0	0	1	0	a	0	0	a ²	0	0	a ³	0

Table 2.2.

operation, as usual with reference to Fig.2.2 is the generalised force vector

$$q \left[\begin{array}{cccccccc} \frac{ab}{4} & \frac{a^2b}{24} & \frac{ab^2}{24} & \frac{ab}{4} & \frac{a^2b}{24} & -\frac{ab^2}{24} & \frac{ab}{4} & -\frac{a^2b}{24} & -\frac{ab^2}{24} & \frac{ab}{4} \\ & & & & & & & & & & -\frac{a^2b}{24} & \frac{ab^2}{24} \end{array} \right]$$

The case of concentrated loads presents no difficulty. Some authors have approximated the generalised forces produced by a uniformly distributed loading by four "lumped" forces at the nodal points only. i.e. $q \left[\frac{ab}{4} \ 0 \ 0 \ \frac{ab}{4} \ 0 \ 0 \ \frac{ab}{4} \ 0 \ 0 \ \frac{ab}{4} \ 0 \ 0 \right]$. In the Author's experience this approximation leads to serious errors. For example an approximate displacement or stress resultant can be calculated as being above the true value whereas using the correct generalised force vector the same quantity becomes less than the true value.

(b) Method of Undetermined Coefficients - Zienkiewicz and Cheung (55)

(i) A displacement function of the form $\{w\} = [D_Z] \{a\}$ is assumed, where $\{a\}$ is a vector of undetermined coefficients. The number of coefficients is fixed by the number of generalised displacements assumed for the element. (The symbols are written out in full in Table 2.2; maintaining the nomenclature of the Melosh method).

(ii) By differentiation and substitution of the nodal coordinates in turn

$$\begin{aligned} \{v\} &= [c] \{a\} \\ \text{or } \{a\} &= [c^{-1}] \{v\} \end{aligned}$$

(iii) As in the first method the stress resultants are written in terms of the generalised displacements

$$\begin{aligned} \{M\} &= [A] \{B\} \{w\} \\ &= [A] \{B\} [D_Z] \{a\} \\ &= [A] \{B\} [D_Z] [c^{-1}] \{v\} \end{aligned}$$

(iv) Applying the principle of virtual work and constraining the displacements such that they are unity in the direction of a selected generalised force and zero in the directions of all other forces, then

$$\text{External work } W_e = \delta \{v\} \{F\}$$

where $\{F\}$ are the generalised forces.

$$\text{Hence } W_e = \{F\}.$$

$$\text{Internal work } dW_i = \delta \left[\{B\} \{w\} \right]^T \{M\}$$

$$\begin{aligned} \text{or } W_i &= \int_A \delta \left[\{B\} \{w\} \right]^T \{M\} dA \\ &= \int_A \delta \left[\{B\} \left[D_Z \right] \left[C^{-1} \right] \{v\} \right]^T \{M\} dA \\ &= \int_A \left[\{B\} \left[D_Z \right] \left[C^{-1} \right] \{ \delta v \} \right]^T \{M\} dA \\ &= \int_A \left[\{B\} \left[D_Z \right] \left[C^{-1} \right] \right]^T \{M\} dA \end{aligned}$$

Equating external and internal work,

$$\begin{aligned} \{F\} &= \int_A \left[\{B\} \left[D_Z \right] \left[C^{-1} \right] \right]^T \left[A \right] \{B\} \left[D_Z \right] \left[C^{-1} \right] \{v\} dA \\ &= \int_A \left[C^{-1} \right]^T \left[D_Z \right] \{B\} \left[A \right] \{B\} \left[D_Z \right] \left[C^{-1} \right] \{v\} dA \end{aligned}$$

where again $[K] = \left[C^{-1} \right]^T \int_A \left[D_Z \right] \{B\} \left[A \right] \{B\} \left[D_Z \right] dA \left[C^{-1} \right]$ is the stiffness matrix relating generalised forces $\{F\}$ to generalised displacements $\{v\}$.

Thus the $[D]$ assumptions of Melosh and of Zienkiewicz and Cheung can be related:

$$\left[D_Z \right] \left[C^{-1} \right] = \left[D_M \right]$$

It is also of interest to compare these $[D]$ assumptions with the Lagrange-Hermite approach. Whereas the first term in the latter vector is

$$D_1 = \frac{1}{a^3} (2x^3 - 3ax^2 + a^3) \frac{1}{b^3} (2y^3 - 3by^2 + b^3),$$

in the former case the corresponding term is

$$\begin{aligned} D_1 &= \frac{2x^3}{a^3} + \frac{2y^3}{b^3} - \frac{3x^2}{a^2} - \frac{3y^2}{b^2} - \frac{2x^3y}{a^3b} - \frac{2xy^3}{ab^3} \\ &\quad + \frac{3x^2y}{a^2b} + \frac{3xy^2}{ab^2} - \frac{xy}{ab} + 1. \end{aligned}$$

The functions of x and of y are not separable, and it can be seen that a simple function in the first twelve obvious undetermined coefficients leads to a very unwieldy $[D]$ vector. It will be seen later that in general it is impossible to guess the function in terms of undetermined coefficients which corresponds to a natural choice of a $[D]$ vector by the Melosh technique.

2.6 Three New Element Stiffness Matrices

Having obtained the cubic Hermitian polynomials which guarantee complete interelement compatibility for 12 generalised displacements per element, Papenfuss (51) evidently extended the method no further. Schmit (58) did not proceed to set up an element stiffness matrix in the conventional manner, as described in the previous section, but employed linear programming techniques to solve the problem:

"Given the potential energy of a system as a function of the generalised displacements

$$\pi = \pi (v_i)$$

find v_i such that $\pi(v_i)$ is a minimum."

The Author however, used the Lagrange-Hermite polynomials to set up a stiffness matrix as usual. A defect in the Lagrange-Hermite method then becomes apparent, perhaps more readily than in the use of Schmit's approach, in that the deformations associated with the so-called twisting action, namely $\partial^2 w / \partial x \partial y$ vanish at every node resulting in an excessively stiff representation of all structures, and producing divergence from the correct solution in certain problems where twisting is significant, as the element mesh is refined (Section 2.8).

This led the Author to an important step, namely the inclusion of $\partial^2 w / \partial x \partial y$ as an additional degree of freedom for the element. Thus the generalised "displacements" need not be recognisable as displacements in a physical sense, and the restricted view of a recent publication by Severn and Taylor (59) is not justified. The work in this section shows the finite element technique to be a basic method of mathematical analysis rather than a restricted means of solving structural analysis problems, a point also very well demonstrated in work by Zienkiewicz and his colleagues (60). The problem of inclusion of $\partial^2 w / \partial x \partial y$ may be stated:

"look for a function $f(x,y)$ such that say,
when $x = y = 0$, $\partial^2 f / \partial x \partial y = 1$, $f = \partial f / \partial x$
 $= \partial f / \partial y = 0$."

Three other conditions apply at the other corners of the rectangle.

Reasoning from the Lagrange-Hermite method that the functions of x and of y are separable, one arrives at further combinations of the cubics already derived for the 12 degree of freedom case, namely:

At node 1 $p_2(x) p_2(y)$
 At node 2 $p_2(x) p_4(y)$
 At node 3 $p_4(x) p_4(y)$
 At node 4 $p_4(x) p_2(y)$

Thus if the generalised displacements are taken in the order:

$$\begin{bmatrix} v \end{bmatrix} = \begin{bmatrix} w_i & (\partial w / \partial x)_i & (\partial w / \partial y)_i & (\partial^2 w / \partial x \partial y)_i \end{bmatrix}$$

$i = 1, 2, 3, 4$

then the $\{D\}$ vector is

$$\{D\} = \left\{ \begin{array}{l} p_1(x) \cdot p_1(y) \\ p_2(x) \cdot p_1(y) \\ p_1(x) \cdot p_2(y) \\ p_2(x) \cdot p_2(y) \\ p_1(x) \cdot p_3(y) \\ p_2(x) \cdot p_3(y) \\ p_1(x) \cdot p_4(y) \\ p_2(x) \cdot p_4(y) \\ p_3(x) \cdot p_3(y) \\ p_4(x) \cdot p_3(y) \\ p_3(x) \cdot p_4(y) \\ p_4(x) \cdot p_4(y) \\ p_3(x) \cdot p_1(y) \\ p_4(x) \cdot p_1(y) \\ p_3(x) \cdot p_2(y) \\ p_4(x) \cdot p_2(y) \end{array} \right\}$$

The stiffness matrix resulting from this assumption is of order $[16 \times 16]$. It is referred to as "modified Lagrange Hermite".

The next step is to observe that any derivative of w can be made continuous across element boundaries by the use of other polynomials. In particular if $\partial^2 w / \partial x^2$ and $\partial^2 w / \partial y^2$ can be made continuous, the moments M_x and M_y are continuous.

For example the cubic

$$w = \frac{1}{6a}(x^3 - a^2x)$$

Satisfies the conditions: $x = 0, w = \frac{\partial^2 w}{\partial x^2} = 0$

$$x = a, w = 0, \frac{\partial^2 w}{\partial x^2} = 1,$$

and a stiffness matrix could be set up corresponding to the generalised displacements

$$[v] = [w_i \left(\frac{\partial^2 w}{\partial x^2} \right)_i \left(\frac{\partial^2 w}{\partial y^2} \right)_i \left(\frac{\partial^2 w}{\partial x \partial y} \right)_i]$$

$i = 1, 2, 3, 4$

Slope compatibility is not maintained in that case, but can be ensured also by raising the order of the polynomial to 5, i.e. in general

$$w = Ax^5 + Bx^4 + Cx^3 + Dx^2 + Ex + F$$

There are six forms of this polynomial as follows:

Boundary Conditions		Polynomial
$x = 0$	$x = a$	
$w = 1 \frac{\partial w}{\partial x} = \frac{\partial^2 w}{\partial x^2} = 0$	$w = \frac{\partial w}{\partial x} = \frac{\partial^2 w}{\partial x^2} = 0$	$q_1(x) = \frac{1}{a^5}(a^5 - 10a^2x^3 + 15ax^4 - 6x^5)$
$\frac{\partial w}{\partial x} = 1 \quad w = \frac{\partial^2 w}{\partial x^2} = 0$	$w = \frac{\partial w}{\partial x} = \frac{\partial^2 w}{\partial x^2} = 0$	$q_2(x) = \frac{1}{2a^3}(a^3x^2 - 3a^2x^3 + 3ax^4 - x^5)$
$\frac{\partial^2 w}{\partial x^2} = 1 \quad w = \frac{\partial w}{\partial x} = 0$	$w = \frac{\partial w}{\partial x} = \frac{\partial^2 w}{\partial x^2} = 0$	$q_3(x) = \frac{1}{a^4}(a^4x - 6a^2x^3 + 8ax^4 - 3x^5)$
$w = \frac{\partial w}{\partial x} = \frac{\partial^2 w}{\partial x^2} = 0$	$w = 1 \quad \frac{\partial w}{\partial x} = \frac{\partial^2 w}{\partial x^2} = 0$	$q_4(x) = \frac{1}{a^5}(10a^2x^3 - 15ax^4 + 6x^5)$
$w = \frac{\partial w}{\partial x} = \frac{\partial^2 w}{\partial x^2} = 0$	$\frac{\partial w}{\partial x} = 1 \quad w = \frac{\partial^2 w}{\partial x^2} = 0$	$q_5(x) = \frac{1}{2a^3}(a^2x^3 - 2ax^4 + x^5)$
$w = \frac{\partial w}{\partial x} = \frac{\partial^2 w}{\partial x^2} = 0$	$\frac{\partial^2 w}{\partial x^2} = 1 \quad w = \frac{\partial w}{\partial x} = 0$	$q_6(x) = -\frac{1}{a^4}(4a^2x^3 - 7ax^4 + 3x^5)$

First of all the generalised displacements were chosen as

$$[v] = [w_i \left(\frac{\partial^2 w}{\partial x^2} \right)_i \left(\frac{\partial^2 w}{\partial y^2} \right)_i \left(\frac{\partial^2 w}{\partial x \partial y} \right)_i]$$

$i = 1, 2, 3, 4.$

and secondly as

$$\{v\} = \left[w_i \left(\frac{\partial w}{\partial x}\right)_i \left(\frac{\partial w}{\partial y}\right)_i \left(\frac{\partial^2 w}{\partial x \partial y}\right)_i \right] \quad i = 1, 2, 3, 4.$$

In the first case the stiffness matrix resulted in unacceptably over-stiff solutions; in the second case the solutions were better but still far less accurate than for the modified Lagrange Hermite method. For example the second set of generalised displacements led to a value of the central deflection of a square, simply supported plate carrying a uniformly distributed load which was 20% too low. For the first set, the value was over 100% too low. Thus it was concluded that for any polynomial assumption there is a unique best solution, which derives from the inclusion of all the derivatives of w in the generalised displacement vector. Hence for the fifth order polynomials, the generalised displacements were taken as:

$$\{v\} = \left[w_i \left(\frac{\partial w}{\partial x}\right)_i \left(\frac{\partial w}{\partial y}\right)_i \left(\frac{\partial^2 w}{\partial x^2}\right)_i \left(\frac{\partial^2 w}{\partial y^2}\right)_i \left(\frac{\partial^2 w}{\partial x \partial y}\right)_i \right] \quad i = 1, 2, 3, 4.$$

and the $\{D\}$ vector is:

$$\{D\} = \left\{ \begin{array}{l} q_1(x) \quad q_1(y) \\ q_3(x) \quad q_1(y) \\ q_1(x) \quad q_3(y) \\ q_2(x) \quad q_1(y) \\ q_1(x) \quad q_2(y) \\ q_3(x) \quad q_3(y) \\ q_1(x) \quad q_4(y) \\ q_3(x) \quad q_4(y) \\ q_1(x) \quad q_6(y) \\ q_2(x) \quad q_4(y) \\ q_1(x) \quad q_5(y) \\ q_3(x) \quad q_6(y) \\ q_4(x) \quad q_4(y) \\ q_6(x) \quad q_4(y) \\ q_4(x) \quad q_6(y) \\ q_5(x) \quad q_4(y) \\ q_4(x) \quad q_5(y) \\ q_6(x) \quad q_6(y) \\ q_4(x) \quad q_1(y) \\ q_6(x) \quad q_1(y) \\ q_4(x) \quad q_3(y) \\ q_5(x) \quad q_1(y) \\ q_4(x) \quad q_2(y) \\ q_6(x) \quad q_3(y) \end{array} \right\}$$

This approach is called "Fifth Order" *Details of the resulting stiffness matrix are given in Appendix 1. It will be seen that the hand calculations are already laborious, and for the next step, seventh order polynomials, a computer program developed by Duncan (61), for application of the polynomials developed by the Author to skew plate problems was modified to enable the stiffness matrix to be built up automatically from simple input data concerning the polynomials. Details of the program are given in Appendix 4.

There are eight seventh order polynomials as follows:

Boundary Conditions		Polynomial
x = 0	x = a	
w = 1	-	$r_1(x) = \frac{1}{a^7}(a^7 - 35a^3x^4 + 84a^2x^5 - 70ax^6 + 20x^7)$
$\frac{\partial w}{\partial x} = 1$	-	$r_2(x) = \frac{1}{a^6}(a^6x - 20a^3x^4 + 45a^2x^5 - 36ax^6 + 10x^7)$
$\frac{\partial^2 w}{\partial x^2} = 1$	-	$r_3(x) = \frac{1}{2a^5}(a^5x^2 - 10a^3x^4 + 20a^2x^5 - 15ax^6 + 4x^7)$
$\frac{\partial^3 w}{\partial x^3} = 1$	-	$r_4(x) = \frac{1}{6a^4}(a^4x^3 - 4a^3x^4 + 6a^2x^5 - 4ax^6 + x^7)$
-	w = 1	$r_5(x) = \frac{1}{a^7}(35a^3x^4 - 84a^2x^5 + 70ax^6 - 20x^7)$
-	$\frac{\partial w}{\partial x} = 1$	$r_6(x) = -\frac{1}{a^6}(15a^3x^4 - 39a^2x^5 + 34ax^6 - 10x^7)$
-	$\frac{\partial^2 w}{\partial x^2} = 1$	$r_7(x) = \frac{1}{2a^5}(5a^3x^4 - 14a^2x^5 + 13ax^6 - 4x^7)$
-	$\frac{\partial^3 w}{\partial x^3} = 1$	$r_8(x) = -\frac{1}{6a^4}(a^3x^4 - 3a^2x^5 + 3ax^6 - x^7)$

For generalised displacements

$$\left[v \right] = \left[w_i \quad \left(\frac{\partial w}{\partial x} \right)_i \quad \left(\frac{\partial w}{\partial y} \right)_i \quad \left(\frac{\partial^2 w}{\partial x^2} \right)_i \quad \left(\frac{\partial^2 w}{\partial y^2} \right)_i \quad \left(\frac{\partial^2 w}{\partial x \partial y} \right)_i \quad \left(\frac{\partial^3 w}{\partial x^3} \right)_i \right. \\
 \left. \quad \left(\frac{\partial^3 w}{\partial y^3} \right)_i \quad \left(\frac{\partial^3 w}{\partial x^2 \partial y} \right)_i \quad \left(\frac{\partial^3 w}{\partial x \partial y^2} \right)_i \right] \quad i = 1, 2, 3, 4.$$

*Note: The Author later observed that this set of generalised displacements is not yet complete. See discussion of the work of Bogner, Fox and Schmit (62), Section 2.7.

the $\{D\}$ vector becomes:

$$\{D\} = \left(\begin{array}{l} r_{11}(x) \quad r_{11}(y) \\ r_{21}(x) \quad r_{11}(y) \\ r_{12}(x) \quad r_{21}(y) \\ r_{31}(x) \quad r_{11}(y) \\ r_{13}(x) \quad r_{31}(y) \\ r_{22}(x) \quad r_{22}(y) \\ r_{41}(x) \quad r_{11}(y) \\ r_{14}(x) \quad r_{41}(y) \\ r_{32}(x) \quad r_{32}(y) \\ r_{23}(x) \quad r_{23}(y) \\ r_{15}(x) \quad r_{15}(y) \\ r_{25}(x) \quad r_{25}(y) \\ r_{16}(x) \quad r_{16}(y) \\ r_{35}(x) \quad r_{35}(y) \\ r_{17}(x) \quad r_{17}(y) \\ r_{26}(x) \quad r_{26}(y) \\ r_{45}(x) \quad r_{45}(y) \\ r_{18}(x) \quad r_{18}(y) \\ r_{36}(x) \quad r_{36}(y) \\ r_{51}(x) \quad r_{51}(y) \\ r_{61}(x) \quad r_{61}(y) \\ r_{52}(x) \quad r_{52}(y) \\ r_{71}(x) \quad r_{71}(y) \\ r_{53}(x) \quad r_{53}(y) \\ r_{62}(x) \quad r_{62}(y) \\ r_{81}(x) \quad r_{81}(y) \\ r_{54}(x) \quad r_{54}(y) \\ r_{72}(x) \quad r_{72}(y) \\ r_{63}(x) \quad r_{63}(y) \\ r_{82}(x) \quad r_{82}(y) \\ r_{55}(x) \quad r_{55}(y) \\ r_{64}(x) \quad r_{64}(y) \\ r_{73}(x) \quad r_{73}(y) \\ r_{83}(x) \quad r_{83}(y) \\ r_{56}(x) \quad r_{56}(y) \\ r_{65}(x) \quad r_{65}(y) \\ r_{74}(x) \quad r_{74}(y) \\ r_{84}(x) \quad r_{84}(y) \\ r_{57}(x) \quad r_{57}(y) \\ r_{66}(x) \quad r_{66}(y) \\ r_{75}(x) \quad r_{75}(y) \\ r_{85}(x) \quad r_{85}(y) \\ r_{58}(x) \quad r_{58}(y) \\ r_{67}(x) \quad r_{67}(y) \\ r_{76}(x) \quad r_{76}(y) \\ r_{86}(x) \quad r_{86}(y) \\ r_{59}(x) \quad r_{59}(y) \\ r_{68}(x) \quad r_{68}(y) \\ r_{77}(x) \quad r_{77}(y) \\ r_{87}(x) \quad r_{87}(y) \\ r_{50}(x) \quad r_{50}(y) \end{array} \right)$$

The explicit, algebraic form of the stiffness matrix in this case is not known (although it could be output by the computer). Appendix 2 gives a specialised numerical stiffness matrix for a square element of side 1.0, flexural rigidity $D = 1.0$ and Poisson's ratio = 0.3.

In some ways, these sophistications of the finite element method are self-defeating; for example it becomes difficult to

specify exactly the boundary conditions at free edges of plates because quantities like $\frac{\partial^2 w}{\partial x^2}$ and $\frac{\partial^2 w}{\partial y^2}$ can only be specified individually and not as the combination $\frac{\partial^2 w}{\partial x^2} + \nu \frac{\partial^2 w}{\partial y^2}$. The quantitative effect of this is discussed in Section 2.8. However, Section 2.9 considers the application of the techniques described in this section to the solution of problems involving moderately thick plates, where the use of polynomials of at least order 5 is essential.

2.7 Parallel Work 1964-1967

The development of finite element methods of analysis for plate bending problems is of such importance that considerable effort is being expended by research teams in this field principally in the U.S.A. The work presented in this chapter has been confined to rectangular elements because it was envisaged that only rectangular plates would be used in the experimental work. More general element shapes are the quadrilateral and the triangle, which are much more difficult to deal with than the rectangle. Either of these shapes can be used for plates with irregular boundaries, or for the refinement of the element mesh in regions of particular interest as shown in Fig.2.1b. The triangle can also be used for the analysis of doubly curved shells of any shape. In this section a discussion of recent developments in the use of triangular elements is included with the discussion of work on rectangular elements which parallels the Author's.

As far as rectangular elements are concerned, Bogner, Fox and Schmit (62), Hansteen (63) and Butlin and Leckie (64) have all independently used the approach in this thesis called "modified Lagrange Hermite". In addition, Bogner, Fox and Schmit's paper, which only became available to the Author during the writing of this thesis contains the development of the fifth order polynomials as well. The Author's ideas centred on ensuring continuity of certain derivatives across element boundaries and he missed what should have been an obvious point after the development of the modified Lagrange Hermite method, namely that every possible combination of first and second order derivatives should ideally be included in the Fifth

Order approach. Bogner, Fox and Schmit observed this, and took the generalised displacements as:

$$\begin{bmatrix} v \end{bmatrix} = \begin{bmatrix} w_i & \left(\frac{\partial w}{\partial x}\right)_i & \left(\frac{\partial w}{\partial y}\right)_i & \left(\frac{\partial^2 w}{\partial x^2}\right)_i & \left(\frac{\partial^2 w}{\partial y^2}\right)_i & \left(\frac{\partial^2 w}{\partial x \partial y}\right)_i \\ & \left(\frac{\partial^3 w}{\partial x^2 \partial y}\right)_i & \left(\frac{\partial^3 w}{\partial x \partial y^2}\right)_i & \left(\frac{\partial^4 w}{\partial x^2 \partial y^2}\right)_i \end{bmatrix}$$

$$i = 1, 2, 3, 4.$$

However it is debatable whether this approach (9 generalised displacements per node) is preferable to the Author's Seventh Order method (10 generalised displacements per node) in practice because at this level of refinement all methods are very accurate, and the Seventh Order method has the advantage of providing shear forces directly. Gallaher (65) has also attempted to obtain moment continuity between elements by using combinations of the Hermitian cubics (6 generalised displacements per node), but the use of the fifth order polynomials seems to the Author to be more logical.

Argyris (66) has extended his method of "natural" or "invariant" stiffness from its initial application in plane stress problems to the plate bending problem, using both parallelogram and triangular elements with three degrees of freedom per node. This method requires the specification of rigid body modes and of straining or natural modes, the number being determined by the number of generalised displacements assumed for the element. The paper (66b) is ambiguous in that in the first instance it is claimed that compatibility is fully satisfied for the parallelogram elements (p103) but the displacement functions shown on p114 do not in fact satisfy interelement compatibility. The Author contends that the introduction either of mid-side nodes, or of additional degrees of freedom at the nodes will be necessary to obtain complete compatibility. The results obtained by Argyris's approach will be shown to be much poorer than those obtained using a compatible field method, both for rectangular and for skew parallelogram plates (Section 2.8).

Bazeley, Cheung, Irons and Zienkiewicz (67) have also concerned themselves with the more difficult problem of deriving

acceptable solutions to plate bending problems using triangular elements. Following Jones (68) they propose a convergence criterion of "constant strain" which is less rigorous than the usual convergence criteria in that complete interelement compatibility need not be maintained. The violation of interelement compatibility does however mean a violation of the Melosh condition for monotonic convergence and for a particular element mesh the solutions for a problem may be either overestimates or underestimates of the true ones and may oscillate about these true solutions as the mesh is further subdivided. The Author disputes the assertion in paper (67) that the results are "of comparable accuracy to those attainable by the use of rectangular elements". Comparisons are given in Section 2.8. When complete interelement compatibility is maintained the results for the analysis of a plate using triangular elements are very "stiff" indeed. The Author suggests that the addition of a degree of freedom $\delta^2_w / \delta x \delta y$ at the three nodes of the triangle would probably result in much better solutions, on the basis of the foregoing work on rectangular elements.

Further analyses using triangular elements are reported by Clough and Tocher (57) who have also evaluated the Melosh 1961, Fitted Lagrange and Lagrange Hermite methods for rectangular elements, although less extensively than in the succeeding pages of this thesis.

Pian's method of assumed stress distributions (69) has been used by Pian himself (70) and by Severn and Taylor (59) to develop stiffness matrices for rectangular elements with three degrees of freedom per node. In this method, a stress distribution in terms of undetermined coefficients β is assumed throughout the element (i.e. within the element and on its boundaries) together with displacement distributions on the boundary only. This is therefore a "mixed" approach in contrast to the pure field approaches developed in this thesis. The question arises, as Gallagher pointed out in connection with plane stress elements (71), of whether the prescribed stresses, integrated along the boundary, give the prescribed displacements. That the prescribed edge displacements predominate over the prescribed

edge stresses can be seen from Severn and Taylor's paper where discontinuities in the stress resultants across element boundaries were observed.

Thus Severn and Taylor's method is completely mixed - compatibility only being assured at element boundaries together with equilibrium only in the element interiors. Although Pian (70) gives no information about stress resultants, the fact that he does not obtain monotonic convergence of the displacement under a single load as the element mesh is subdivided implies that his stress distribution assumptions also lead to a completely mixed solution. However, Pian's ideas could be used within the framework of a pure compatible method to obtain a better satisfaction of equilibrium within element boundaries. The Author has pointed out elsewhere (72) misconceptions in Severn and Taylor's paper.

2.8 Evaluation of Rectangular Finite Elements for the Analysis of Thin Elastic Plates in Bending

Before the finite element methods described in this chapter can be applied with confidence in the solution of problems for which no analytical solutions exist, the methods must first be evaluated in the solution of problems for which exact, or at least good approximate solutions are known. Such an evaluation of the Melosh 1961, Fitted Lagrange, Lagrange Hermite, modified Lagrange Hermite, Fifth Order and Seventh Order methods is given in this section. In addition the results obtained by these six methods are compared with other recent methods which were described in the previous section.

Tables 2.3-2.10 indicate the convergence trends for the displacement of a point on a plate for four different plate structures each subjected to two different loadings, as the finite element mesh is refined. The structures chosen were:

- (i) A square plate clamped at all four edges,
- (ii) A square plate simply supported at all four edges,
- (iii) A square plate supported at the four corners only,
- (iv) A square cantilever plate,

and the loadings were:

NUMBER OF SUBDIVISIONS PER SIDE

14

12

10

8

6

4

2

0.00150

0.00145

0.00140

0.00135

0.00130

0.00125

0.00120

CENTRAL DEFLECTION $\times q D^4$

MELOSH
1961

FINITE DIFFERENCES

FITTED
LAGRANGE

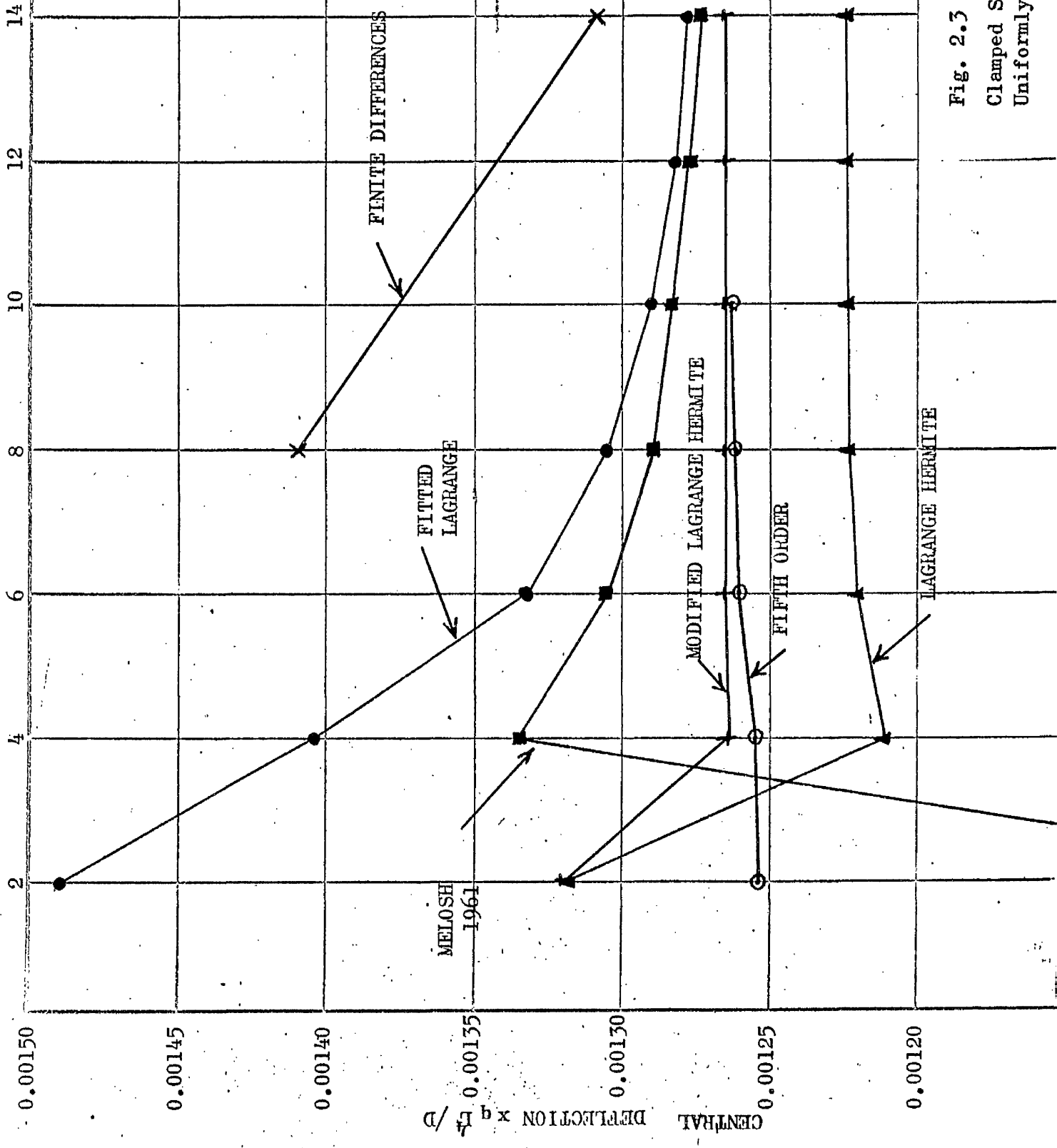
MODIFIED LAGRANGE HERMITE

FIFTH ORDER

LAGRANGE HERMITE

Fig. 2.3

Clamped Square Plate:
Uniformly Distributed Load



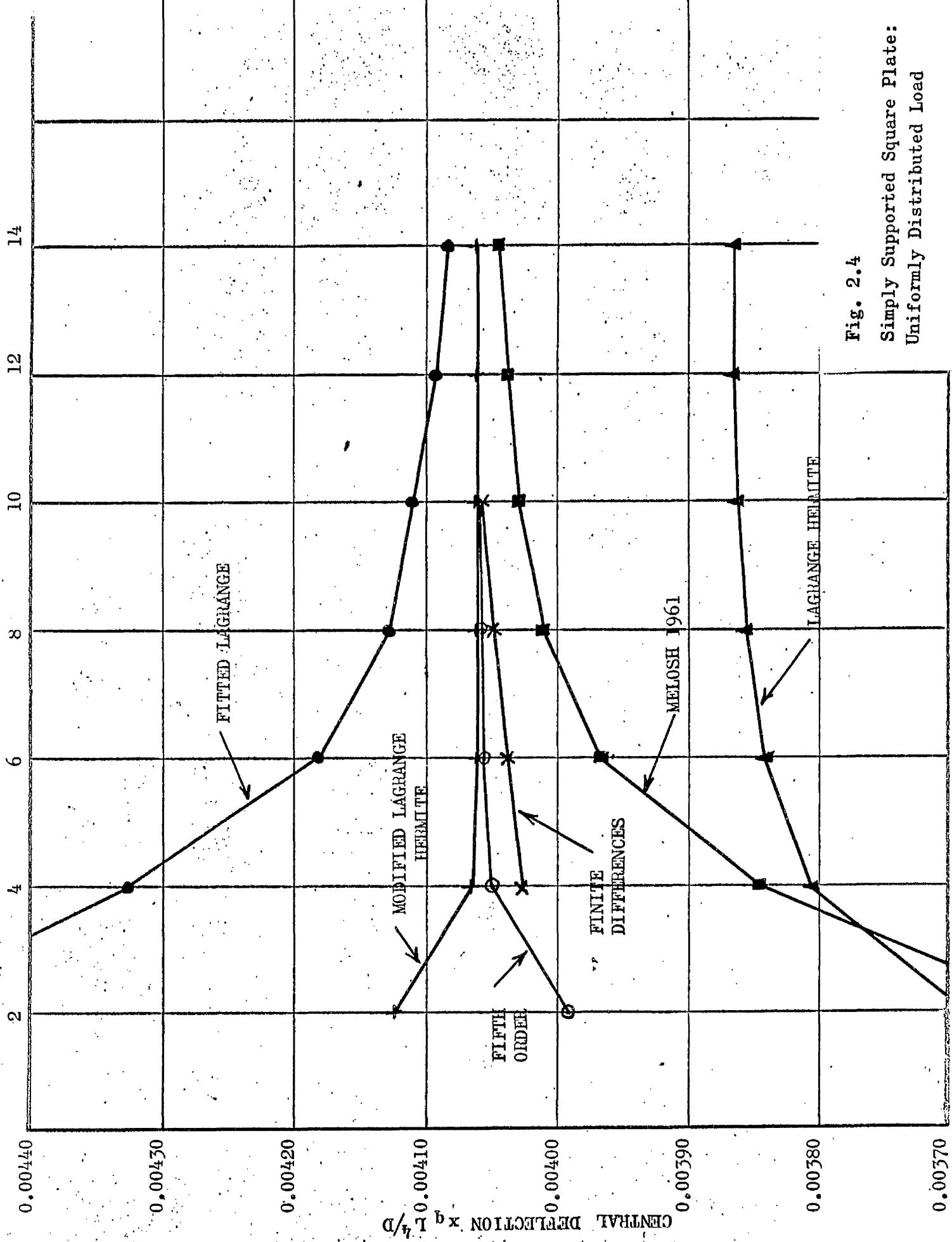


Fig. 2.4
Simply Supported Square Plate:
Uniformly Distributed Load

METHOD	FINITE ELEMENTS					FINITE DIFFERENCES	
TYPE	MELOSH 1961	FITTED LAGRANGE	LAGRANGE HERMITE	MODIFIED LAGRANGE HERMITE	FIFTH ORDER	FOURTH ORDER APPROXS.	SEVENTH ORDER
MESH 2 x 2	1060	1490	1320	1324.8	1253.7	-	1569.1
4 x 4	1333.8	1403.3	1211.3	1264.9	1255.3	-	1263.9
6 x 6	1304.6	1332.3	1220.1	1265.1	1261.3	-	1265.0
8 x 8	1289.1	1303.8	1226.6	1265.2	1263.3	1410	-
10 x 10	1281.1	1290.3	1230.1	1265.3	1264.1	-	-
12 x 12	1276.5	1282.8	1232.5	1265.3	-	-	-
14 x 14	1273.6	1278.2	1233.5	1265.3	-	1310	-

Exact value (6) = 1265.

Table 2.3.

Clamped Square Plate:
Uniformly Distributed Load:
Central Deflection:
Multiplier $qL^4/10^6D$.

METHOD	FINITE ELEMENTS					FINITE DIFFERENCES	
TYPE	MELOSH 1961	FITTED LAGRANGE	LAGRANGE HERMITE	MODIFIED LAGRANGE HERMITE	FIFTH ORDER	FOURTH ORDER APPROXS.	SEVENTH ORDER
MESH 2 x 2	3033	5063	3651	4123	3993	-	4052.2
4 x 4	3846.2	4328.2	3805.2	4065.3	4049.9	4028	4061.5
6 x 6	3968.9	4181.2	3841.8	4062.9	4057.2	4040	4062.1
8 x 8	4010.2	4129.3	3854.7	4062.5	4059.6	4050	-
10 x 10	4029.1	4105.2	3860.7	4062.4	4060.6	4060	-
12 x 12	4039.3	4092.1	3863.9	4062.4	-	-	-
14 x 14	4045.5	4084.2	3865.9	4062.4	-	-	-

Exact value (6) = 4060.

Table 2.4.

Simply Supported Square Plate:
Uniformly Distributed Load:
Central Deflection:
Multiplier $qL^4/10^6D$.

NUMBER OF SUBDIVISIONS PER SIDE

14

12

10

8

6

4

2

FINITE DIFFERENCES

MODIFIED LAGRANGE
HERMITE

FIFTH
ORDER

LAGRANGE HERMITE

FITTED
LAGRANGE

MELOSH 1961

0.0260

0.0250

CENTRAL DEFLECTION $\times q L^4 / D$

0.0240

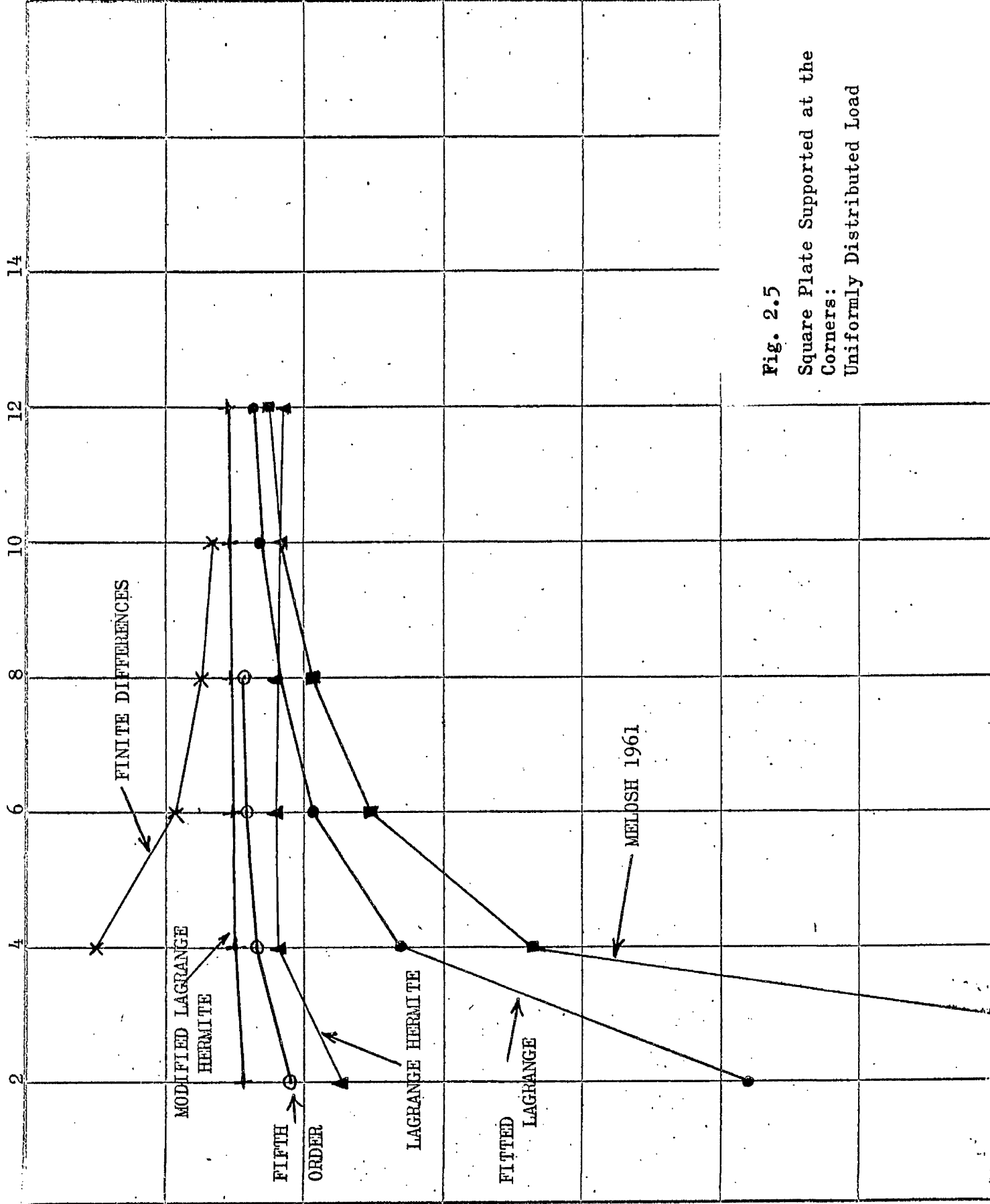
0.0230

0.0220

0.0210

Fig. 2.5

Square Plate Supported at the
Corners:
Uniformly Distributed Load



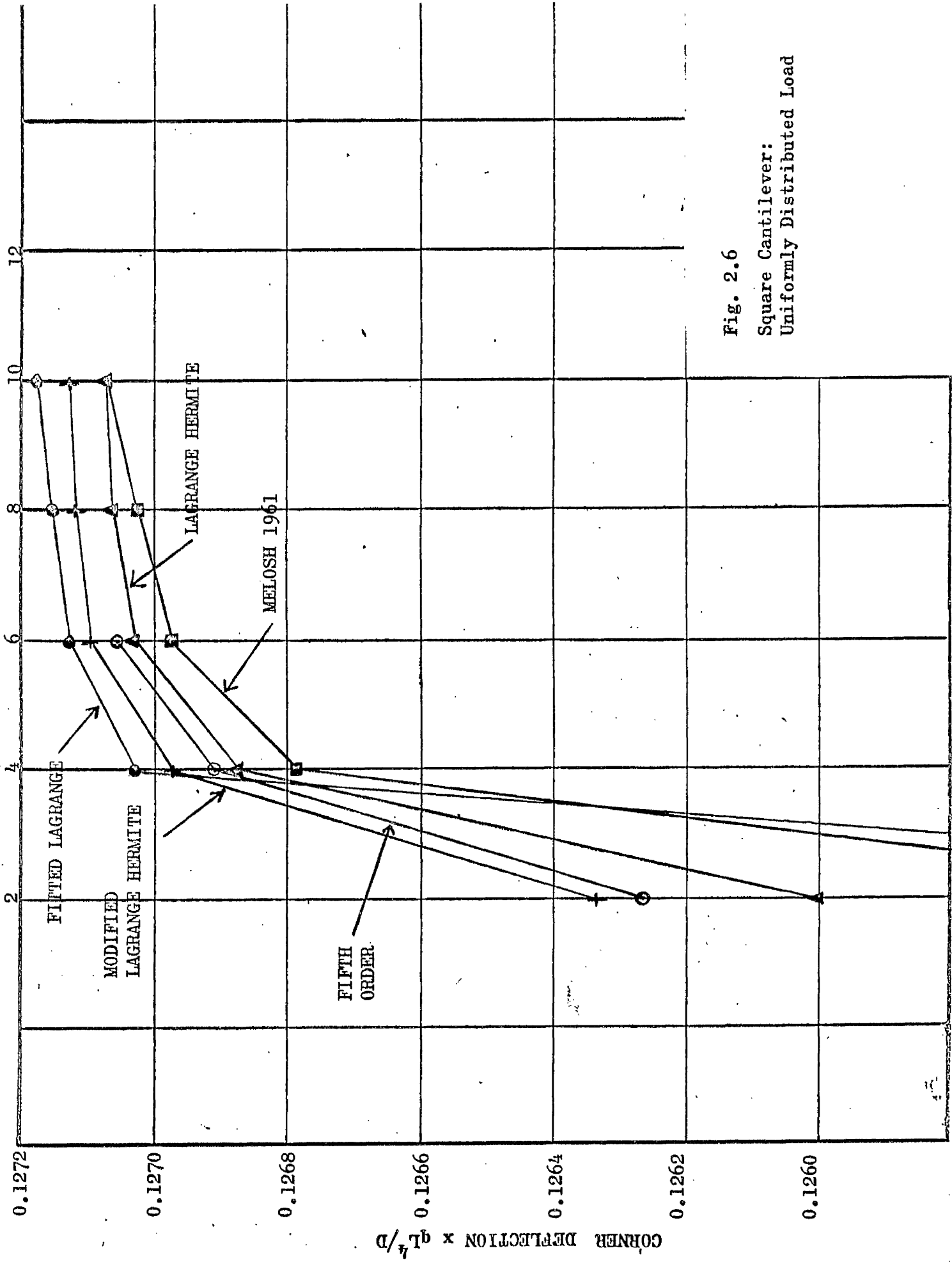


Fig. 2.6
Square Cantilever:
Uniformly Distributed Load

METHOD	FINITE ELEMENTS					FINITE DIFFERENCES
TYPE	MELOSH 1961	FITTED LAGRANGE	LAGRANGE HERMITE	MODIFIED LAGRANGE HERMITE	FIFTH ORDER	FOURTH ORDER APPROXS.
MESH 2 x 2	1811	2179	2470	2542.9	2534.3	-
4 x 4	2335.3	2429.6	2518.7	2550.1	2548.1	2650.0
6 x 6	2451.3	2493.6	2519.4	2550.5	2549.5	2593.8
8 x 8	2493.9	2517.8	2518.1	2550.6	2550.0	2574.7
10 x 10	2514.0	2529.3	2516.8	2550.6	-	2566.0
12 x 12	2525.1	2535.7	2515.8	2550.6	-	-

Analytical solution (84) = 2650.

Table 2.5.

Square Plate Supported at the Corners:
 Uniformly Distributed Load:
 Central Deflection:
 Multiplier $qL^4/10^5D$.

METHOD	FINITE ELEMENTS				
TYPE	MELOSH 1961	FITTED LAGRANGE	LAGRANGE HERMITE	MODIFIED LAGRANGE HERMITE	FIFTH ORDER
MESH 2 x 2	819	726	1260	1263.5	1262.6
4 x 4	1267.9	1270.3	1268.9	1269.5	1268.6
6 x 6	1269.9	1271.3	1270.4	1271.0	1270.5
8 x 8	1270.7	1271.7	1271.0	1271.5	-
10 x 10	1271.2	1271.9	1271.2	1271.5	-

Table 2.6.

Square Cantilever Plate:
 Uniformly Distributed Load:
 Corner Deflection:
 Multiplier $qL^4/10^4D$.

NUMBER OF SUBDIVISIONS PER SIDE

2 4 6 8 10 12 14 16

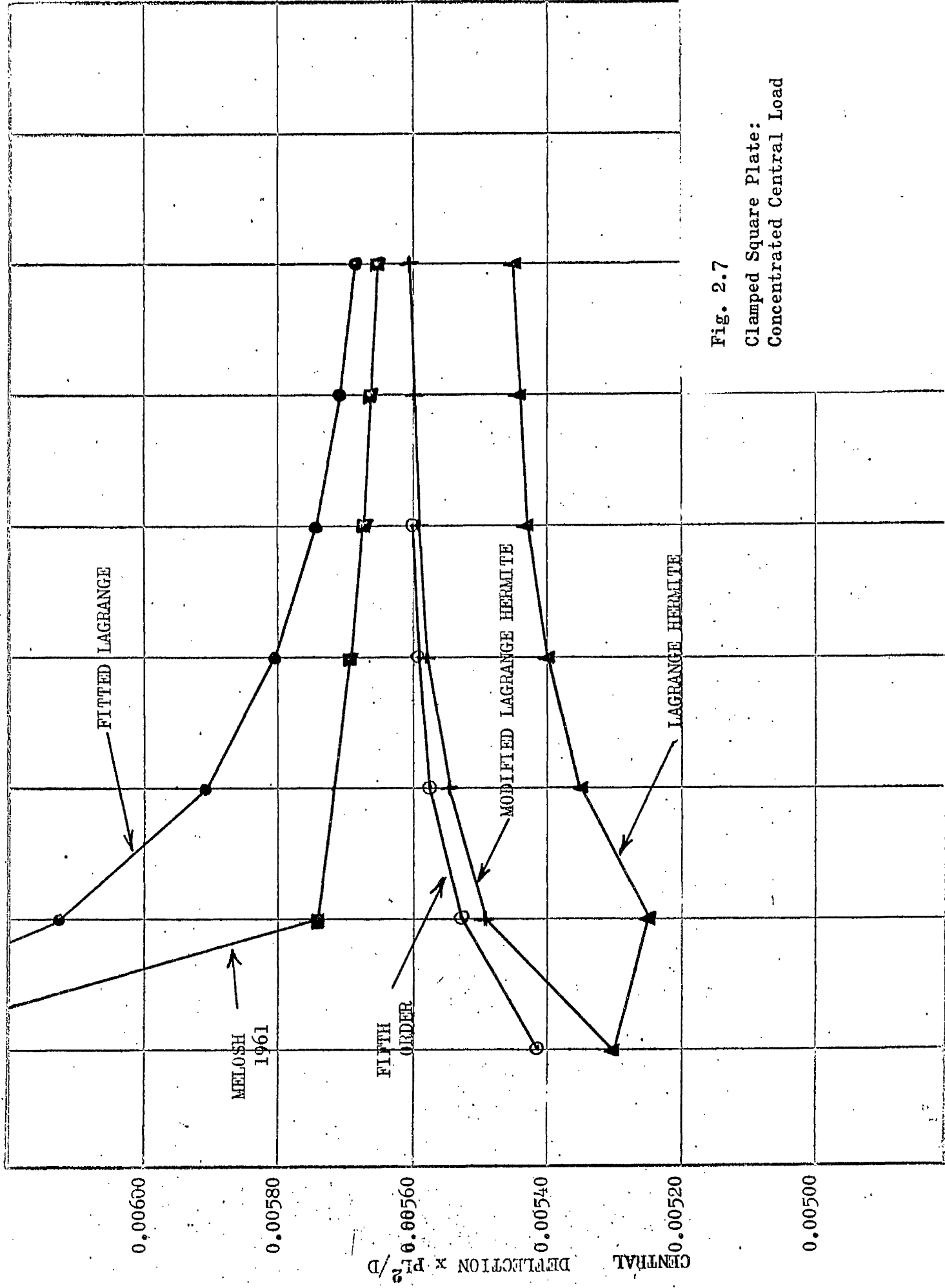


Fig. 2.7
Clamped Square Plate:
Concentrated Central Load

NUMBER OF SUBDIVISIONS PER SIDE

14

12

10

8

6

4

2

0.0130

0.0125

0.0120

0.0115

0.0110

0.0105

CENTRAL DEFLECTION $\times P L^3 / D$

FINITE DIFFERENCES

FITTED LAGRANGE

MELOSH 1961

FIFTH ORDER

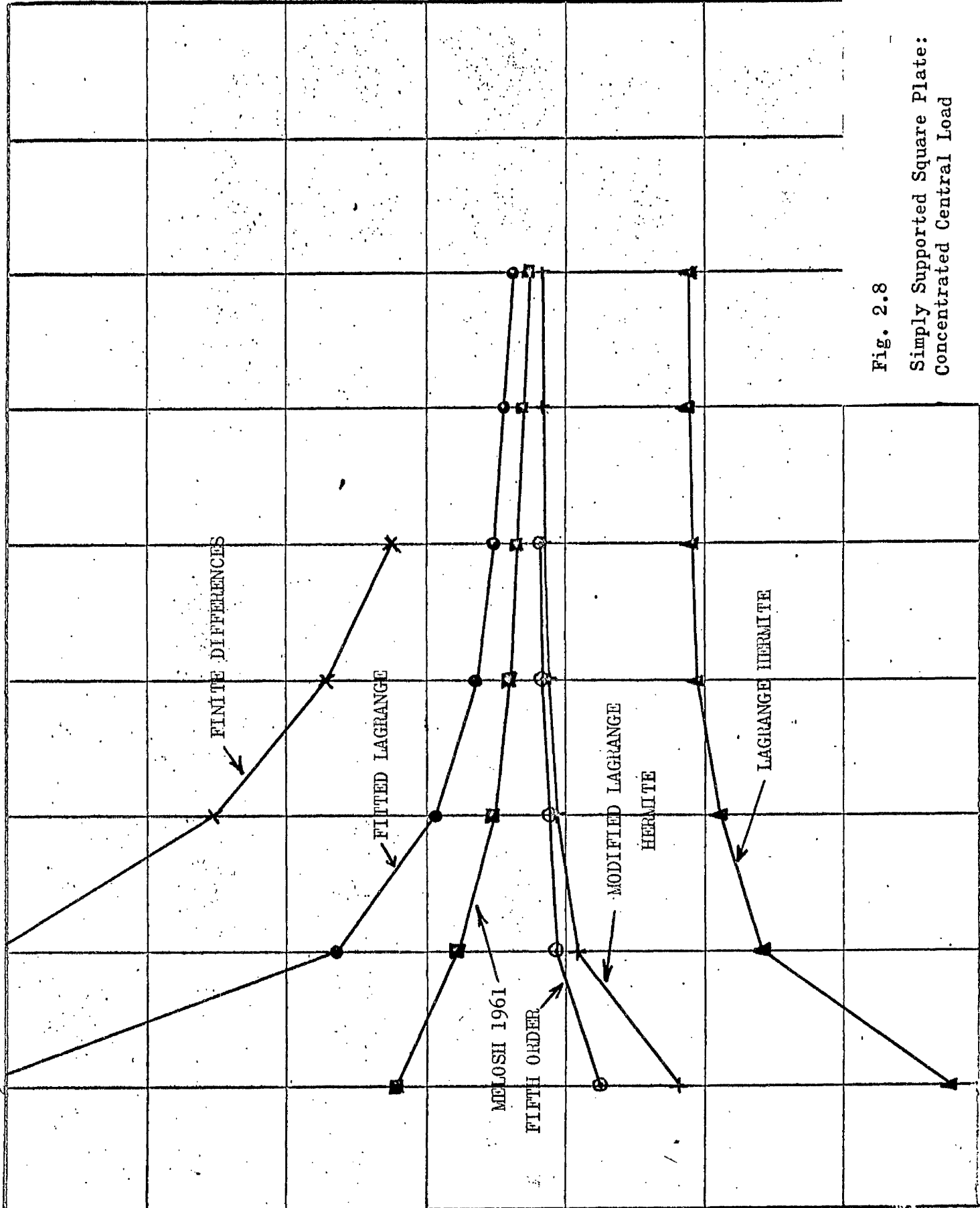
MODIFIED LAGRANGE

HERMITE

LAGRANGE HERMITE

Fig. 2.8

Simply Supported Square Plate:
Concentrated Central Load



METHOD		FINITE ELEMENTS					
TYPE		MELOSH 1961	FITTED LAGRANGE	LAGRANGE HERMITE	MODIFIED LAGRANGE HERMITE	FIFTH ORDER	SEVENTH ORDER
MESH	2 x 2	4240	5920	5300	5300	5407	5330.7
	4 x 4	5738.9	6134.5	5246.6	5484.3	5533.4	5537.5
	6 x 6	5719.8	5910.4	5345.4	5554.6	5577.2	5579.2
	8 x 8	5689.7	5802.6	5396.4	5579.7	5592.2	-
	10 x 10	5669.5	5744.6	5423.3	5591.4	5599.1	-
	12 x 12	5656.1	5709.9	5438.9	55.97.7	-	-
	14 x 14	5646.9	5687.5	5448.7	5601.5	-	-

Exact solution (6) = 5600.

Table 2.7.

Clamped Square Plate:
 Concentrated Central Load:
 Central Deflection:
 Multiplier $PL^2/10^6D$.

METHOD		FINITE ELEMENTS				FINITE DIFFERENCES		
TYPE		MELOSH 1961	FITTED LAGRANGE	LAGRANGE HERMITE	MODIFIED LAGRANGE HERMITE	FIFTH ORDER	FOURTH ORDER APPROXs.	SEVENTH ORDER
MESH	2 x 2	1210	1380	1010	1107.8	1137.7	-	1129.4
	4 x 4	1189.1	1232.7	1078.7	1147.1	1153.2	1367.2	1152.7
	6 x 6	1176.5	1197.1	1094.8	1154.4	1156.7	1276.9	1156.8
	8 x 8	1170.6	1182.9	1100.9	1156.9	1158.1	1235.1	-
	10 x 10	1167.5	1175.6	1103.8	1158.0	1158.8	1212.7	-
	12 x 12	1165.6	1171.4	1105.5	1158.7	-	-	-
	14 x 14	1164.4	1168.7	1106.6	1159.0	-	-	-

Exact solution (6) = 1160.

Table 2.8.

Simply Supported Square Plate:
 Concentrated Central Load:
 Central Deflection:
 Multiplier $PL^2/10^5D$.

NUMBER OF SUBDIVISIONS PER SIDE

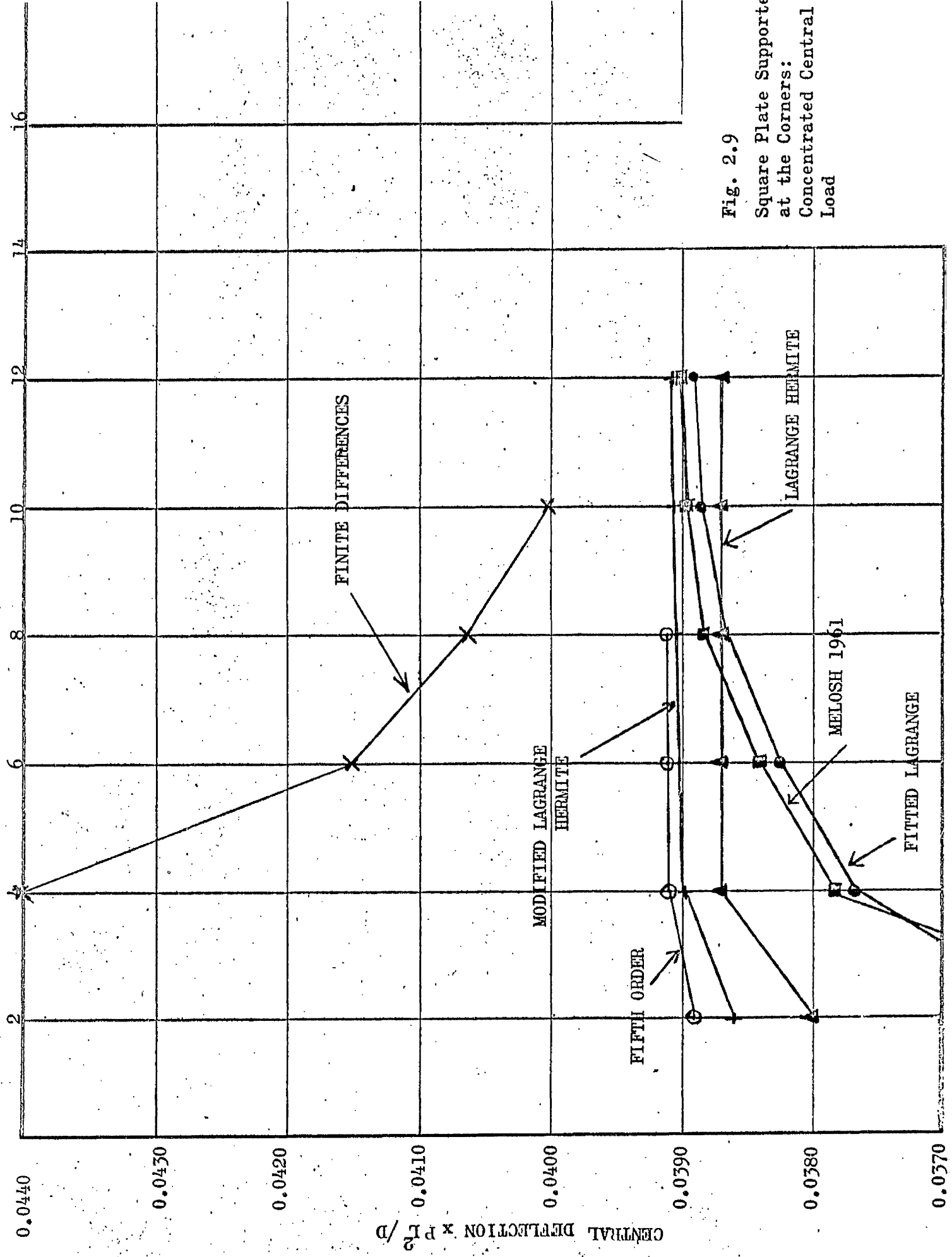


Fig. 2.9
Square Plate Supported
at the Corners:
Concentrated Central
Load

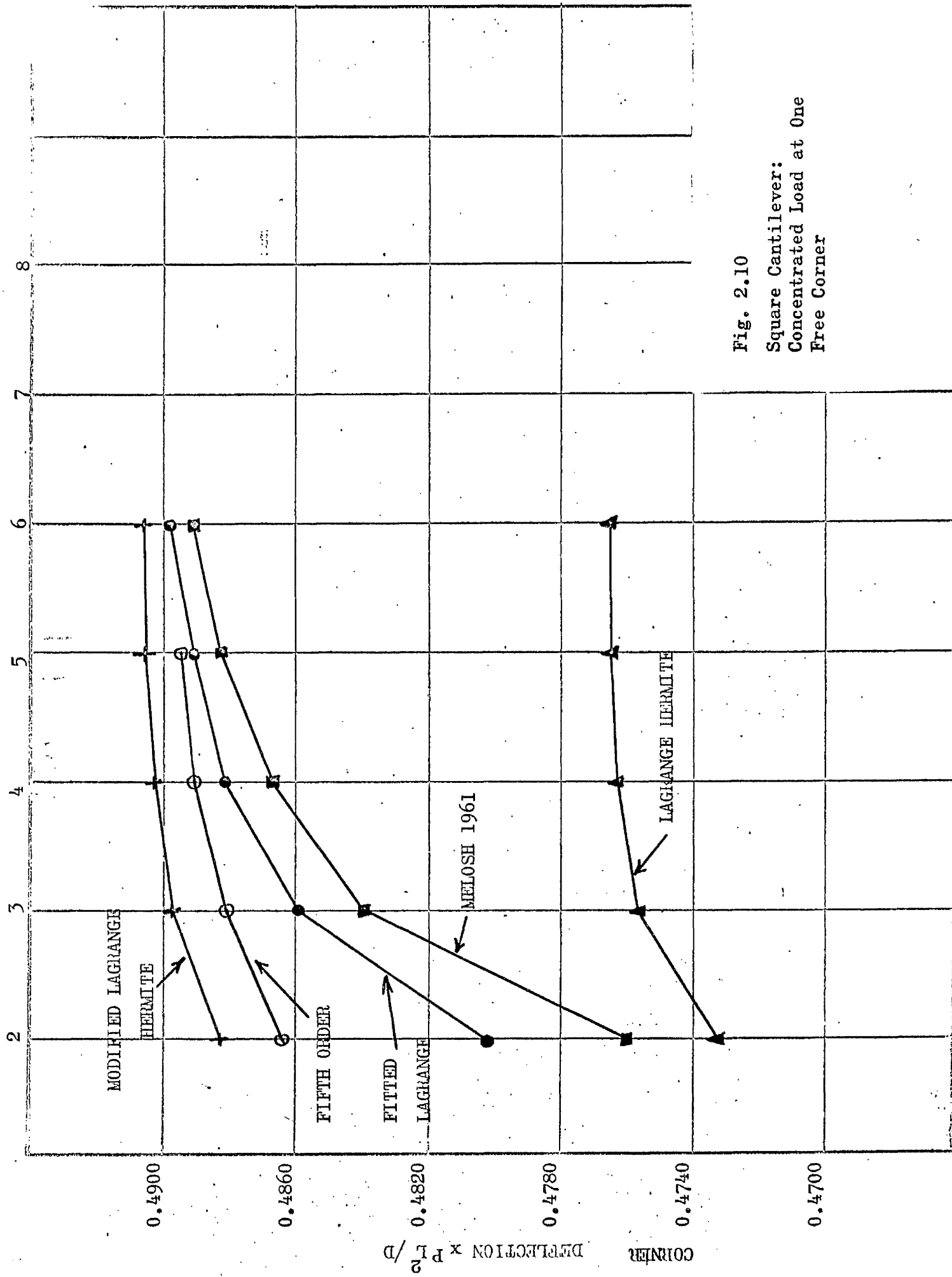


Fig. 2.10
 Square Cantilever:
 Concentrated Load at One
 Free Corner

METHOD	FINITE ELEMENTS					FINITE DIFFERENCES
TYPE	MELOSH 1961	FITTED LAGRANGE	LAGRANGE HERMITE	MODIFIED LAGRANGE HERMITE	FIFTH ORDER	FOURTH ORDER APPROXS.
MESH 2 x 2	3490	3470	3800	3864.7	3885.1	-
4 x 4	3772.1	3781.6	3872.1	3901.5	3907.2	4403.1
6 x 6	3849.7	3856.3	3878.1	3908.5	3910.9	4148.7
8 x 8	3878.1	3882.6	3879.5	3911.0	3912.2	4054.0
10 x 10	3891.4	3894.6	3879.6	3912.1	-	4007.8
12 x 12	3898.6	3901.0	3879.4	3912.8	-	-

Gridwork solution (40) 3900.

Table 2.9.

Square Plate Supported at the Corners:
 Concentrated Central Load:
 Central Deflection:
 Multiplier $PL^2/10^5D$.

METHOD	FINITE ELEMENTS				
TYPE	MELOSH 1961	FITTED LAGRANGE	LAGRANGE HERMITE	MODIFIED LAGRANGE HERMITE	FIFTH ORDER
MESH 2 x 2	4759.9	4807.7	4734.3	4882.7	4877.7
4 x 4	4837.4	4859.8	4757.7	4897.9	4893.5
6 x 6	4867.7	4881.0	4763.6	4903.5	4900.2
8 x 8	4882.5	4891.4	4765.3	4906.2	-
10 x 10	4890.8	4897.3	4765.3	4907.7	-

Table 2.10.

Square Cantilever Plate:
 Concentrated Load at One Free Corner:
 Deflection Under Load:
 Multiplier $PL^2/10^4D$.

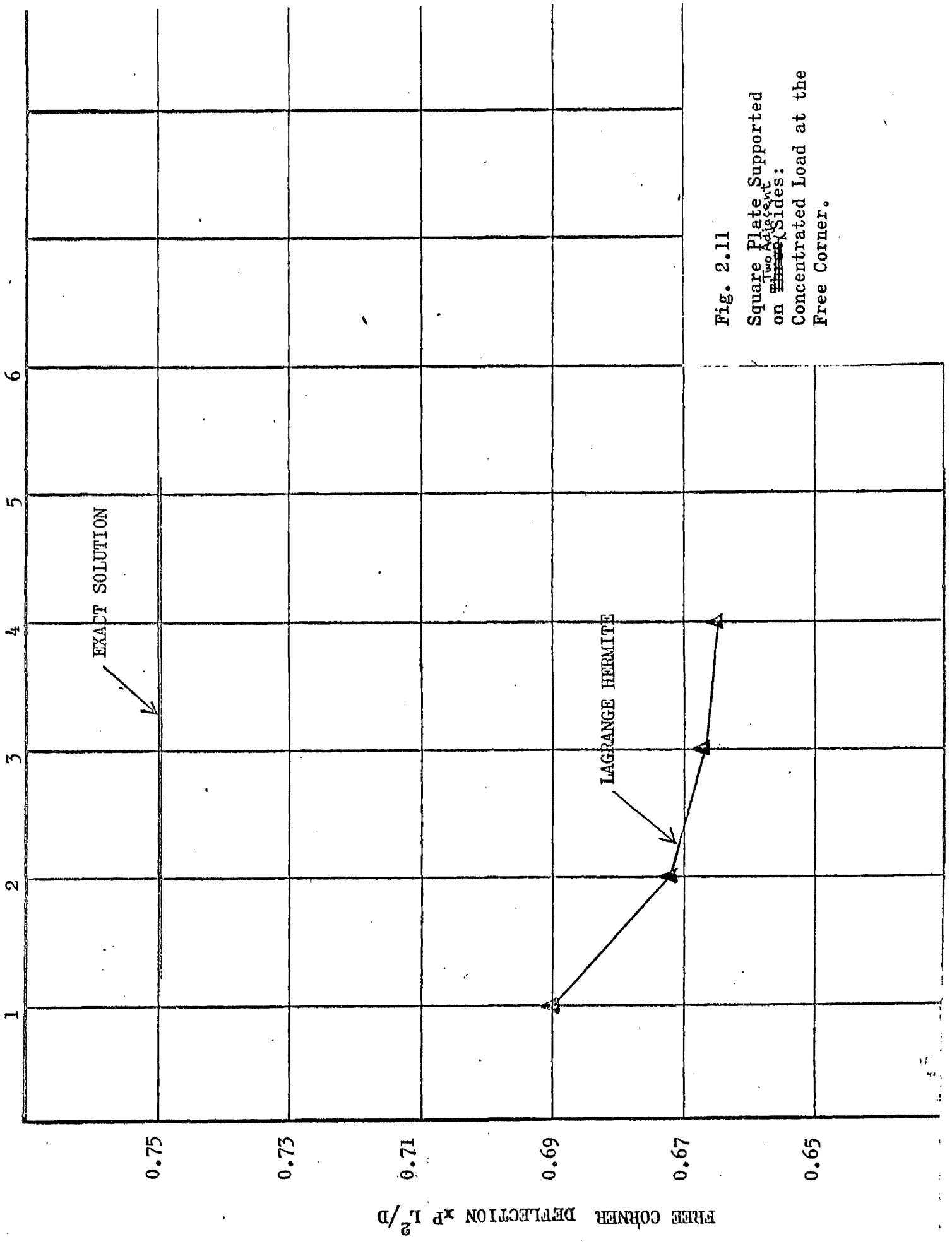


Fig. 2.11
 Square Plate Supported
 on ~~Three~~ Two Adjacent
 Sides:
 Concentrated Load at the
 Free Corner.

- (a) A uniformly distributed loading covering the whole plate.
- (b) In cases (i) (ii) and (iii) a concentrated load at the centre of the plate and in case (iv) a concentrated load at one free corner of the cantilever. For structures (i), (ii) and (iii) the displacement of the centre of the plate has been tabulated, while in structure (iv) the displacement of a free corner has been tabulated (in case (iv)(b) the loaded corner). These tables are shown graphically in Figs.2.3-2.10, although to avoid crowding the diagrams, the results for the Seventh Order method have not been plotted. However the results for the finite difference method described in Chapter 4 have been shown on these figures for convenience.

From an examination of the results the following points should be made:

I. For plate subdivisions of four elements per side and finer all of the six methods, with the exception of the Lagrange Hermite method, give results for displacements which are of acceptable accuracy for many engineering purposes. Fig.2.10 shows the Lagrange Hermite method providing a poor answer even with a fine mesh subdivision, and another example, originally given by Butlin and Leckie (64) of the free corner deflection of a plate simply supported along three sides and loaded at the free corner shows the solution by the Lagrange Hermite method diverging from the true one (Fig.2.11). Therefore the use of the Lagrange Hermite method should be discontinued. However, the lack of monotonic convergence for pure compatible methods reported by Butlin and Leckie has not been confirmed; e.g. compare their Fig.5 with Fig.2.8.

II. The pure compatible methods - Lagrange Hermite, modified Lagrange Hermite, Fifth Order and Seventh Order have been shown to provide lower bound solutions for all of the cases examined i.e. the displacement curves in Figs.2.7-2.10 converge to the true answer from below as the element mesh is refined. In contrast if complete compatibility is not maintained, for example in the Fitted Lagrange method, the displacement under a single load is sometimes overestimated,

Figs.2.7,2.8,and sometimes underestimated Figs.2.9,2.10. In only one of the cases considered, Fig.2.3, does a pure compatible method overestimate any displacement, when the modified Lagrange Hermite method slightly overestimates the central deflection of a simply supported square plate carrying a uniformly distributed load.

When the fifth and seventh order functions are used, difficulties arise in prescribing the correct boundary conditions at free edges. Along a free edge OY for example, $\frac{\partial^2 w}{\partial x^2} + \nu \frac{\partial^2 w}{\partial y^2}$ should be set equal to zero, but one can only control $\frac{\partial^2 w}{\partial x^2}$ and $\frac{\partial^2 w}{\partial y^2}$ independently. In the examples of Tables 2.3-2.10, $\frac{\partial^2 w}{\partial x^2}$ and $\frac{\partial^2 w}{\partial y^2}$ have been left to take up their own values at free edges. The moment normal to a free edge tends to zero quite rapidly as the mesh is refined. As a typical example consider structure (iii) with loading (b). The moment normal to an edge at the mid-point of that edge, for a load P, takes the values

<u>Mesh</u>	<u>Normal Moment</u>	<u>Central Moment</u>
2 x 2	0.0154P	0.34324P
4 x 4	0.00467P	0.41781P
6 x 6	0.00287P	0.46058P
8 x 8	0.00194P	0.49060P

The central bending moment has also been tabulated for comparison. To this extent the Fifth Order results of Tables 2.5,2.6,2.9,2.10 are approximate.

To allow further comparison between the pure compatible approaches, a series of values of stress resultants are tabulated in Tables 2.11-2.14. Structures (i) and (ii) are considered, subjected to loadings (a) and (b). The results show that the modified Lagrange Hermite method gives stress resultants of comparable accuracy to the Fifth Order method for uniform loadings, but of inferior accuracy for concentrated loadings. The effect of using only six generalised displacements per node in the Fifth Order method rather than the complete nine is demonstrated in Table 2.11 for example, in that the moments do not converge to the exact values as the element mesh is refined. The discrepancies are however quite small.

ACTION		CENTRAL MOMENT			MID EDGE MOMENT		
METHOD		Mod L.H.	5th Ord.	7th Ord.	Mod L.H.	5th Ord.	7th Ord.
MESH	2 x 2	0.041333	0.021375	0.036128	0.031795	0.054233	0.061210
	4 x 4	0.025102	0.021957	0.022668	0.043469	0.052771	0.045506
	6 x 6	0.023736	0.022467	0.022714	0.047312	0.051847	0.047589
	8 x 8	0.023344	0.022646	-	0.048914	0.051590	-
	10 x 10	0.023178	0.022737	-	0.049723	0.051482	-
	12 x 12	0.023091	-	-	0.050186	-	-
	14 x 14	0.023041	-	-	0.050475	-	-

Exact solutions (6) 0.0231 0.0513

Table 2.11.

Clamped Square Plate:
 Uniformly Distributed Load q : Actions:
 Multiplier qL^2 .

ACTION		CENTRAL MOMENT		
METHOD		Mod L.H.	5th Ord.	7th Ord.
MESH	2 x 2	0.057203	0.045663	0.045393
	4 x 4	0.049217	0.047036	0.047238
	6 x 6	0.048402	0.047480	0.047590
	8 x 8	0.048162	0.047652	-
	10 x 10	0.048058	0.047735	-
	12 x 12	0.048004	-	-

Exact solution (6) 0.0479

Table 2.12.

Simply Supported Square Plate:
 Uniformly Distributed Load q :
 Actions:
 Multiplier qL^2 .

ACTION	CENTRAL MOMENT			MID EDGE MOMENT		
	METHOD	Mod L.H.	5th Ord.	7th Ord.	Mod L.H.	5th Ord.
MESH 2 x 2	0.16533	0.21096	0.17170	0.12718	0.12020	0.10575
4 x 4	0.22063	0.28383	0.23961	0.11502	0.12626	0.11458
6 x 6	0.26265	0.32543	0.28140	0.11868	0.12613	0.11834
8 x 8	0.29262	0.35511	-	0.12109	0.12591	-
10 x 10	0.31583	0.37817	-	0.12250	0.12584	-
12 x 12	0.33477	-	-	0.12336	-	-
14 x 14	0.35077	-	-	0.12393	-	-

Exact solution (6)

0.1257

Table 2.13.

Clamped Square Plate:
 Concentrated Central Load P:
 Actions:
 Multiplier P.

ACTION	CENTRAL MOMENT		
	METHOD	Mod L.H.	5th Ord.
MESH 2 x 2	0.19814	0.26811	0.22031
4 x 4	0.27261	0.33760	0.29263
6 x 6	0.31584	0.37922	0.33528
8 x 8	0.34609	0.40889	-
10 x 10	0.36941	0.43193	-
12 x 12	0.38840	-	-

Table 2.14.

Simply Supported Square Plate:
 Concentrated Central Load P:
 Actions:
 Multiplier P.

This feature is even more marked in the Seventh Order method where only ten of a possible sixteen generalised displacements per node have been used. Table 2.11 also demonstrates an interesting feature in that the central displacement and central bending moment are underestimated by the Fifth Order method while the edge bending moment is overestimated. Exactly the reverse trend is exhibited by the modified Lagrange Hermite method. The direction of convergence of any one action in a plate is therefore no guide to the behaviour of any other action. In the case of plates subjected to a single concentrated load however, the pure compatible approaches invariably underestimated all the displacements and stress resultants.

Due to the inclusion of only ten out of sixteen possible generalised displacements per node in the Author's Seventh Order method, the stress resultants obtained by this method are of inferior accuracy to those obtained by the Author's Fifth Order method. However the inclusion of the third order derivatives as degrees of freedom enables shear forces to be calculated directly from the Seventh Order solutions. These forces cannot be obtained by any of the lower order methods (unless by differencing the lower order derivatives). Table 2.15 shows that the shear forces computed by the Seventh Order method are very accurate but unless these accurate values of shear force are desired, the Seventh Order method cannot be recommended over the Fifth Order and modified Lagrange Hermite methods. In fact in the Author's opinion the latter method is the optimum method for analysis of thin plates which can be subdivided into rectangular elements. It should be noted that $\partial^2 w / \partial x \partial y$ should not be constrained to be continuous between elements of different thickness, or in any other case where it is not physically continuous. Fuller justification for the development of the higher order polynomials comes in the next section, where, due to the necessity of carrying up to fourth order derivatives in the calculations, the cubic functions of the modified Lagrange Hermite method are inadequate.

As confirmation of the accuracy of Tables 2.3-2.10 the results given by Hamsteen (63) will be found to be identical with the results of Tables 2.4 and 2.8, while the results given by Bogner, Fox and Schmit (62) agree exactly with Table 2.3. The accuracy of displacements reported by the same authors for their complete fifth order method, i.e. nine generalised displacements per node, is very good as shown by Table 2.16. They give no information about stress resultants.

Comparison between pure compatible methods and mixed methods can be made by considering Table 2.17 computed from Severn and Taylor's results (59) and Table 2.18 computed from Pian's results (70). These two sets of results should be compared with Tables 2.3 and with Tables 2.7 and 2.8 respectively. The displacements computed from the mixed methods are of comparable accuracy to those computed by the pure methods, but the stress resultants are of inferior accuracy. Table 2.18 demonstrates the lack of monotonic convergence prevalent in mixed methods.

Argyris (66) gives one result for his method of "natural stiffnesses" for rectangular elements. With a 20 x 20 mesh he computes the central deflection of a square, simply supported plate carrying a uniformly distributed load as $0.004052 qL^4/D$ and the central bending moment as $0.04754 qL^2$. These figures are of comparable accuracy to those obtained with a 6 x 6 mesh in the Fifth Order method or with an 8 x 8 mesh in the modified Lagrange Hermite method. (Tables 2.4, 2.12). Since Argyris's method also involved the insertion of special narrow elements at the supports of the plate the results obtained would seem to be considerably poorer than the results obtained by the Author's methods. In addition Duncan (61) has obtained results for skew plates, using the Author's displacement functions, which are more accurate than those quoted by Argyris (66).

The validity of the claim by Bazeley et al (67) that the results obtained by using triangular elements are of "comparable accuracy" to those obtained by using rectangular elements (67) can be examined by comparing Tables 2.19 and 2.20 with Tables 2.8 and 2.7 respectively.

MESH	SHEAR
2 x 2	0.035811
4 x 4	0.033732
6 x 6	0.033796

Exact value (6) 0.0338.

Table 2.15. Maximum Shear in Simply Supported Square Plate:
Uniformly Distributed Load q :
Multiplier qL :
Seventh Order Method.

MESH	DEFLECTION
2 x 2	1265.3
8 x 8	1265.3

Exact value (6) 1265

Table 2.16. Central Deflection of Clamped Square Plate:
Uniformly Distributed Load q :
Multiplier $qL^4/10^6D$.
After Bogner, Fox and Schmit (62).

MESH	CENTRAL DEFLECTION	CENTRAL MOMENT	MID EDGE MOMENT
2 x 2	1330	0.0440	0.0461
4 x 4	1240	0.0473	0.0256
6 x 6	1250	0.0491	0.0244
8 x 8	1260	0.0500	0.0237

Table 2.17. Deflection and Actions for a Clamped Square Plate:
Uniformly Distributed Load q :
Multipliers $qL^4/10^6D$ and qL^2 .
After Severn and Taylor (59).

STRUCTURE	SIMPLY SUPPORTED PLATE				CLAMPED PLATE			
	STIFFNESS MATRICES COMPATIBLE WITH BOUNDARY STRESS CONDITIONS				RESTRAINED EDGES			
	up to β_9	up to β_{15}	up to β_{23}	up to β_{23}	up to β_9	up to β_{15}	up to β_{23}	up to β_{23}
2 x 2	0.02188	0.01279	0.01124	0.01022	0.008446	0.005608	0.005410	0.005410
4 x 4	0.01191	0.01142	0.01133	0.01125	0.005806	0.005375	0.005276	0.005276
8 x 8	0.01169	0.01156	0.01153	0.01151	0.005689	0.005556	0.005514	0.005514
12 x 12	0.01164	0.01157	0.01159	0.01159	0.005650	0.005587	0.005572	0.005572
16 x 16	-	-	-	-	0.005633	0.005593	0.005601	0.005601

Table 2.18.

Square Plates:
 Concentrated Central Load:
 Central Deflections:
 Multiplier PL^2/D .
 After Pian (70).

MESH	INCOMPATIBLE SOLUTION	COMPATIBLE SOLUTIONS		
2 x 2	1302	855	854	798
4 x 4	1176	1057	1056	1039
6 x 6	1211	1117	1116	1108
8 x 8	1165	-	-	-

Table 2.19. Simply Supported Square Plate:
 Concentrated Central Load:
 Central Deflection:
 Multiplier $PL^2/10^5D$.
 After Bazeley, Cheung, Irons and Zienkiewicz (67).

MESH	INCOMPATIBLE SOLUTION	COMPATIBLE SOLUTIONS		
2 x 2	521	193	186	169
4 x 4	589	474	472	461
6 x 6	583	511	510	503
8 x 8	572	-	-	-

Table 2.20. Clamped Square Plate:
 Concentrated Central Load:
 Central Deflection:
 Multiplier $PL^2/10^5D$.
 After Bazeley et. al. (67).

Completely unbiased comparisons are hard to draw among all of the finite element methods available for the analysis of thin plates in bending. However in the first place the superiority of rectangular elements over triangular elements seems now to be well established, for the solution of problems where rectangular elements fit the plate geometry. In the second place, among rectangular finite element methods, one has a choice among pure approaches (e.g. modified Lagrange Hermite, Fifth Order and Seventh Order), mixed approaches (e.g. Pian (70) or Severn and Taylor (59)) and incompatible displacement approaches (e.g. Melosh 1961, Fitted Lagrange or Argyris (66)). The only advantage of the mixed and incompatible displacement methods is that only three degrees of freedom per node are specified, so that the demands on computer storage are less, although in the future this is liable to become a less and less important point. But a basic dilemma in finite element analysis is whether to use many "crude" elements or fewer "sophisticated" elements for the solution of a given problem. For thin plates, the Author's inclination would be to use a fairly sophisticated pure method, for example the modified Lagrange Hermite method, where at least monotonic convergence of results as the mesh is refined can be guaranteed. Pian's method could be used to optimise the results without increasing the number of degrees of freedom. The simple plate examples chosen here for the element evaluation may not have brought out the full advantages of pure methods. Duncan's experience for skew plates (61) is that the discrepancies between pure and incompatible methods become much more marked.

2.9 Analysis of "Moderately Thick Plates" by Means of Rectangular Finite Elements

Mention has already been made of the assumptions involved in treating real foundation materials as being, for example, perfectly elastic media. An assumption more often glossed over is that involved in treating a thick, heavily reinforced concrete raft as a Kirchhoff plate. Being concerned with the effects of this approximation in the analysis of foundation rafts, the Author first

considered the possibility of applying Reissner's theory, including the effect of transverse shear deformations in the bending of elastic plates (73). The use of the complete theory allied with the finite element approach seemed to pose large problems, principally because it is impossible to write the stress resultants as distinct functions of the derivatives of the transverse displacement. However the theory of "moderately thick plates" proposed by Love (74) yielded stress resultants in an acceptable form and was used in this study. The seventh order displacement functions were used, since up to the fourth derivatives of displacement were involved; displacement functions of order less than 5 would be unacceptable. The extension of the finite element method to higher order problems such as this is a justification for the development of the higher order polynomials which may be too sophisticated for thin plate work.

The stress resultants are taken in the form:

$$M_x = -D \left(\frac{\partial^2 w}{\partial x^2} + \nu \frac{\partial^2 w}{\partial y^2} \right) + \frac{h^2}{5} D \frac{\partial^2 \nabla^2 w}{\partial y^2} - \frac{2-\nu}{1-\nu} \frac{h^2}{10} q$$

$$M_y = -D \left(\frac{\partial^2 w}{\partial y^2} + \nu \frac{\partial^2 w}{\partial x^2} \right) + \frac{h^2}{5} D \frac{\partial^2 \nabla^2 w}{\partial x^2} - \frac{2-\nu}{1-\nu} \frac{h^2}{10} q$$

$$M_{xy} = -(1-\nu) D \frac{\partial^2 w}{\partial x \partial y} - \frac{h^2}{5} D \frac{\partial^2 \nabla^2 w}{\partial x \partial y}$$

$$V_x = -D \left(\frac{\partial^3 w}{\partial x^3} + \frac{\partial^3 w}{\partial x \partial y^2} \right)$$

$$V_y = -D \left(\frac{\partial^3 w}{\partial y^3} + \frac{\partial^3 w}{\partial x^2 \partial y} \right)$$

and the substitution $q = D \nabla^4 w$ is made. The first three equations above are found by substituting the ~~second~~ ^{last} two in equations [II], [III], [IV], reference (73).

The equations can then be written using the notation of the discussion of thin plates as

$$\{ M \} = [A] \{ B \} \{ w \}$$

where the new meanings of the symbols are given in Table 2.21. The assumed stress resultants again lead to a strain energy expression

$$dU = \frac{1}{2} [S] \{M\}$$

$$\{S\} = [Q^T] \{B\} \{w\}$$

where $[Q]$ is defined in Table 2.22. The matrix formulation is thus identical to the thin plate case:

$$dU = \frac{1}{2} [v] \{D\} [B] [Q] [A] \{B\} [D] \{v\}$$

$$\text{and } [K] = \int_A \{D\} [B] [Q] [A] \{B\} [D] dA,$$

but in this case the kernel $[Q][A]$ is of order 12 instead of order 3. The amount of computing involved in the development of the 40 x 40 stiffness matrix for a moderately thick plate is heavy, the generation of a dimensionless 1 x 144 vector from which any element stiffness matrix could quickly be computed taking about 100 minutes on a KDF9 computer. The relevant (ALGOL) computer program is given in Appendix 4.

Some results for moderately thick plates are shown in Table 2.23. No theoretical results are available to enable direct comparisons to be made but the problem of the simply supported square plate carrying a uniformly distributed load has been solved by Salerno and Goldberg (75) using the complete Reissner theory. For a thickness/length ratio of 0.1, Salerno and Goldberg found an increase in central deflection over the thin plate value of about 4%. The moderately thick plate theory using finite elements and the Seventh Order displacement assumptions gives about 3%. For other problems, the increases are larger. It can be concluded that this computer aided method provides reasonable estimates of the effect of transverse shear deformations on the bending of elastic plates and the capability of solving a far larger range of problems than has previously been possible. It is perhaps worth pointing out the relative ease with which the finite element method can cope with this more complex theory within an already established framework of matrix manipulations. It would appear to the Author that this is one example where the use of finite elements is considerably superior to the use of finite differences.

$$\begin{aligned}
 [M] &= \begin{bmatrix} M_x & M_y & M_{xy} & V_x & V_y \end{bmatrix} \\
 [B] &= \begin{bmatrix} \frac{\partial^2}{\partial x^2} & \frac{\partial^2}{\partial y^2} & \frac{\partial^2}{\partial x \partial y} & \frac{\partial^3}{\partial x^3} & \frac{\partial^3}{\partial y^3} & \frac{\partial^3}{\partial x^2 \partial y} & \frac{\partial^3}{\partial x \partial y^2} & \frac{\partial^4}{\partial x^4} & \frac{\partial^4}{\partial y^4} & \frac{\partial^4}{\partial x^2 \partial y^2} & \frac{\partial^4}{\partial x^3 \partial y} & \frac{\partial^4}{\partial x \partial y^3} & \frac{\partial^4}{\partial x \partial y \partial y^2} \end{bmatrix}
 \end{aligned}$$

$$[A] = \begin{bmatrix}
 -D & -\nu D & 0 & 0 & 0 & 0 & 0 & 0 & 0 & 0 & 0 & 0 & 0 & 0 \\
 -\nu D & -D & 0 & 0 & 0 & 0 & 0 & 0 & 0 & 0 & 0 & 0 & 0 & 0 \\
 0 & 0 & -(1-\nu)D & 0 & 0 & 0 & 0 & 0 & 0 & 0 & 0 & 0 & 0 & 0 \\
 0 & 0 & 0 & -D & 0 & 0 & 0 & 0 & 0 & 0 & 0 & 0 & 0 & 0 \\
 0 & 0 & 0 & 0 & -D & 0 & 0 & 0 & 0 & 0 & 0 & 0 & 0 & 0 \\
 0 & 0 & 0 & 0 & 0 & -D & 0 & 0 & 0 & 0 & 0 & 0 & 0 & 0 \\
 0 & 0 & 0 & 0 & 0 & 0 & -D & 0 & 0 & 0 & 0 & 0 & 0 & 0 \\
 0 & 0 & 0 & 0 & 0 & 0 & 0 & -D & 0 & 0 & 0 & 0 & 0 & 0 \\
 0 & 0 & 0 & 0 & 0 & 0 & 0 & 0 & -D & 0 & 0 & 0 & 0 & 0 \\
 0 & 0 & 0 & 0 & 0 & 0 & 0 & 0 & 0 & -D & 0 & 0 & 0 & 0 \\
 0 & 0 & 0 & 0 & 0 & 0 & 0 & 0 & 0 & 0 & -D & 0 & 0 & 0 \\
 0 & 0 & 0 & 0 & 0 & 0 & 0 & 0 & 0 & 0 & 0 & -D & 0 & 0 \\
 0 & 0 & 0 & 0 & 0 & 0 & 0 & 0 & 0 & 0 & 0 & 0 & -D & 0 \\
 0 & 0 & 0 & 0 & 0 & 0 & 0 & 0 & 0 & 0 & 0 & 0 & 0 & -D
 \end{bmatrix}$$

Table 2.21.

-1	0	0	0	0	0	0	0	0	0	$\frac{-2}{1-\nu^2} \frac{h^2}{10}$	0	0
0	-1	0	0	0	0	0	0	0	0	$\frac{-\nu-2}{1-\nu^2} \frac{h^2}{10}$	$\frac{-2}{1-\nu^2} \frac{h^2}{10}$	0
0	0	-2	0	0	0	0	0	0	0	0	0	$-\frac{2h^2}{5(1-\nu)}$
0	0	0	$-\frac{h^2}{5(1-\nu)}$	0	0	$-\frac{h^2}{5(1-\nu)}$	0	0	0	0	0	0
0	0	0	0	$-\frac{h^2}{5(1-\nu)}$	$-\frac{h^2}{5(1-\nu)}$	0	0	0	0	0	0	0

$$[Q]^T =$$

Table 2.22.

CASE	1	2	3	4
Thin Plate	4062.1	1156.8	5579.1	1265.0
$k/L = 0.005$	4062.5	1157.1	5582.0	1265.4
0.01	4063.6	1157.9	5590.6	1266.7
0.05	4098.7	1174.1	5759.4	1301.5
0.1	4205.1	1200.0	5974.6	1371.7

Table 2.23. Central deflection of square plates, transverse shear included.

Case 1: Simply Supported: Uniformly Distributed Load.

Case 2: Simply Supported: Concentrated Central Load.

Case 3: Clamped: Concentrated Central Load.

Case 4: Clamped: Uniformly Distributed Load.

Mesh 6 x 6 throughout.

Only one other finite element analysis incorporating the effect of transverse shear deformations is known to the Author, Herrmann (76) having used triangular elements for the solution of a circular plate problem. Herrmann also used a theory of moderately thick plates, and despite the fact that w , M_x , M_y and M_{xy} vary only linearly within each triangle, the finite element results are in excellent agreement with theory.

2.10 Finite Element Method For Axisymmetric Plates in Bending

One of the reasons for developing finite element methods for the analysis of plates in bending was in order to couple the plate with a semi-infinite elastic medium, also analysed by finite elements (Chapter 3), in which the elastic properties could be varied at will, horizontally and vertically. However it was found that for a rectangular plate bearing on a semi-infinite medium, very large sets of equations with large band widths would be involved, which would tax the capacity of the computer readily available (16K immediate access storage at that time). Although the rectangular plate problem could no doubt have been solved by subdividing the medium and analysing it in successive "blocks" or by matrix partitioning schemes, it was decided that a study of the problem of the axisymmetric plate bearing on a semi-infinite medium would fulfil the aims of the research just as well. Due to the radial symmetry this problem is virtually two-dimensional. The Author was not aware of a published finite element method for axisymmetric plates in bending (although it was later found that such a plate can be treated as a special case in Grafton and Strome's method (77) for axisymmetric shells.) However, by taking the elements in the form of annular rings of uniform thickness, and using a method analogous to the "slope deflection" method for beams it proved very simple to set up an explicit stiffness matrix. The details are given in Appendix 3. The same stiffness matrix can be obtained by the pure finite element approach of Section 2.6.

The results obtained by the finite element method were checked against some known analytical solutions (6).

(a) Annular plate, with outside radius/inside radius = 5, simply supported at the outer edge and carrying a uniformly distributed load

	<u>Finite Elements</u>	<u>Analytical</u>
Deflection at inner edge	0.813 qa^4/Eh^3	0.813 qa^4/Eh^3

(b) Annular plate, with outside radius/inside radius = 5, simply supported at the outer edge and carrying a uniform line load along the inner edge

	<u>Finite Elements</u>	<u>Analytical</u>
Deflection at inner edge	0.704 Pa^2/Eh^3	0.704 Pa^2/Eh^3

(c) Circular plate simply supported at the outer edge, carrying a uniformly distributed load

	<u>Finite Element</u> (5 elements)	<u>Analytical</u>
Central deflection	0.684 qa^4/Eh^3	0.696 qa^4/Eh^3

(d) Circular plate clamped at the outer edge, carrying a central point load

	<u>Finite Element</u> (10 elements)	<u>Analytical</u>
Central deflection	0.0197 Pa^2/D	0.0199 Pa^2/D

In cases (a) and (b) the finite element solutions agree exactly with the analytical solutions, as they should as no approximations have been made for the moments and forces distributed along the edges of the elements (in the same way as the finite element method gives the exact answer for the analysis of a line structure). In cases (c) and (d) a slight error is incurred because at the centre of a solid plate the $\log_e a/b$ term becomes infinite. This is overcome by leaving a small hole in the innermost element. The effect on the results is seen to be negligible.

The coupling of a circular plate to a Winkler-type foundation is a simple process by finite element procedures. All that is involved is the addition of the foundation stiffness to the stiffness of the annular plate elements, where the contribution to the strain energy of the foundation can be written:

$$U_F = \int_b^a \int_0^{2\pi} \frac{1}{2} k(r) [w] \{w\} r \, dr \, d\theta$$

As usual the displacement assumption is

$$\{w\} = [D] \{v\}$$

and when $\delta \pi / \delta v$ is formed, there is an additional contribution to an element stiffness matrix of

$$\int_b^a \int_0^{2\pi} k(r) \{D\} [D] \cdot r \cdot dr \cdot d\theta$$

A computer program was written permitting a linear variation $k(r) = k_b + \frac{(k_a - k_b)(r-b)}{a-b}$ across any element and using a cubic displacement form (Hermitian cubics). For the special case $k_a = k_b = k$ (constant), the results from the program could be checked against reference (6) p264 as shown below

Radius (inches)	Deflection (in x 10 ⁻³)	
	Finite Elements	Reference (6)
0	43.2	43.0
1	42.9	-
2	42.0	-
3	41.1	-
4	40.2	-
5	39.4	39.1

The agreement is seen to be satisfactory.

2.11 Computation

Many ALGOL computer programs were written to perform the numerical work described in this thesis. These programs were of two basic types, firstly the generation and solution of typical symmetrical banded structural analysis equations, and secondly the generation of element stiffness matrices for complex displacement function assumptions. For the first type of program the Author is indebted to Macleod (78) for a procedure capable of solving symmetrical, banded equations by the Choleski square root method, and for the second type to Duncan (61) whose program written originally for skew plate problems was adapted by the Author. Details of these two types of program are given in Appendix 4.

CHAPTER 3.

ELASTIC SOLID FOUNDATIONS ANALYSED BY FINITE ELEMENT METHODS.

3.1 Introduction.

As the work on the finite element method for the analysis of plates in bending progressed it became apparent that the same method might also provide a means of analysing a solid foundation whose properties were variable throughout the mass, thereby going at least part of the way towards a truer representation of actual foundation materials. Linear elastic behaviour was assumed for the solid, nonlinear elasticity presenting only computational problems beyond that assumption. The elastic solid finite elements could only be evaluated in the solution of problems involving homogeneous solids since these are the only problems for which analytical solutions exist.

3.2 Previous Work.

Some preliminary studies by Melosh (79) were available, dealing with tetrahedral and rectangular right prismatic elements. Later work by Argyris (80), (81) examined the tetrahedral element more fully, the former reference dealing with the assumption of constant strain in the element, the latter with the assumption of linearly varying strain. However, as has already been mentioned in conjunction with the development of the circular plate analysis, it was decided that the study of the full three-dimensional problem of a rectangular plate bearing on an elastic solid foundation would place very heavy demands on the capacity of the computing equipment available. It was therefore decided to deal with the axisymmetric problem first.

A study of axisymmetric elastic solid problems by the finite element method, due to Clough and Rashid (82) was available and the stiffness properties of a solid ring element of triangular cross-section, shown in Fig. 3.1, were derived following the assumptions of that reference; that is, two degrees of freedom per node, and linear edge displacements (implying constant strain within an individual element).

Argyris (83) has also more recently described two elements suitable for the analysis of axisymmetric elastic solids.

Referring to Fig. 3.1 the stiffness matrix relating the nodal forces $P_A F_A P_B F_B P_C F_C$ to the nodal displacements $\Delta_A \delta_A \Delta_B \delta_B \Delta_C \delta_C$ is rather complex and will not be given explicitly here. It is in fact formed automatically, from basic input, by the computer.

3.3 Evaluation of the Element.

The correctness of the derived stiffness matrix was checked by applying it to two problems (the same problems as were chosen by Clough and Rashid). The first problem was a thick-walled pressure vessel, idealised as shown in Fig. 3.2, subjected to external pressure. The results for radial displacements are shown in Table 3.1. As might be expected for a compatible finite element method the displacements are underestimated - by about 5% in all cases.

Secondly, Boussinesq's problem of a concentrated load applied to a semi-infinite homogeneous elastic medium was analysed. Several ways of subdividing the medium were attempted, as shown in Figs. 3.3, 3.4 but the subdivision shown in Fig. 3.3 was eventually adopted. This led to the surface displacements shown in Fig. 3.5, together with the corresponding Boussinesq predictions. It can be seen that the absolute displacements differ from the true ones by about 10%, but that the relative displacement pattern is accurate. The 10% discrepancy (which as far as one can tell agrees with the result shown in Clough and Rashid's Fig. 11) may be due in part to the limited number of elements used but is also probably due to the assumed boundary conditions of roller supports at the edges of the finite zone, and to the necessity of introducing a small hole at the centre of the medium just as was done for the circular plate. Since the main point of interest in this research was the variation in foundation stiffness throughout a foundation, rather than the absolute value of that stiffness, the results were considered satisfactory for the analysis of the tests on sand foundations described in Chapter 5.

3.4 Circular Plate Bearing on a Semi-Infinite Elastic Medium.

Finally a problem of a circular plate coupled to a

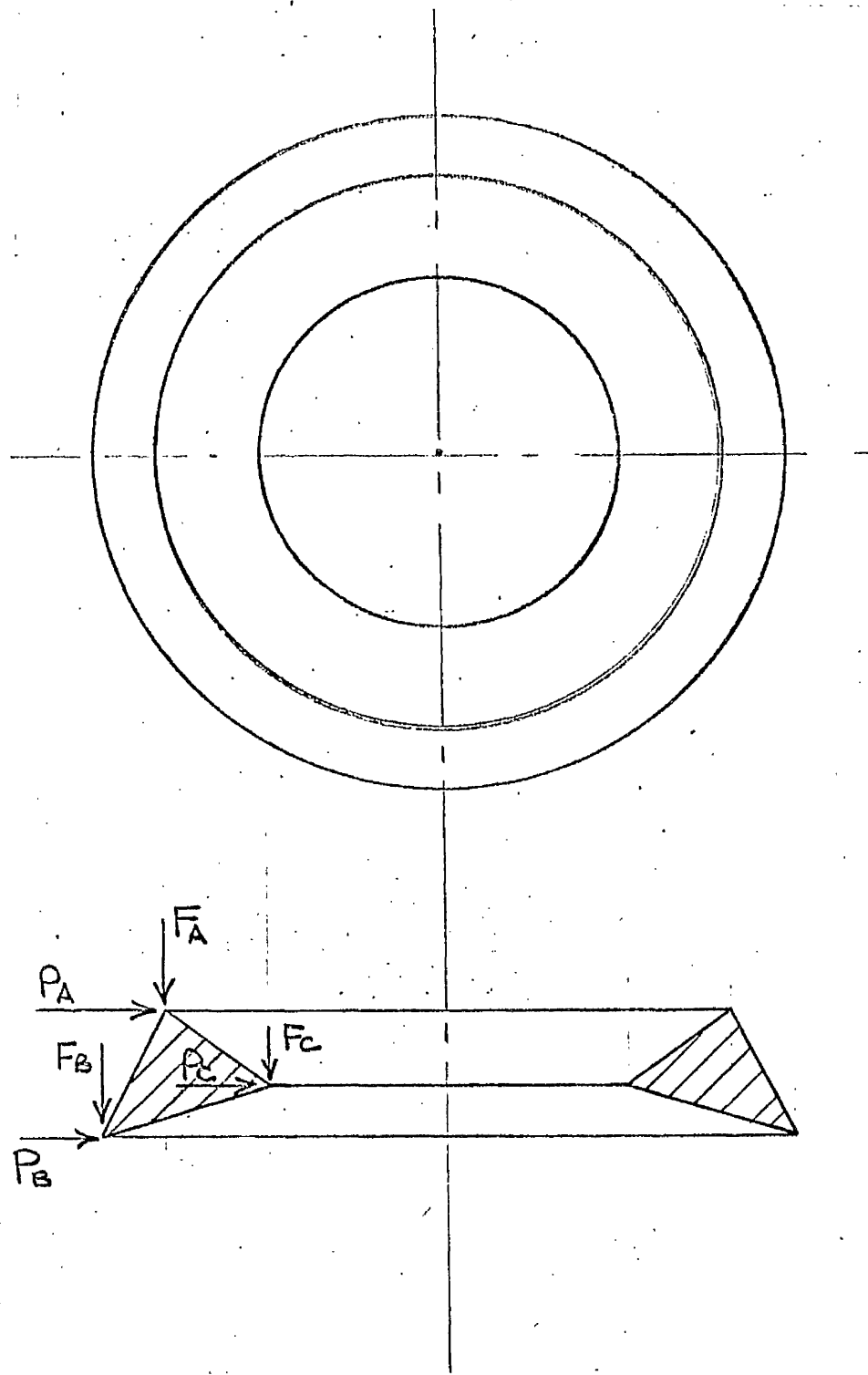


Fig. 3.1 Axisymmetric Solid Element

$E = 900 \text{ lb/in}^2 \quad \nu = 0.49$

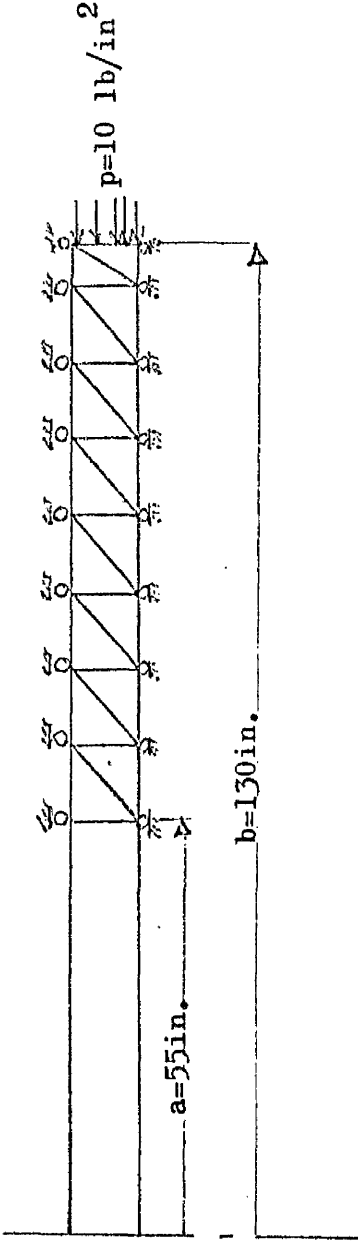


Fig. 3.2 Idealisation of Thick-Walled Cylinder

Radius (in)	55	65	75	85	95	105	115	125	130
Radial Disp. (in)	1.070	0.915	0.800	0.713	0.646	0.593	0.548	0.512	0.497
Theoretical Value	1.131	0.964	0.843	0.752	0.680	0.623	0.576	0.538	0.522

$$\text{Theoretical Radial Displacement} = \frac{b^2 p}{E(b^2 - a^2)} \left[\frac{(1+\nu)a^2}{r} - (1-2\nu) \right]$$

Table 3.1 Comparison of Finite Element and Exact Radial Displacements of a Thick-Walled Cylinder

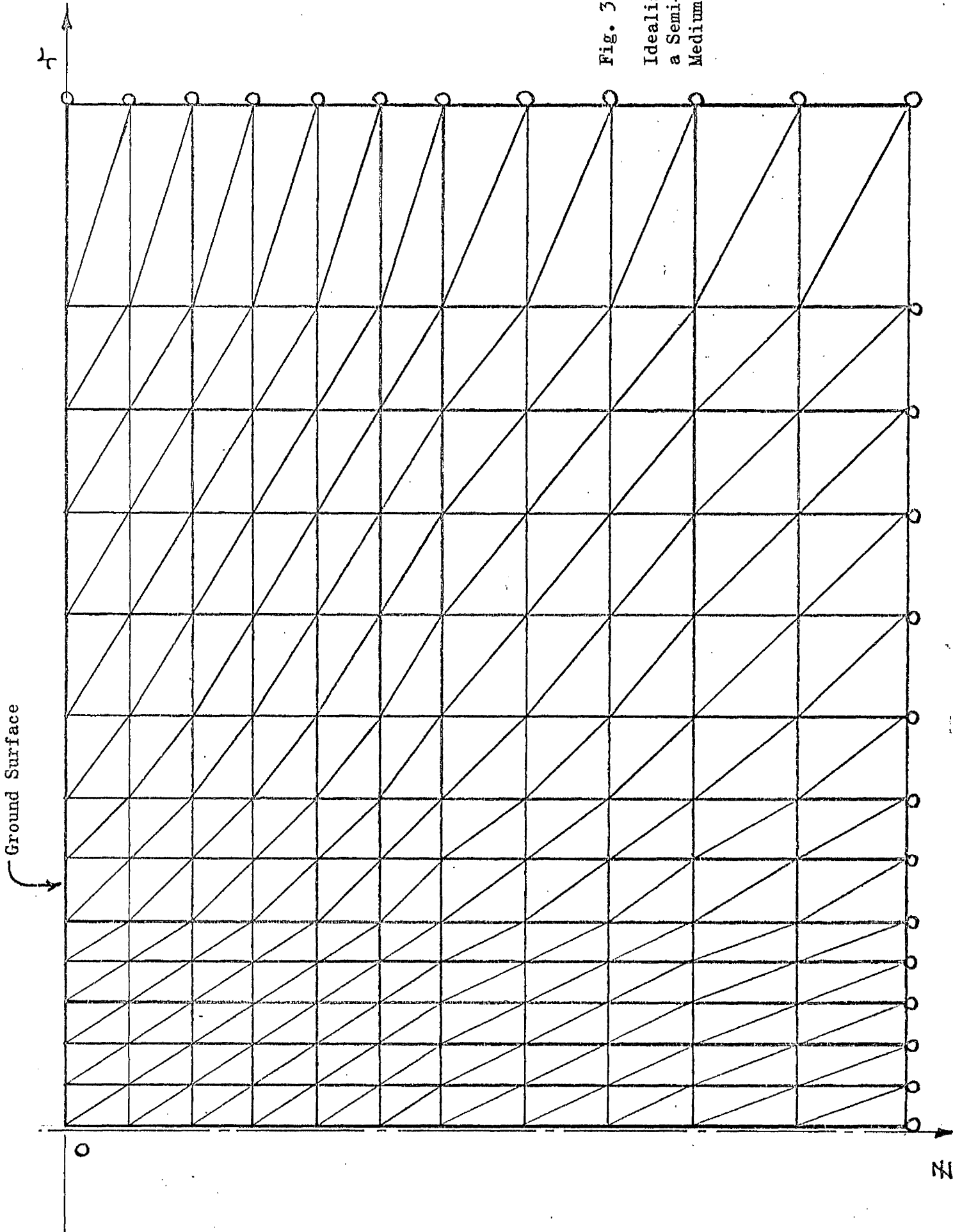


Fig. 3.3

Idealisation of
a Semi-Infinite
Medium

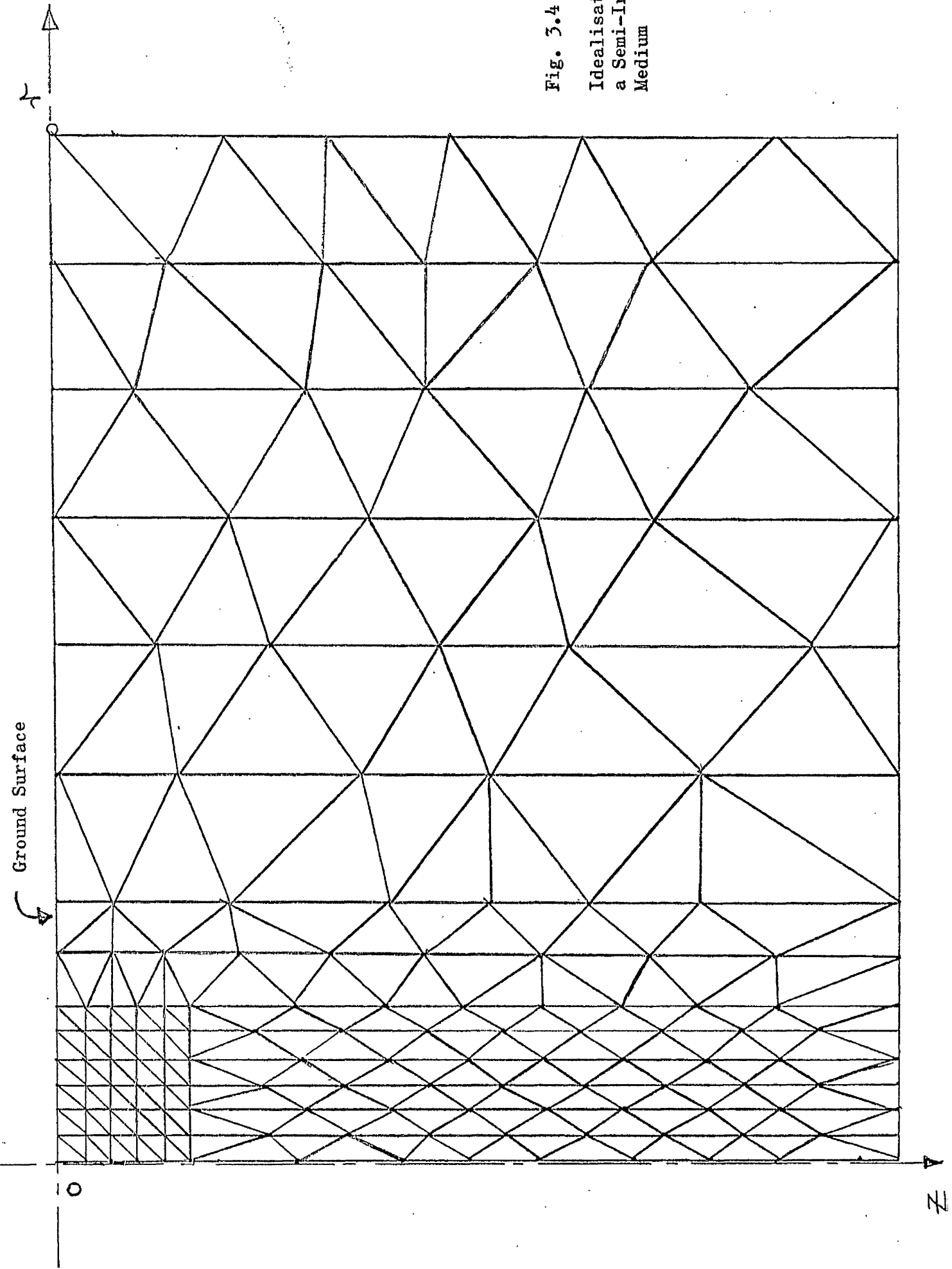


Fig. 3.4
Idealisation of
a Semi-Infinite
Medium

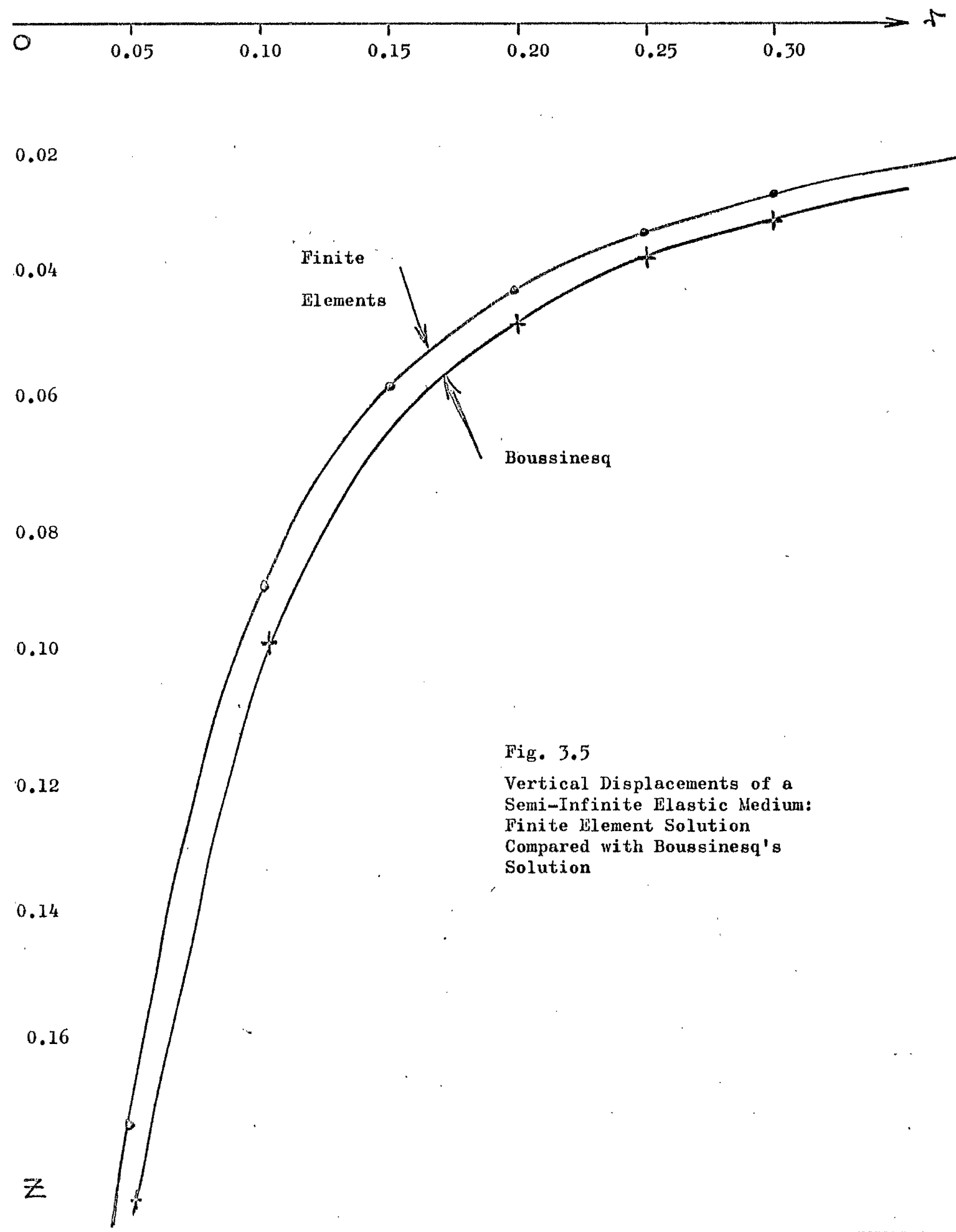


Fig. 3.5

Vertical Displacements of a
Semi-Infinite Elastic Medium:
Finite Element Solution
Compared with Boussinesq's
Solution

semi-infinite elastic medium was analysed. The example is given by Pickett and McCormick (20). The following data were used for the finite element solution :-

Subgrade : $E = 30$, $\nu = 0.3$

Plate : $E = 1$, $t = 1$, $\nu = 0.3$

Loading : $P = 100$ (concentrated central load).

This leads to a value of a/ℓ (Pickett and McCormick's notation) of 1.98 implying a theoretical displacement under the load of $0.198 \frac{P\ell^2}{D}$. The finite element value is $0.178 \frac{P\ell^2}{D}$, 11% lower than the theoretical value, a discrepancy again attributable to the factors quoted above.

The method of solving the coupled plate on elastic medium problem was first to develop a flexibility matrix for the foundation, invert this matrix, and add the resultant foundation stiffness matrix terms to the appropriate terms of the plate stiffness matrix. Since no rotational degrees of freedom were incorporated in the solid analysis, the stiffness of the foundation against a radially symmetric line moment could not be added to the rotational stiffness of the plate elements, and complete compatibility was not guaranteed between plate and foundation. It may be mentioned that this method of first finding the flexibility matrix for part of a structure or medium could be used to obtain a much finer mesh subdivision for the foundation. This could be divided into sections cut by horizontal planes and, working from the bottom of the medium, the flexibility of each section could be found in turn, and the stiffness of that section added to the next section, so that one would only carry forward a matrix of the order of the number of degrees of freedom on the cut plane.

3.5 Conclusions.

The conclusions drawn from this section of the work were that the method described for the analysis of axisymmetric plates bearing on elastic solid media with variable properties could be expected to give an adequate representation of the distribution of stiffness in the foundation, but that the absolute values of that stiffness would be overestimated by about 10%.

CHAPTER 4.

FINITE DIFFERENCE METHOD FOR THE SOLUTION OF PLATE FLEXURE PROBLEMS.

4.1 Introduction

Although the theoretical work in this thesis has been primarily concerned with the finite element method, the Author does not consider that that method is necessarily superior to the older established finite difference method for the solution of all problems. In fact, in the Author's opinion, too little effort has been concentrated on the use of the latter method with specific reference to digital computers. The finite element method has naturally lent itself to computer - oriented development, whereas the earlier method has suffered through older, manual calculation methods being programmed directly for computers rather than new, superficially more complex methods being sought. At the beginning of this research study the Author had an open mind regarding the use of either method and the finite difference method has been used for the solution of a few problems, some of which protagonists of the finite element method have described as "very difficult to deal with by finite differences" (55). The method of solving these problems is now presented.

4.2 Solutions by Fourth Order Finite Differences.

To obtain solutions for a thin elastic plate bearing on a Winkler foundation, one looks for solutions to the familiar differential equation.

$$D \nabla^4 w = q - kw \dots\dots\dots \text{Eq. (4.1)}$$

in terms of the values of w (and sometimes its derivatives) at a number of discrete points within the area of the plate, these points being most conveniently arranged in some form of regular mesh pattern.

For the purposes of hand calculation, usually involving Southwell's relaxation method (37) the biharmonic equation has often been split into two second order equations, as follows :-

$$\begin{aligned} D \nabla^2 w &= -M \\ \nabla^2 M &= -(q - kw) \end{aligned} \quad (11)$$

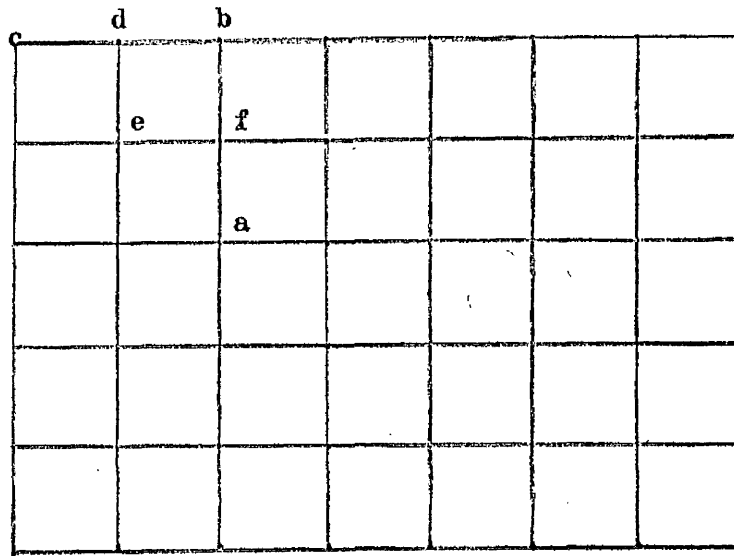


Fig. 4.1a
 Subdivision of a Rectangular Plate

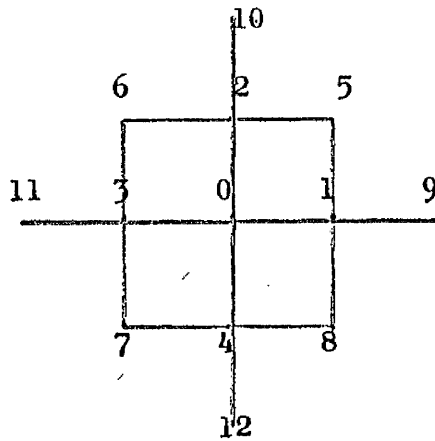


Fig. 4.1b
 Standard Mesh Numbering System

Whatever the merits of this approach for hand calculations, the Author does not consider it advisable for computer applications since it leads to twice the necessary number of unknowns and hinders the symmetrical and logical construction of the equilibrium equations, causing ill-conditioned, unsymmetric matrices which are prone to numerical difficulties when solved by standard matrix handling routines.

By far the more effective method for computer purposes is to use fourth order finite difference approximations. Consider a rectangular plate covered by a square mesh as shown in Fig. 4.1a. The conventional mesh numbering system is shown in Fig. 4.1b. With respect to this mesh numbering system, the fourth order finite difference approximation to eq. (4.1) is :

$$(20 + h^4k) w_0 - 8w_1 - 8w_2 - 8w_3 - 8w_4 + 2w_5 + 2w_6 + 2w_7 + 2w_8 + w_9 + w_{10} + w_{11} + w_{12} = h^4 q_0$$

where h is the distance between the mesh lines and q_0 is the intensity of loading at point o. This equation may be applied directly at plate nodes such as (a) where w_1 to w_{12} all lie within the area of the plate. If for the moment the discussion is restricted to rectangular plates with free edges, the required boundary conditions are that zero shear and zero moment exist along all of the plate edges. In that case, five other independent positionings of the standard mesh are possible, as follows :-

(b) At an edge, not adjacent to a corner

$$(16 - 8\nu - 6\nu^2 + h^4k) w_0 + (-12 + 4\nu) w_1 + (-8 + 4\nu + 4\nu^2) w_2 + (-8 + 4\nu + 4\nu^2) w_4 + (4 - 2\nu) w_5 + (4 - 2\nu) w_8 + 2w_9 + (1 - \nu^2) w_{10} + (1 - \nu^2) w_{12} = h^4 q_0$$

(c) At a corner

$$(12 - 8\nu - 4\nu^2 + h^4k) w_0 + (-12 + 8\nu + 4\nu^2) w_4 + (8 - 8\nu) w_8 + (2 - 2\nu^2) w_9 + (2 - 2\nu^2) w_{12} = h^4 q_0$$

(d) At an edge, adjacent to a corner

$$(15 - 8\nu - 5\nu^2 + h^4k) w_0 + (-12 + 4\nu) w_1 + (-6 + 4\nu + 2\nu^2) w_2 + (-8 + 4\nu + 4\nu^2) w_4 + (4 - 2\nu) w_5 + (4 - 2\nu) w_8 + 2w_9 + (1 - \nu^2) w_{12} = h^4 q_0$$

(e) At an interior point, adjacent to a corner

$$(18 + h^4 k)w_0 - 8w_1 + (-6 + 2\nu)w_2 + (-6 + 2\nu)w_3 - 8w_4 \\ + (2 - \nu)w_5 + (2 - \nu)w_6 + (2 - 2\nu)w_7 + 2w_8 \\ + w_9 + w_{12} = h^4 q_0$$

(f) At an interior point adjacent to an edge

$$(19 + h^4 k)w_0 - 8w_1 - 8w_2 + (-6 + 2\nu)w_3 - 8w_4 \\ + 2w_5 + (2 - \nu)w_6 + (2 - \nu)w_7 + 2w_8 \\ + w_9 + w_{10} + w_{12} = h^4 q_0$$

Then for rectangular plates having $m \times n$ node points located on a square mesh, a set of $m \times n$ simultaneous equations can be formed by applying the equations given above as appropriate. Simple instructions enable digital computers to build up the $m \times n$ equation coefficients automatically. These coefficients are in band form, and by multiplying the equations for corner points by four and the equations for edge points by two, this band becomes symmetrical and the same solution technique (Choleski method) as was used for the finite element equations can be applied.

A further important point is that only terms on the leading diagonal of the symmetric band matrix are affected by arbitrary assumptions for the value of k at any node so that for any such assumption, the matrix retains its symmetry. Rigid support conditions can then be approximated at any node by allowing that particular k to assume a value large enough to ensure that the deflection at the node is negligible. At a free, unsupported node, k merely takes the value zero.

Thus, in addition to plates on Winkler foundations, plates on point, or line supports can be analysed by the method described in this section, and rectangular plates simply supported around all four edges, or simply supported at the four corners only have been successfully analysed. A "rigid" support, for which k was assumed to be 1×10^{10} deflected only by 1×10^{-9} of the maximum deflection in a typical example.

The results of applying the finite difference method for the above problems are plotted on Figs. 2.4, 2.5, 2.8, 2.9, in conjunction

with the finite element solutions to the same problems. It should be remembered that a comparison of methods on the basis of "number of subdivisions per side" is unfair to the finite difference method which only involves one degree of freedom per node. A better comparison would be on the basis of the number of unknowns involved, or the number of computer stores taken up by the respective equation coefficients.

It is interesting to note that the finite difference method leads, with one exception, to overestimates of the deflections of the structures analysed, and may therefore be an important "dual" method to a compatible finite element method, enabling bounds on the displacements and stresses in a structure to be determined. Such bounds appear to have been determined for the problem of the square plate simply supported at the four corners and subjected to a uniformly distributed load. Lee and Ballerteros (84) obtained a theoretical central displacement for this problem of $0.0265 qL^4/D$, whereas the bounded solution obtained by approximate methods is about $0.0255 qL^4/D$. This difference is about 4% and illustrates a case where "approximate" methods can achieve greater accuracy than "analytical" methods.

The above work indicates how solutions to other problems might be obtained conveniently by finite difference methods allied with the use of a computer. Clamped plates could be analysed by considering torsion springs along the free boundaries, and then making these springs very stiff, thus preventing edge rotations.

There is no reason to suppose, therefore, that the finite difference method is necessarily inferior to the finite element method. In the Author's opinion, however, the latter is better equipped to handle higher order problems, for example the analysis of moderately thick plates described in Section 2.9. The use of finite differences in such a problem would be very cumbersome.

CHAPTER 5

EXPERIMENTAL WORK.

5.1 Introduction: Previous Work

The majority of observations of the interaction between structures and soil foundations has been concerned with rigid footings, for example the widely quoted work by Faber (85) who measured a parabolic contact pressure distribution between a rigid circular footing and a sand compared with an inverse parabolic distribution between the same footing and a stiff clay. Early work concerning flexible rectangular plates bearing on idealised foundations has already been mentioned in Chapter 1, Vint and Elgood (8) having used a spring bed foundation while Murphy (9) used a hard rubber subgrade 3 inches thick. Murphy found the coefficient of subgrade reaction by pressing rigid punches into the subgrade and his experimental results are in reasonable agreement with the Winkler predictions as are those of Vint and Elgood. It should be pointed out that the subgrade used by Murphy is far too thin to represent a semi-infinite medium.

Wright (86) investigated the variation in subgrade modulus with the breadth of flexible beams, assuming the modulus to be constant for any individual beam. The accuracy of his results may be questioned due to the small container used, because the side walls almost certainly influenced the results (See Section 5.4). However the trend of Wright's results is confirmed by Lenczner (87) in that the subgrade modulus was found to decrease with increasing width of footing, eventually reaching a limiting value. Lenczner went a step further than Wright in investigating the variation of subgrade modulus along the beam, rather than assuming it to be constant. He found that the variation was related to the curvature of the beam, that the conventional Winkler assumption overestimated the maximum bending moments by about 15%, and that analyses based on an assumption of uniform contact pressure yielded results which were very conservative. These observations are compared with the Author's in Section 5.10.

Barden (4) found good agreement between experimental results for beams bearing on sand and the Winkler predictions for all but rigid beams, and this conclusion is confirmed by Vesic (25)

who also obtained good agreement between theory and experiment assuming the foundation to be a semi-infinite homogeneous elastic medium, analysed by an approximate method.

The only laboratory tests on plates bearing on sand known to the Author were carried out by Brand (88) on flexible circular plates loaded with concentrated central loads. Brand states that his experimental results "could not be compared with theory". He gives no results for deflections, but gives some contact pressures which are compared with the Author's results in Section 5.10.

A larger scale observation is reported by l'Herminier, Bachelier and Soeiro (89) who, using vibrating wire gauges, measured the contact pressures beneath a 36 x 29 x 3.8 metre raft bearing on a gravel. The stress distribution proved to be intermediate between a uniform distribution and the distribution determined by elastic theory.

5.2 Determination of Contact Pressures

The contact pressure distribution between a flexible slab and the subsoil can be determined either directly or indirectly. The direct method involves the presence of some kind of pressure sensing device at the soil-structure interface while the most commonly used indirect method, for the case of a beam, has been the double differentiation of the curvature of the beam. Of the investigations described in the previous section, Wright, Lenczner and Vesic used the latter method and Barden and Brand the former.

The Author preferred the direct method, because numerical differentiation is an inaccurate process, the inaccuracy being compounded with the number of differentiations. In addition, for circular plates axisymmetrically loaded, the contact pressure is a function of d^4w/dr^4 , d^3w/dr^3 , d^2w/dr^2 and dw/dr , so that it would be far more complex and inaccurate to use an indirect method for that case.

There is a voluminous literature on the subject of "earth" pressure cells, and several theses known to the Author contain exhaustive reviews, e.g. Brand (88) and Neale (90), so that another such review would be superfluous. Much of the work is of secondary interest, referring as it does to "embedded" pressure cells rather

than contact pressure cells. As far as the latter are concerned, when used on sand foundations the requirements are simply that the pressure cell should be initially flush with the base of the structure, and that the deflection of the cell under load should be the minimum consistent with reasonable sensitivity, in order to avoid excessive arching action. Thirdly the cell should not radically affect the flexural rigidity of the structure. Two basic types of contact pressure cell have been used in the past, the diaphragm type and the piston type. In the former case the cell face (usually circular) displaces by bending from clamped edges whereas in the latter case the whole face of the cell slides inwards under pressure. The diaphragm type was chosen for this investigation because piston cells are subject to high stress concentrations at their edges and, more importantly, when set in a flexible structure, their freedom of sliding is affected by the deformation of the structure, the piston slot becoming a truncated cone as deformation proceeds. Of course the deformation of the structure also affects the performance of a diaphragm cell since the diaphragm is subjected to in-plane tensile or compressive stresses which alter its sensitivity to applied pressure. This factor, not considered by Bardon or Brand is dealt with in later sections.

Many measuring systems have been used to record the responses of the various types of cell to applied pressure. The three basic methods involve:

- (i) Measurement of the displacement of the diaphragm or piston by the displacement of a fluid contained behind it.
- (ii) A closed system of type (i) where the pressure in a confined fluid due to the displacement is measured.
- (iii) Measurement of the strain in the cell diaphragm by some sort of strain gauge.

Option (i) was adopted because it was comparable to but simpler than option (ii), and because it was felt that it would be difficult to separate the diaphragm strains into those caused by bending of the diaphragm under pressure and those caused by in-plane stresses due to the bending of the structure.

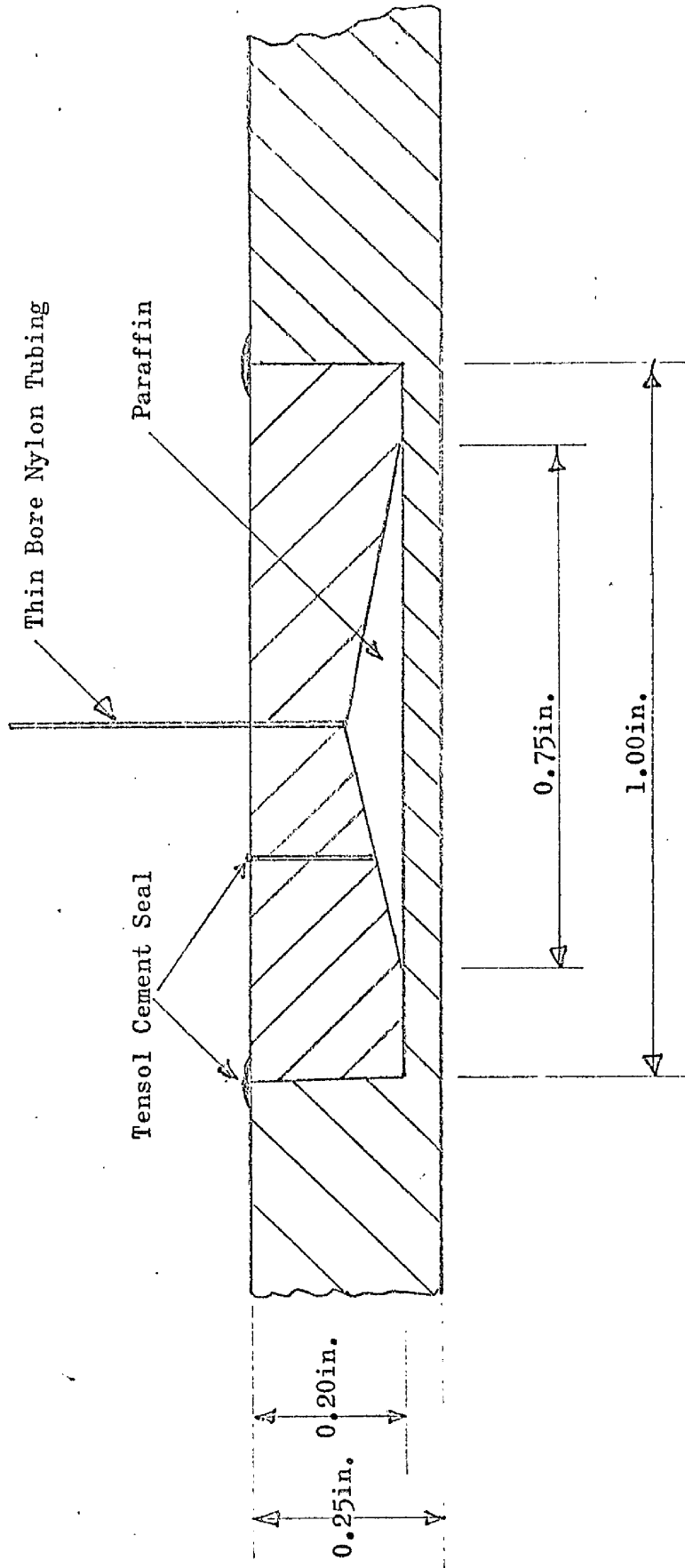
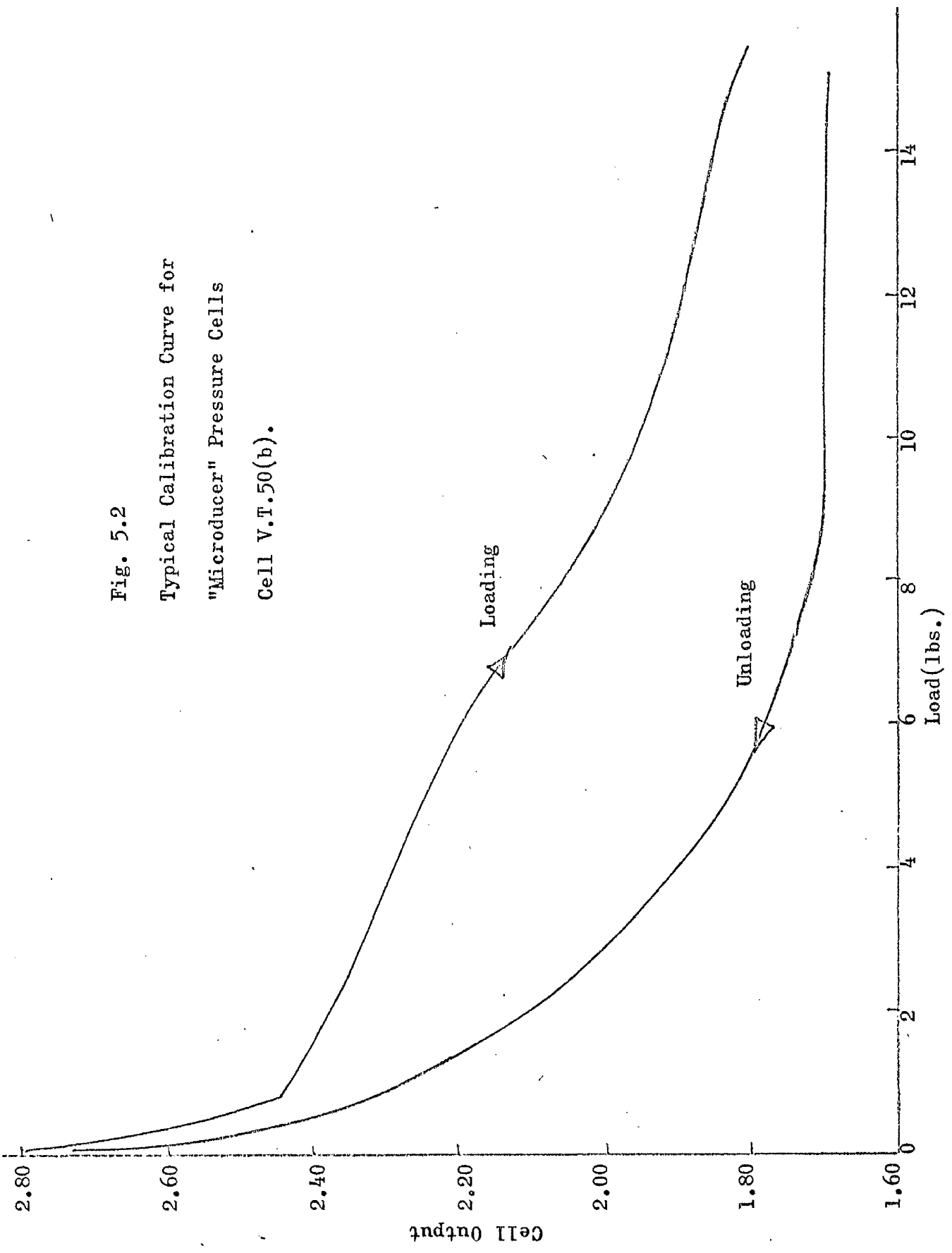


Fig. 5.1
 Cross-section through Perspex Pressure Cell
 (Four times full size).

Fig. 5.2
Typical Calibration Curve for
"Microducer" Pressure Cells
Cell V.T.50(b).



The design finally adopted is shown in Fig.5.1. It is based on previous designs by Rowe and Briggs (91) and by Peaker (92) and conforms to the W.E.S. requirements for diaphragm displacement (93) although not to the more stringent criteria of Trollope and Lee (94). However, all cells were identical and were used on the same soil, so that the cell action factor could be assumed to be constant. A slot was first sunk from the top of the perspex plate, leaving the desired thickness of diaphragm still in position. The shaped disc was then inserted and glued in position with Tensol No.7 perspex cement. Finally the cell was filled with paraffin and the filling hole blocked. Readings of the fluid level in the very thin bore (0.5 mm.) nylon tubing were obtained by fixing the tubing to a graduated scale. Originally a temperature compensation chamber was included in the disc but this was found to be unnecessary due to the short duration of any individual experiment and the good temperature control available in the laboratory. The cell had the following advantages:

- (i) it was very simple and required no complex ancillary electronic equipment,
- (ii) the face of the plate presented to the soil was completely smooth.
- (iii) the minimum effect on the flexibility of the structure had been achieved since the cell was predominantly of the same material as the structure. The calibration of the cells is described in the next section.

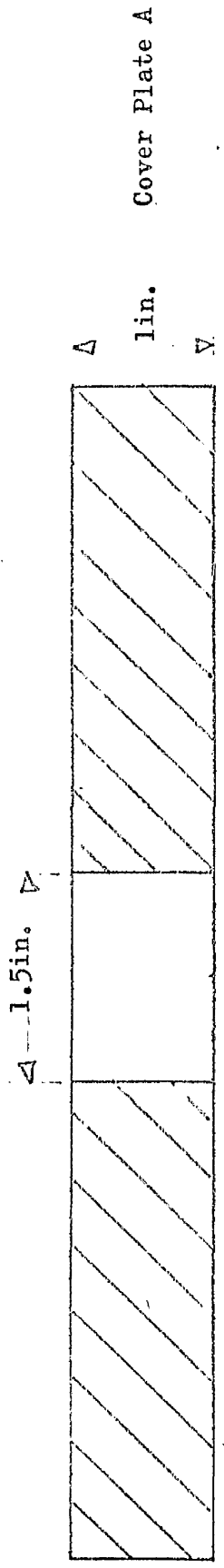
A seemingly promising new ~~departure~~ in the field of pressure cell design was also investigated. Very small cells, the smallest about $\frac{1}{8}$ inch diameter and $\frac{1}{32}$ inch thick are manufactured by Clark Electronic Laboratories in the U.S.A., and consist of two very thin plates, to which terminals are attached, separated by a layer of pressure sensitive paint. When calibrated however, these cells had a very unstable response to pressure because of their extreme sensitivity to eccentricity of loading. A typical calibration curve is shown in Fig.5.2, and even if this were reproduceable it would not inspire confidence in the use of the cell for absolute measurement of pressures. In the Author's opinion, these devices are pressure sensors in a qualitative way rather than quantitative pressure gauges.

5.3 Calibration of Pressure Cells and Determination of the Flexural Rigidities of the Test Plates

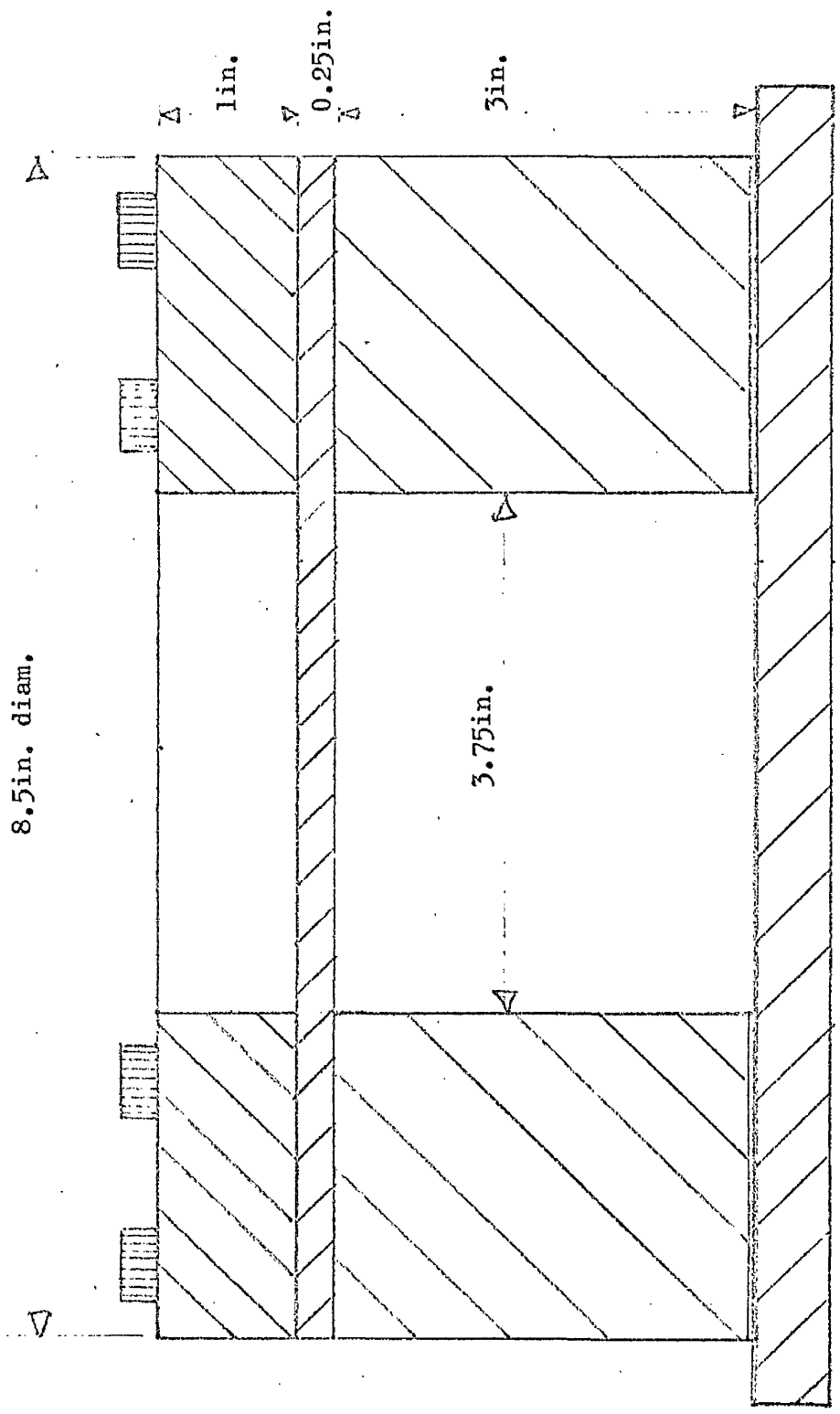
The pressure chamber used for the calibration of the pressure cells is shown in Fig.5.3, and this same chamber was also used to find the flexural rigidities of the perspex test plates. The chamber is $3\frac{3}{4}$ inches internal diameter and the various cover plates are secured to the chamber by 16 Allen screws. With cover plate "A" in position, a pressure cell could be calibrated without allowing the plate in which it was inserted to bend. With cover plate "B" for example, the flexure of the plate came into play and the effect of this on the cell calibration is shown in Fig.5.4. It was shown therefore that the cells had a linear response to applied pressure, but that the curvature of the plate in which they were inserted might introduce serious non-linearity. The magnitude of the non-linearity in the actual experiments is discussed in Section 5.9.

The flexural rigidities of some aluminium plates were first measured using the apparatus because these plates were of a more uniform thickness than the perspex plates and because the E value of the aluminium was known from previous work by Macleod (78) to be less subject to variations from plate to plate than might be expected for the perspex plates. The results of a typical test are shown in Fig.5.5 where the central deflection of the clamped circular plate ($\frac{1}{16}$ inch thick) is recorded against applied pressure. The average deflection of several aluminium plates was found to be 0.00088 inches per lb/in^2 compared with a theoretical value using Macleod's results of 0.00087 inches per lb/in^2 . Since the limit of measuring accuracy was 0.0001 inch, this agreement was thought to be satisfactory, indicating an E value for Aluminium of $10.1 \times 10^6 \text{ lb}/\text{in}^2$ at a Poisson's Ratio of 0.3.

The flexural rigidities of some perspex plates were then measured and some typical results for three $\frac{1}{4}$ inch thick (nominally) plates cut from the same 8 ft. by 4 ft. sheet are shown in Fig.5.6. Plate 1 deflected by 0.00038 inches per lb/in^2 , plate 2 by 0.00034 and plate 3 by 0.00042. At first sight this implied large fluctuations in E from plate to plate, but on measurement of the



Cover Plate A



Cover Plate B
(Secured by 16
Allen Screws)

Perspex Test Plate

Pressure Chamber

Fig. 5.3

Pressure Chamber for
Calibration of Test
Plates and Pressure
Cells.

Cross-section through a Diameter

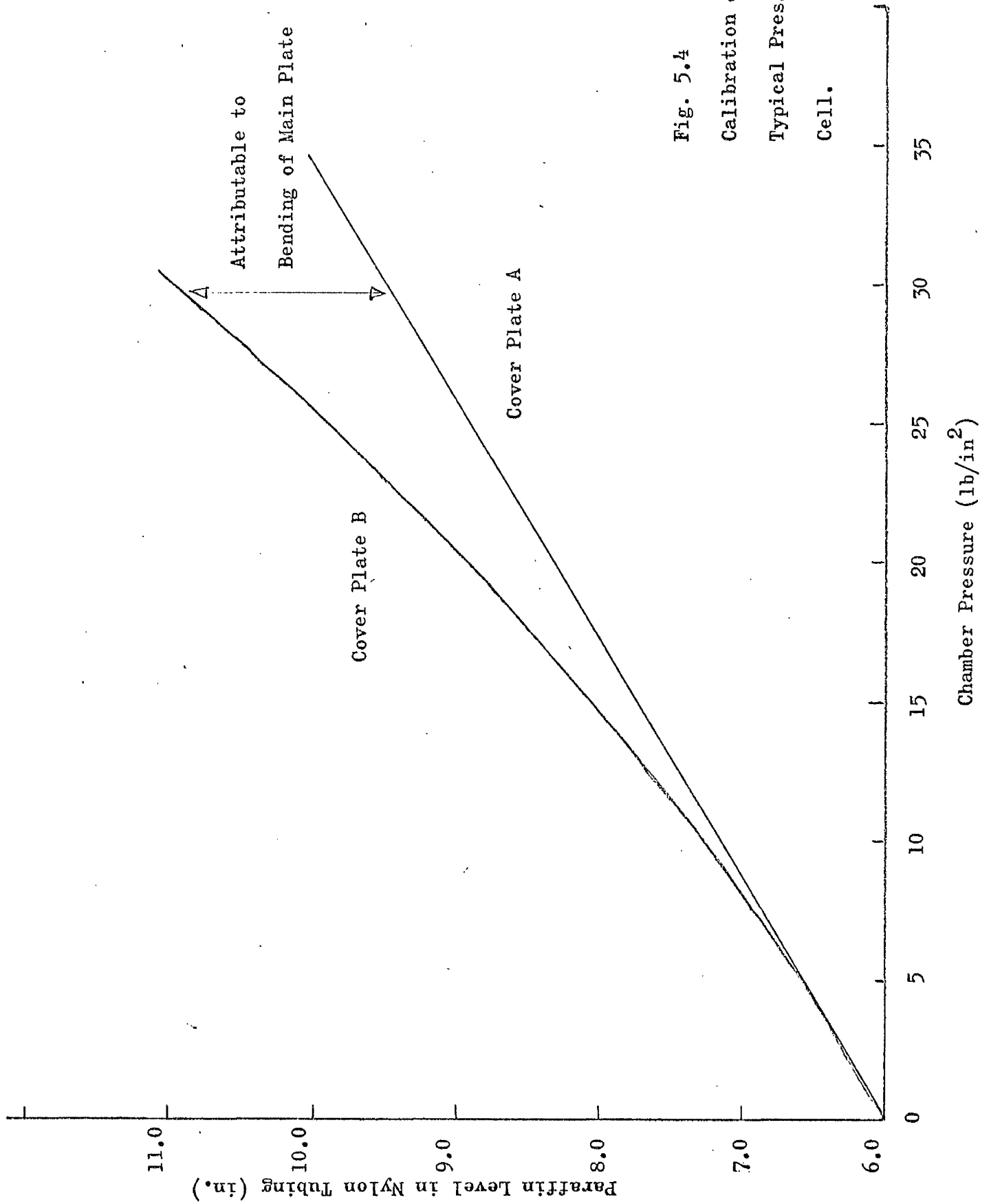


Fig. 5.4
 Calibration of a
 Typical Pressure
 Cell.

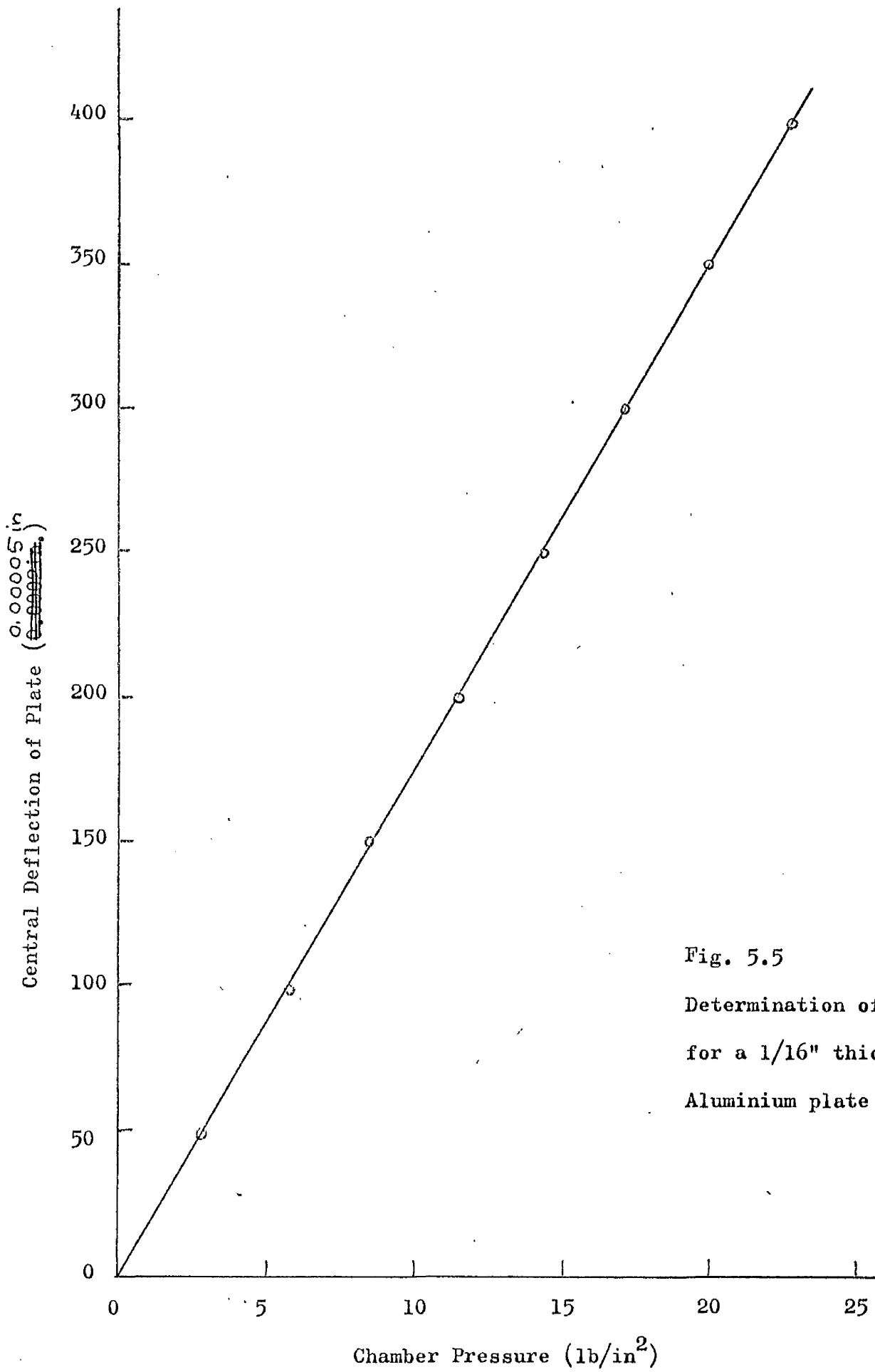


Fig. 5.5
Determination of E
for a 1/16" thick
Aluminium plate

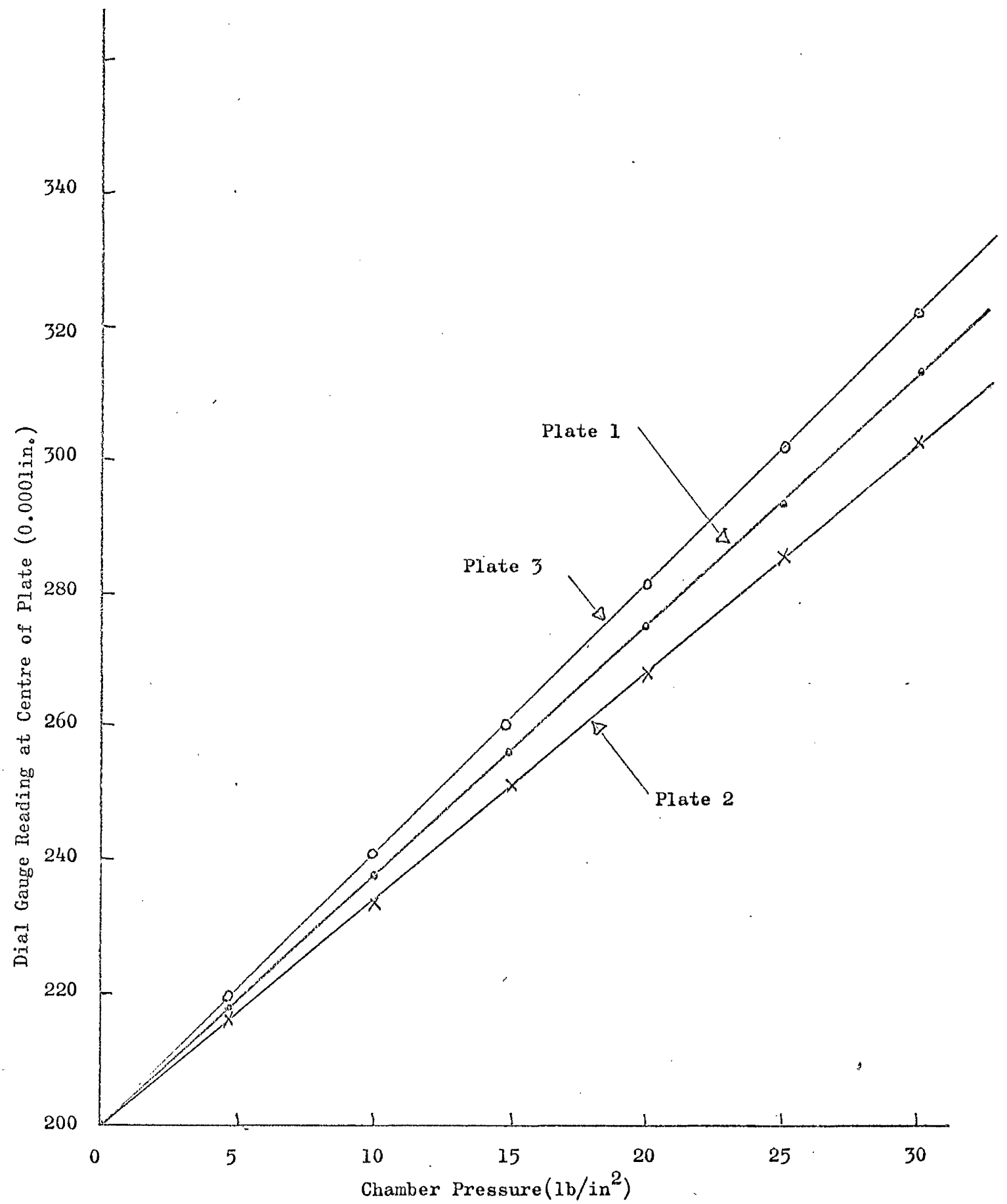


Fig. 5.6 Determination of E for 1/4" (nominally) thick Perspex Plates

plate thicknesses, plate 1 was found to be on average 0.255 inch thick, plate 2 0.263 and plate 3 0.243, giving E values of 3.09×10^5 lb/in², 3.15 lb/in² and 3.23×10^5 lb/in² respectively, reflecting a variation of only $\pm 2\%$ in the E value for that particular sheet. It should be pointed out that, using this apparatus, the E values of all the perspex plates tested were of the order of 3×10^5 lb/in² compared with the usually quoted value of nearer 4×10^5 lb/in². If the low value were due to defects in the apparatus one would expect that the results for the aluminium plates would also be low and that the results for the perspex plates would be less consistent. Since neither of these expectations is fulfilled the apparatus must be assumed to be reliable. In any case, only the relative values of E for the various plates was of interest in this work and the apparatus provided this information. From Macleod's work (78) Poisson's Ratio for perspex was taken to be 0.4 in every case.

5.4 Determination of the Required Size of Sand Container

It became obvious early in the experimental phase of the work that the labour in handling large quantities of sand was going to restrict the number of tests which could reasonably be conducted. On the one hand it was desirable to use as large plates as possible so that the effects of non-uniformity in the foundation would be minimised and deflection measurements readily made at a large number of points on the plate; on the other hand, the minimum volume of sand consistent with these requirements was sought.

Pilot tests were therefore conducted using a bin 30 inches in diameter and 12 inches deep, with auxiliary ring walls 15, $22\frac{1}{2}$ and 25 inches in diameter and 12 inches deep. A rigid test plate 5 inches square and $\frac{3}{8}$ inch thick was used, giving ratios of container width: plate width of 3, $4\frac{1}{2}$, 5 and 6. Leighton Buzzard sand was poured into the container from a tin with a perforated lid held 3 inches from the sand surface. Five layers, each of 2 inches compacted depth, filled the bin to a depth equal to twice the breadth of the plate, compaction being effected by a 10 inch diameter,

Vane Reading (degrees)

20

40

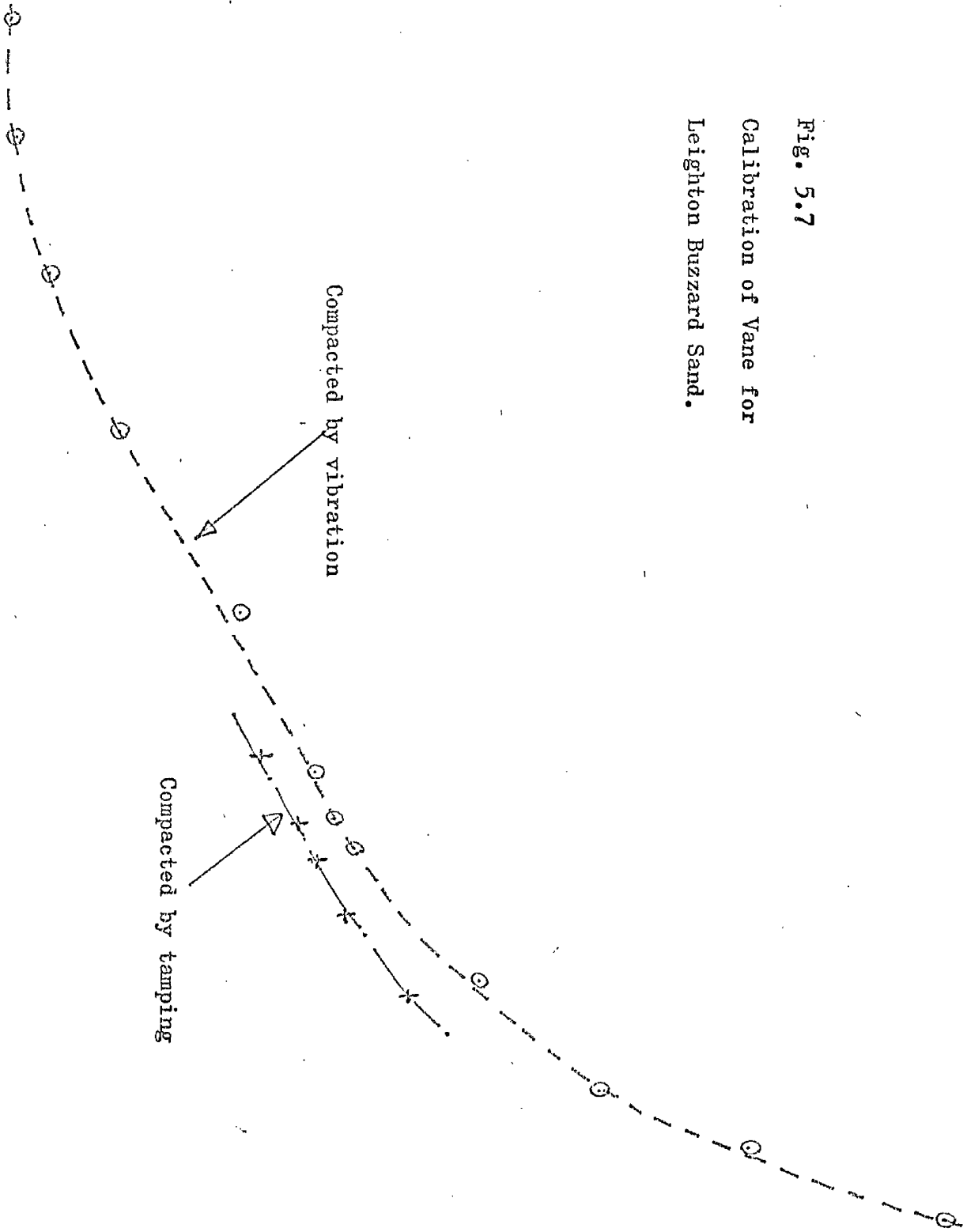
60

80

100

Fig. 5.7

Calibration of Vane for
Leighton Buzzard Sand.



Deflection of Rigid Plate - 5" square (0.0002in.)

0 100 200 300 400 500 600 700

Note: Each curve represents the
average of three tests.

Uniform Pressure (lb/in²)

1.0 2.0 3.0 4.0 5.0

Container Width=22.5in.

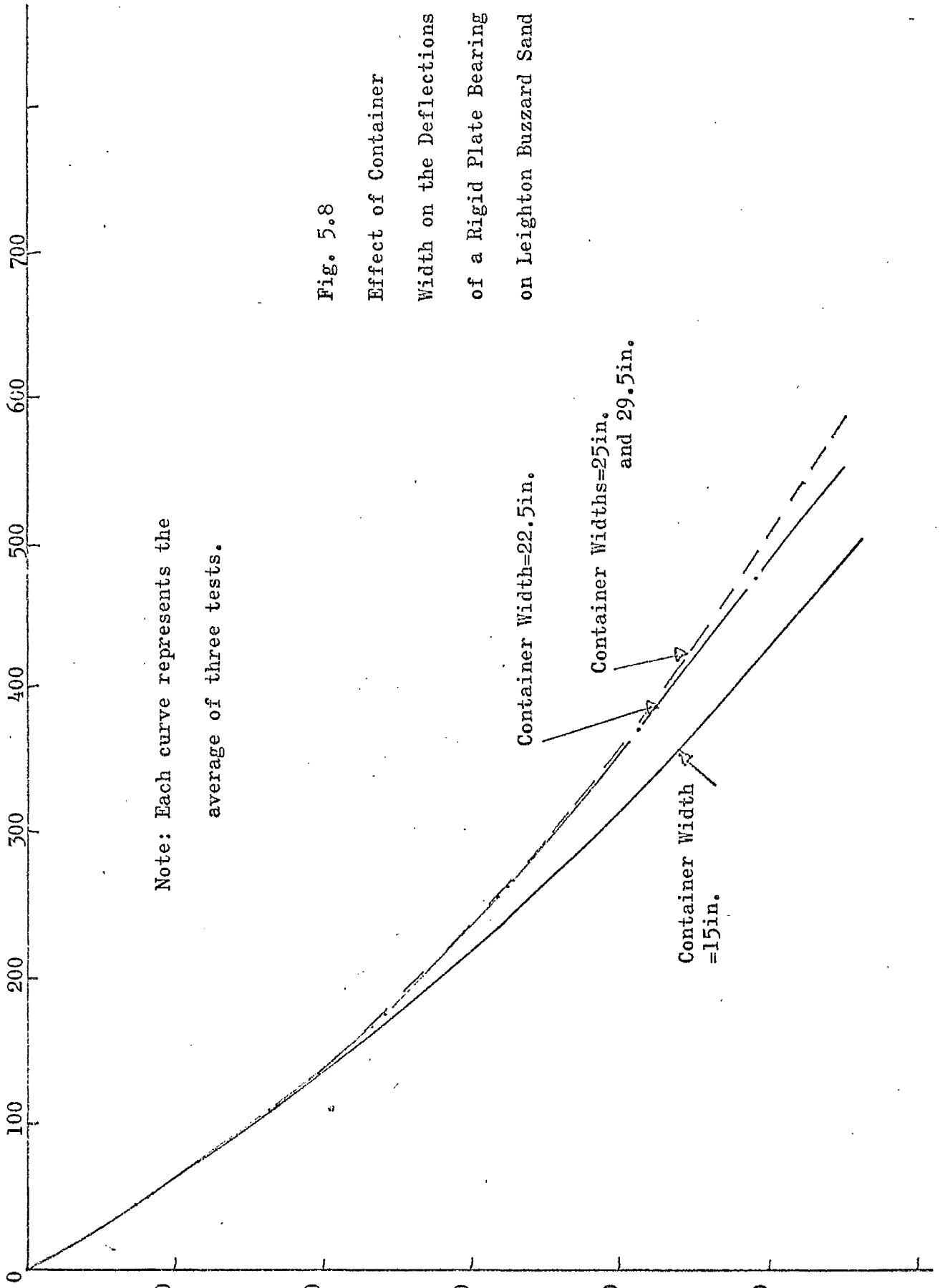
Container Widths=25in.
and 29.5in.

Container Width
=15in.

Fig. 5.8

Effect of Container

Width on the Deflections
of a Rigid Plate Bearing
on Leighton Buzzard Sand



20 pound flat weight. (The necessary depth of 2 times the plate breadth seemed to be universally accepted in the literature, e.g. Allwood (95) whereas the necessary container width was not clearly agreed upon.) A check was also carried out on the uniformity of placement of the sand by a method first used by Allwood (95) and subsequently by Neale (90). In this method, miniature vane shear tests were carried out at various positions in the bin, the vane being driven half way into the uppermost layer each time. (The vane is $\frac{1}{2}$ inch diameter and $\frac{1}{2}$ inch deep.) Calibration tests on the same sand, Fig.5.7, show that the failure torque is highly sensitive to changes in the density of the sand. Fig.5.7 also shows that the method of compaction, in one case vibration while in another tamping, also affects the failure torque. This is attributable to the different grain arrangements due to the two methods, and would be expected to be more pronounced with angular grained sands. That this is true will be seen later. However, for a constant mode of compaction, the vane test is seen to be a good guide to density variations. Vane tests on the compacted sand in the bin indicated density variations of the order of $\pm 0.5 \text{ lb/ft}^3$, which, being comparable with the results for vibrated sands (90), were considered reasonable.

When the bin had been filled, the test plate was levelled and loaded with a uniform pressure, a small "seating" pressure having been first applied, in steps of 1 lb/in^2 up to 6 lb/in^2 and the deflection of the plate after each step was noted. Five minutes were allowed to elapse between each increment because this would subsequently be necessary to permit time for creep of the perspex. The results for 3 tests in each of the 4 bin sizes are plotted together in Fig.5.8. This shows that the 15 inch bin is definitely too small, but that there is little to choose between the other three, especially at the subsequently adopted maximum working pressure of about 4 lb/in^2 . To minimise the sand volume therefore, a minimum container width of $4\frac{1}{2}$ times the plate width was adopted.

5.5 Classification of the Sand Used for the Full Scale Tests

It was decided that the criteria described in the previous section i.e. reasonable plate size together with a reasonable quantity of sand could be met by using plates in the range 8 inch diameter to 12 inch diameter. This implied container sizes of 36 inches to 54 inches and a maximum quantity of about 2 tons of sand. Leighton Buzzard sand had been used for the pilot tests, but the purchase of 2 tons of this sand would have been very expensive and in any case it was felt that a finer sand would minimise the effects of variations in the density of the foundation, especially as far as the pressure cells were concerned since there would be more grains in contact with the cell.

After several trials, a fine Tey river sand was adopted. The grain size distribution of this sand is shown in Fig.5.9 and it can be seen that the sand is very uniform, 70% of its particles passing the 36 sieve but being retained on the 52 sieve. The specific gravity of the sand particles was found to be 2.77, the maximum porosity by the tilting test to be 0.47 and the minimum porosity, after vibration under water, to be 0.38. The sphericity and roundness of the sand were found to be 0.80 and 0.45 respectively, by a method developed by Neale (90). This indicated a rather angular sand and confirmed visual inspections which revealed a proportion of flaky mica particles. Finally the moisture content of the sand as delivered (washed, sieved, dried and bagged) was found to be 0.05% and it was assumed that this small amount of moisture would not affect the behaviour of the sand by causing significant capillary forces.

5.6 Placement of the Sand in the Full Scale Tests

A considerable amount of work was involved in the investigation of the behaviour of plates of varying thickness and diameter bearing on just one sand foundation (i.e. a single sand placed at a single density), and this limited objective formed the scope of the experimental work. This considerably simplified the requirements of apparatus for depositing the sand in the containers,

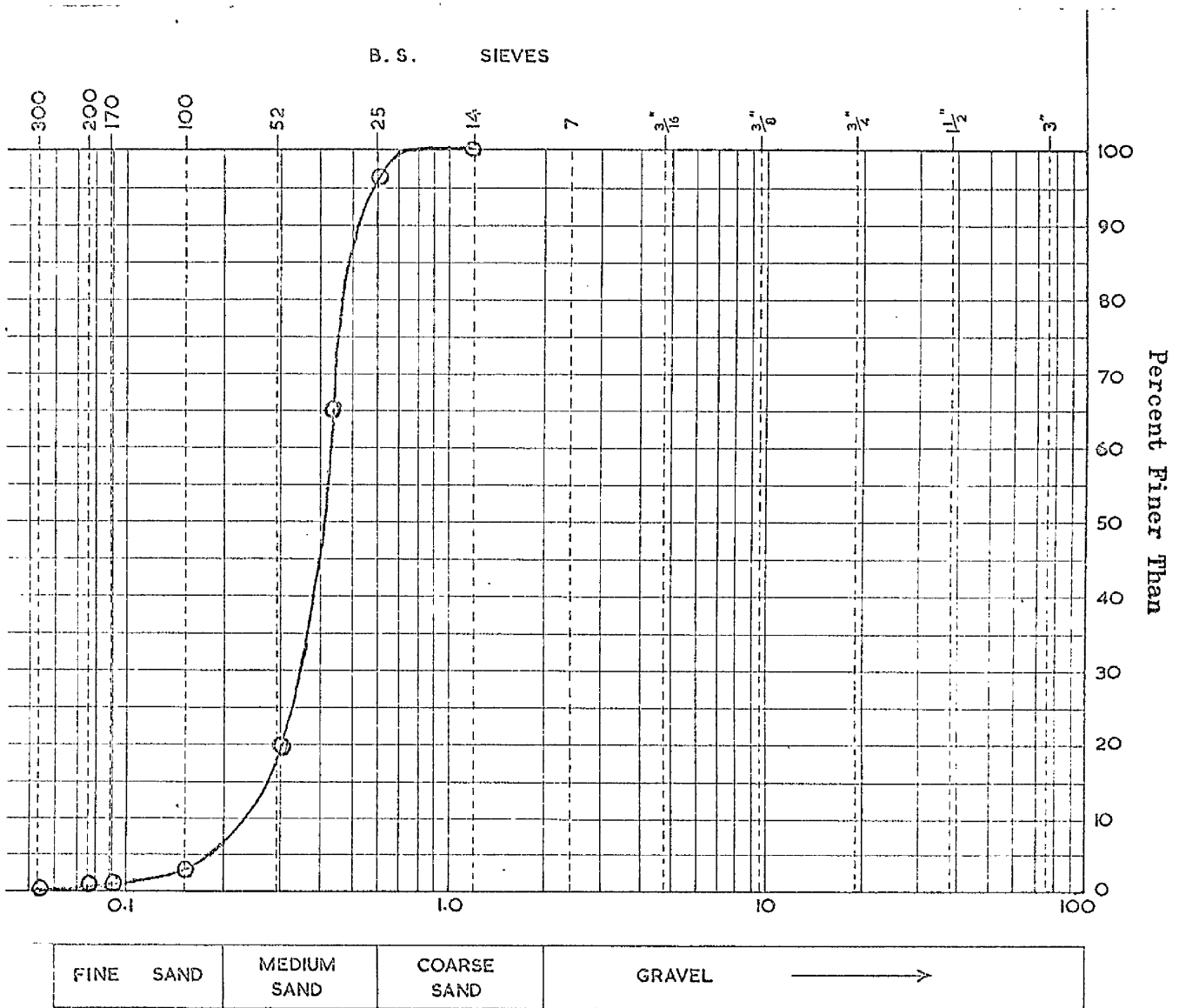
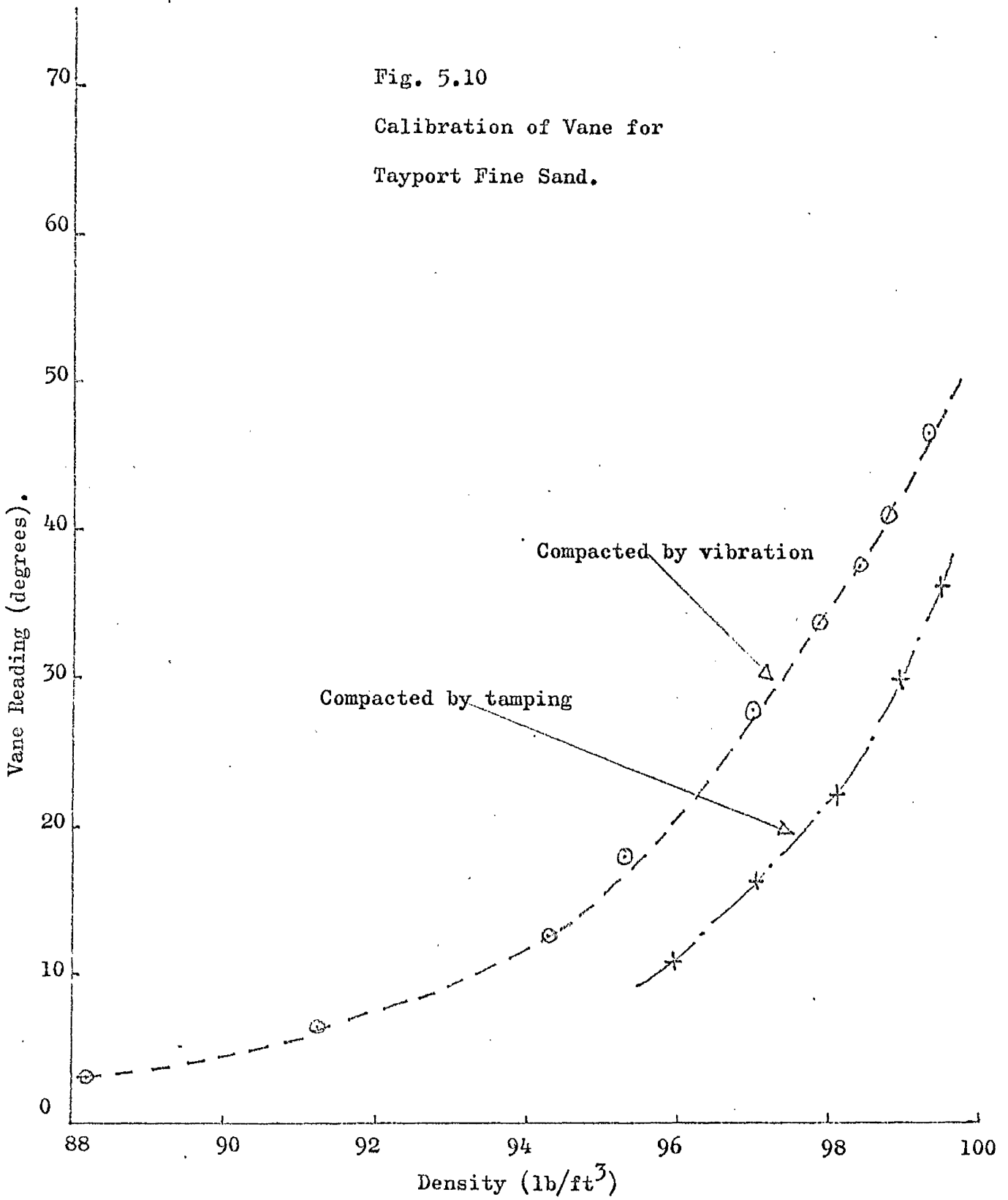


Fig. 5.9

Particle size distribution for Tayport Fine Sand.

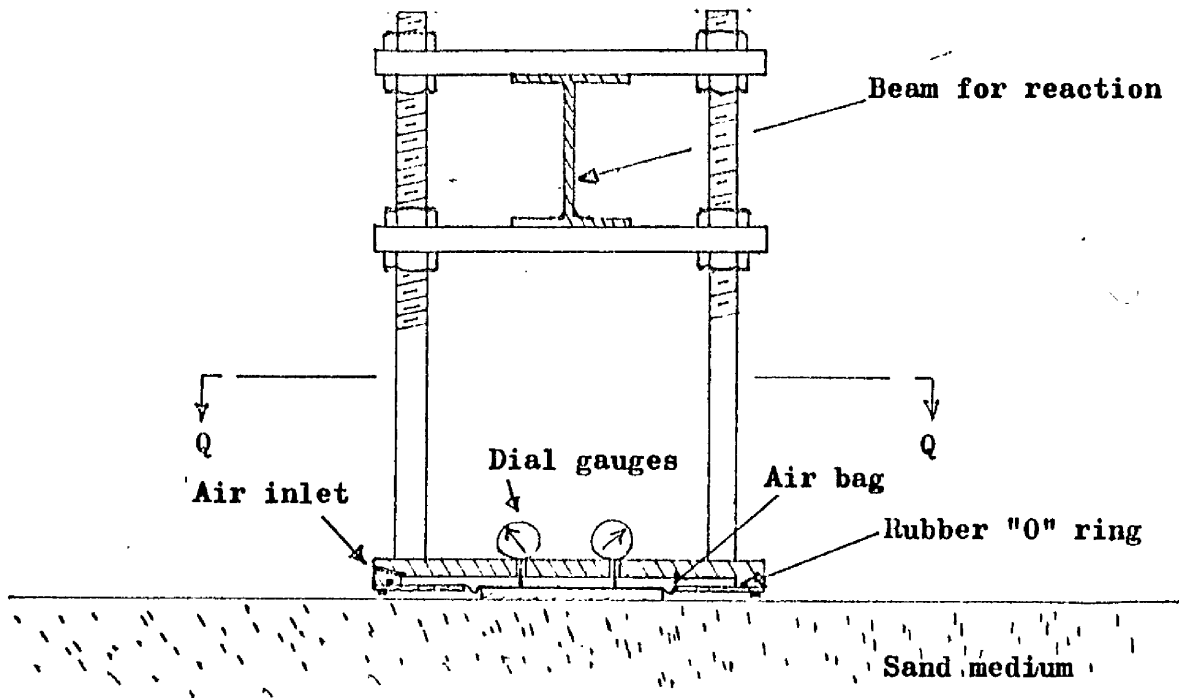
Fig. 5.10
Calibration of Vane for
Tayport Fine Sand.



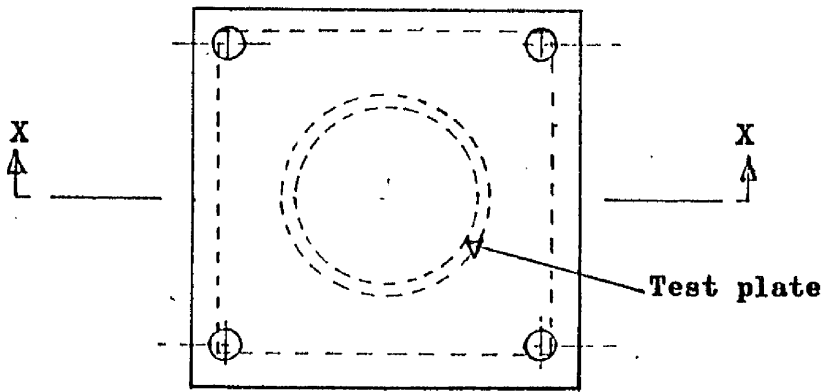
and all that was required was the ability to deposit reasonably uniform layers of sand over areas from 36 inches square to 54 inches square, ready for compaction. A simple hopper arrangement was adopted, consisting of two $\frac{1}{2}$ inch thick blockboard panels, one fixed to supports and the other free to slide, perforated by $\frac{1}{4}$ inch diameter holes at 1 inch centres. The hopper was 5 feet square overall, so that a complete layer could be deposited in one pour. Since the sand always dropped through a distance of at least 18 inches, no facility for adjusting the dropping distance was provided. The sand was poured into the containers in layers which, after compaction, were nominally 4 inches thick, the tamper being 10 inches square and weighing 28 lb. The uniformity of the layers was tested in the same way as in the pilot tests, the vane having been calibrated as shown in Fig.5.10. This time the method of compaction had more influence on the ultimate torque/density relationship because of the more angular sand grains. The variation in density of the compacted sand in the containers was again of the order of $\pm 0.5 \text{ lb/ft}^3$, which was considered acceptable.

5.7 Plates Bearing on Sand and Subjected to Uniformly Distributed Loads

The original aim in the research project was the examination of the behaviour of flexible plates, bearing on sands and subjected to uniformly distributed loads on their upper faces. To this end, at the time of the pilot tests to determine the size of container required, a small apparatus was constructed, capable of applying a uniform pressure to plates up to about 6 inches square. This apparatus was in fact used in the pilot tests, and the experience thus gained utilised for the construction of a larger apparatus capable of applying uniform pressures to plates up to 12 inches square. Drawings of this larger apparatus are shown in Fig.5.11. The rubber air bag was formed by slitting open a 6 inch diameter triaxial test membrane, and the range of plate displacements over which the full pressure was transmitted to a given plate was checked by gradually moving the plate away from the pressurised air bag and recording



Elevation on X-X



Plan on Q-Q

Fig. 5.11 Apparatus for applying uniform pressure to plates bearing on sand (1/8 full size)

the position at which the load began to decrease. Unfortunately, no plate of practicable flexibility could be induced to bend on the medium-dense sand foundation under the pressures which could be applied. The most flexible plate tried was 12 inches in diameter and $1/16$ inch thick. More flexible plates would have been closer to membranes than to plates. At this scale therefore, and given the stiffness of the foundation, the tests using uniform loadings had to be abandoned.

5.8 Circular Plates Bearing on Sand and Subjected to Concentrated Central Loadings

It was then decided to attempt to use the next simplest loading, namely, a concentrated central load. Concentrated loads present the problem that theoretically they have no area of application whereas in practice a certain undefined area of application exists. The first task was therefore to ascertain whether the proposed loading system gave nearly the correct results when applied to a situation in which a theoretical answer was known. The circular calibration chamber described in Section 5.3 was used for this purpose the test plate ($1/4$ inch thick perspex) having a small dimple, formed by a drill tip, made at its centre. The load was applied through a $1/4$ inch diameter stainless steel ball-bearing. The measured deflection was 23.5×10^{-4} inches per 10 proving ring divisions (16.38 lb) while the theoretical deflection, $Pa^2/16\pi D$ was 22.55×10^{-4} inches per 16.38 lb, the difference being 4%. It seemed reasonable to assume, therefore, that the concentrated load, applied in the above manner, was close to the theoretical conception of a concentrated load.

A second complication when using circular plates bearing on sand and centrally loaded is that there is a relatively small range of plate flexibilities within the thin plate range, for which bending of the plate occurs without the edges of the plate losing contact with the sand. As this loss of contact does not usually occur in practice and as it presents complications in the theoretical analysis, only plates with flexibilities such that their edges did not rise were tested.

After preliminary trials, the following 9 plates were selected, all of perspex:

<u>Diameter (inches)</u>	<u>Nominal Thickness (inches)</u>		
8	$\frac{1}{4}$ (+ 13)	$\frac{5}{16}$ (+ 2)	$\frac{3}{8}$ (+ 2)
9	$\frac{5}{16}$ (+ 1)	$\frac{3}{8}$ (- 15)	0.42(+ 1)
10	$\frac{3}{8}$ (+ 27)	0.42 (+ 1)	$\frac{1}{2}$ (- 7)

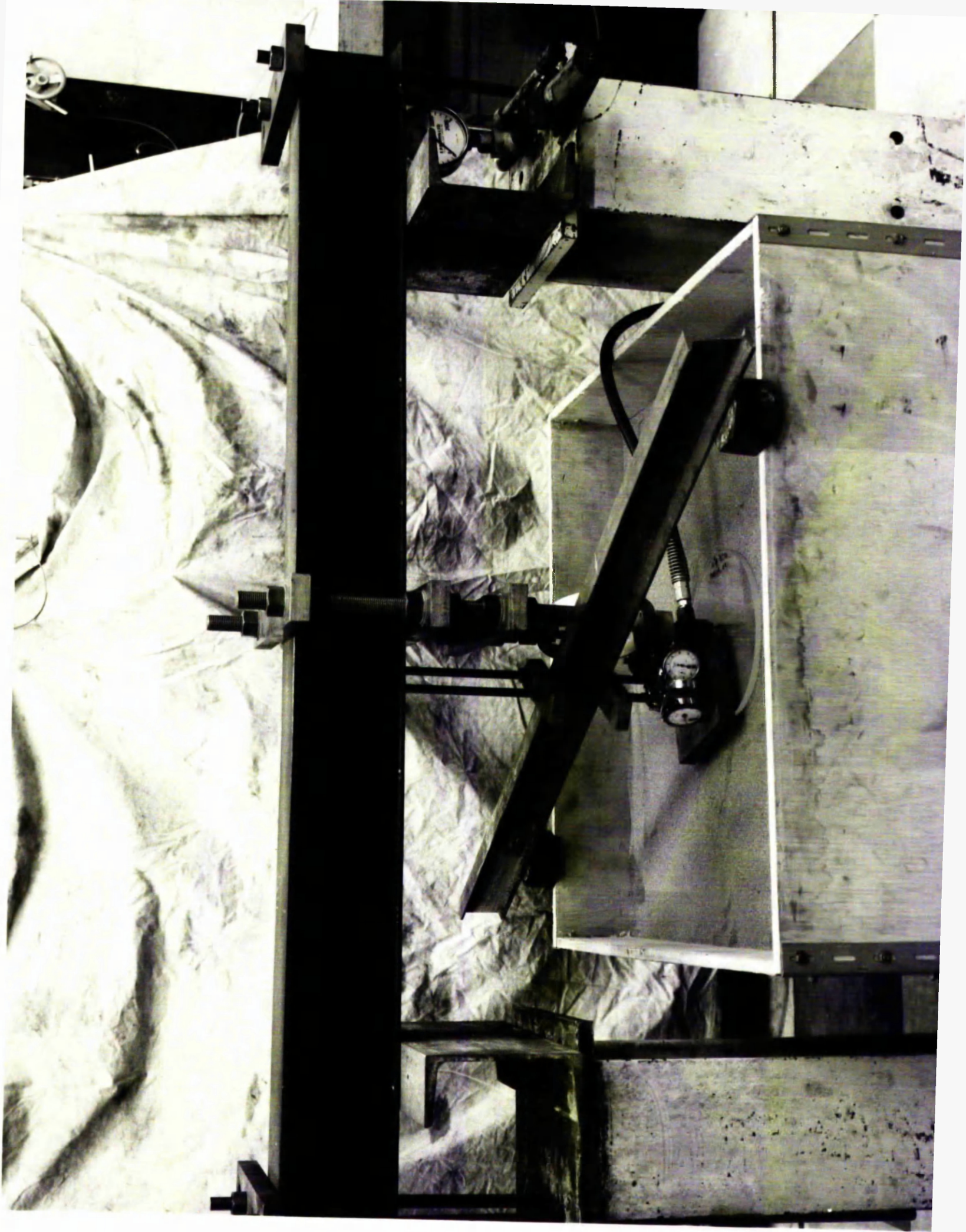
The figures in brackets indicate the average variation from the nominal size in ten-thousandths of an inch. The 0.42 inch thick plates were not available as standard sizes and had to be machined down from the $\frac{1}{2}$ inch size.

Calibration pieces were cut from the perspex sheets, immediately adjacent to the test plates, and the following E values determined as described in Section 5.3.

<u>Nominal Plate Thickness (inches)</u>	<u>E (lb/in²)</u>
$\frac{1}{4}$	3.09×10^5
$\frac{5}{16}$	3.01×10^5
$\frac{3}{8}$	3.19×10^5
0.42	3.07×10^5
$\frac{1}{2}$	3.25×10^5

5.9 Apparatus and Testing Procedure

The experimental set-up is shown in Plate 1. After the container had been filled to the required depth, the circular test plate was placed on the sand surface and levelled. The load was applied by a hydraulic jack and measured by a proving ring. In order to measure the deflections of the plate at radii $\frac{1}{2}$ inch apart, conventional dial gauge supports could not be used, being too bulky. To obtain the necessary cluster of gauges a holder was used embodying the principle shown in the sketch of the pressure chamber (Fig.5.11). The lugged back plates of the dial gauges were replaced by plain back plates, allowing 7 gauges to be positioned on the holder at radii $\frac{1}{2}$ inch apart. Other dial gauges with conventional supports were positioned round the circumference of the plate to check that no tilting occurred under load. All of the dial gauges were graduated to $\frac{1}{10,000}$ inch.



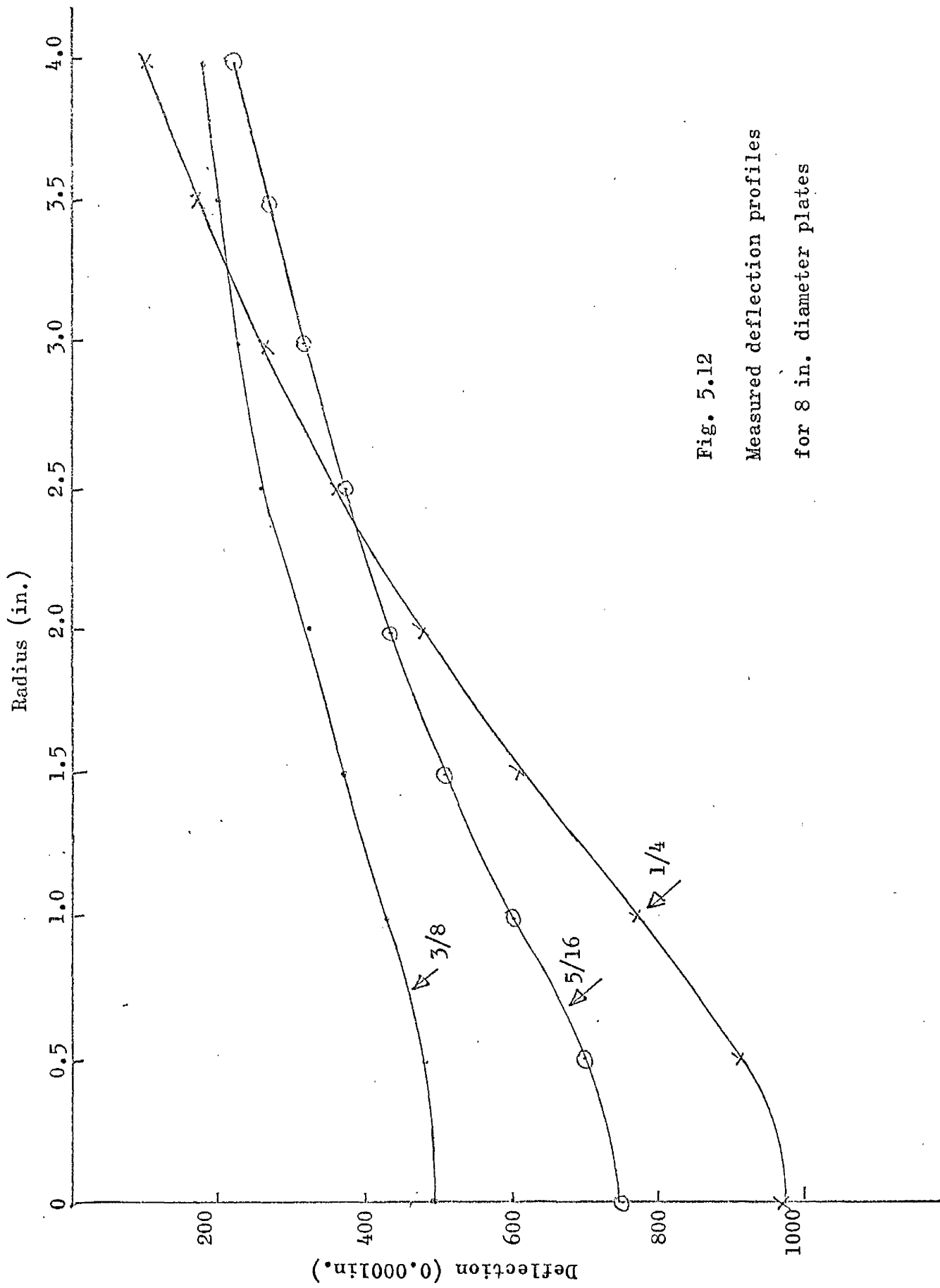


Fig. 5.12
 Measured deflection profiles
 for 8 in. diameter plates

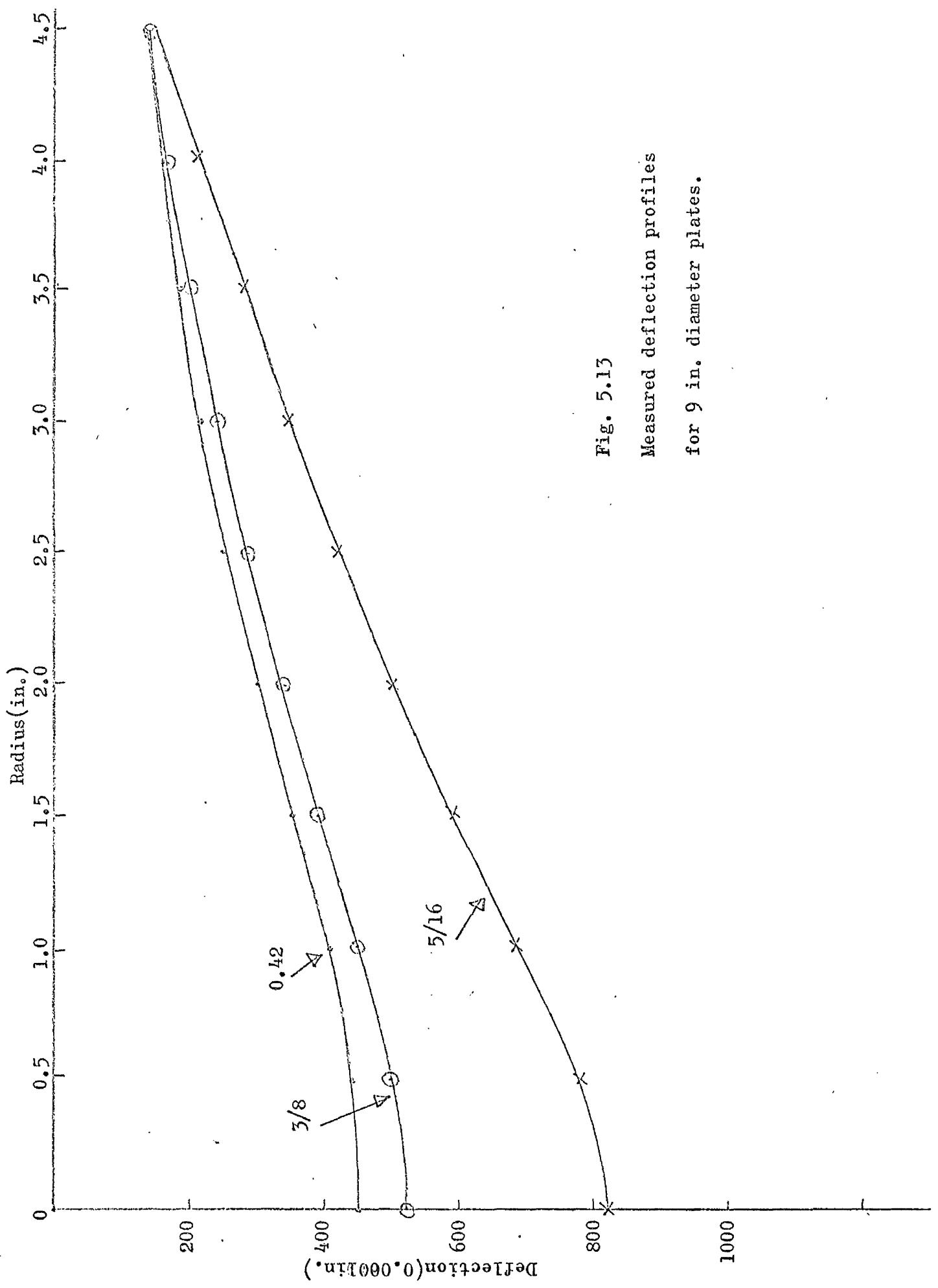


Fig. 5.13

Measured deflection profiles
for 9 in. diameter plates.

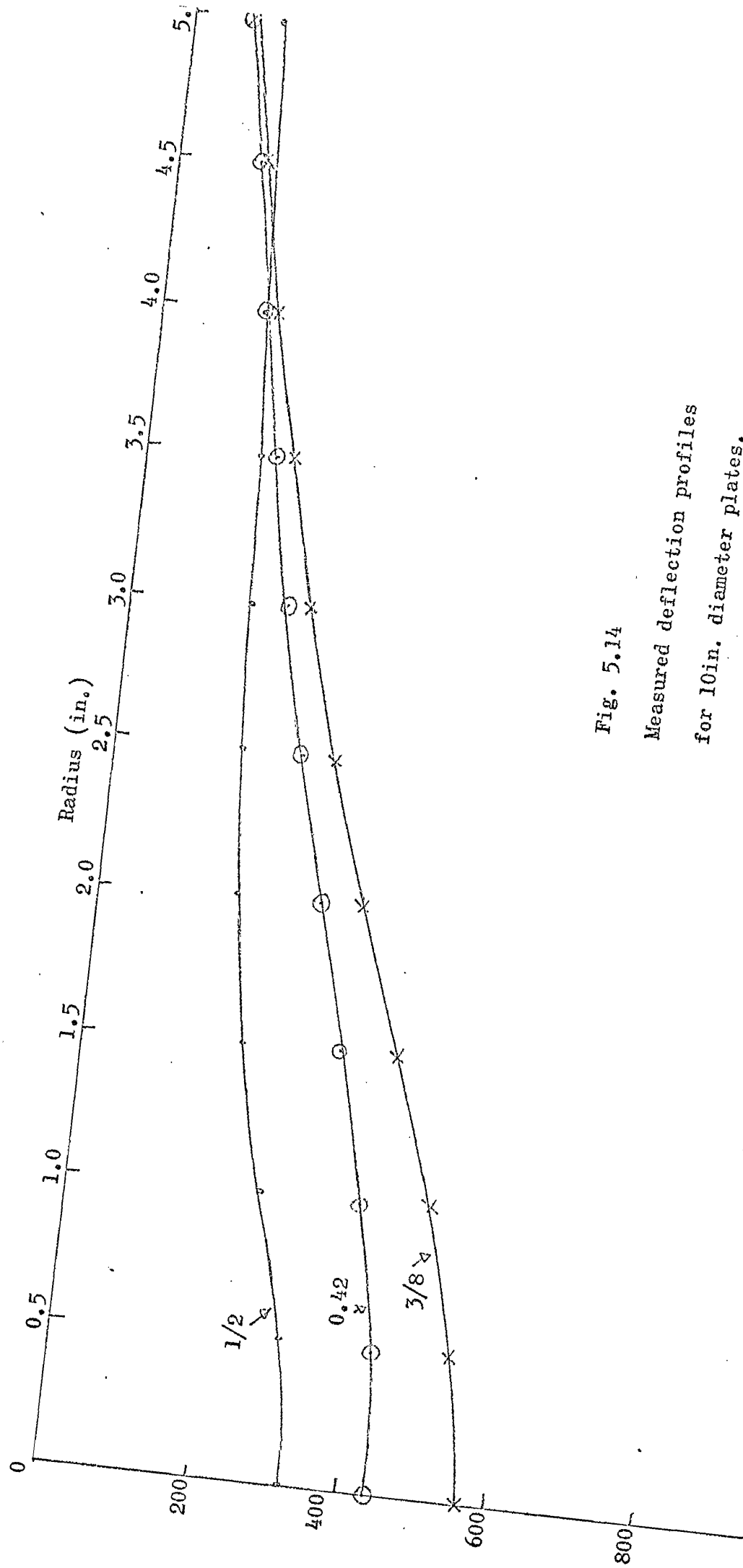


Fig. 5.14

Measured deflection profiles
for 10in. diameter plates.

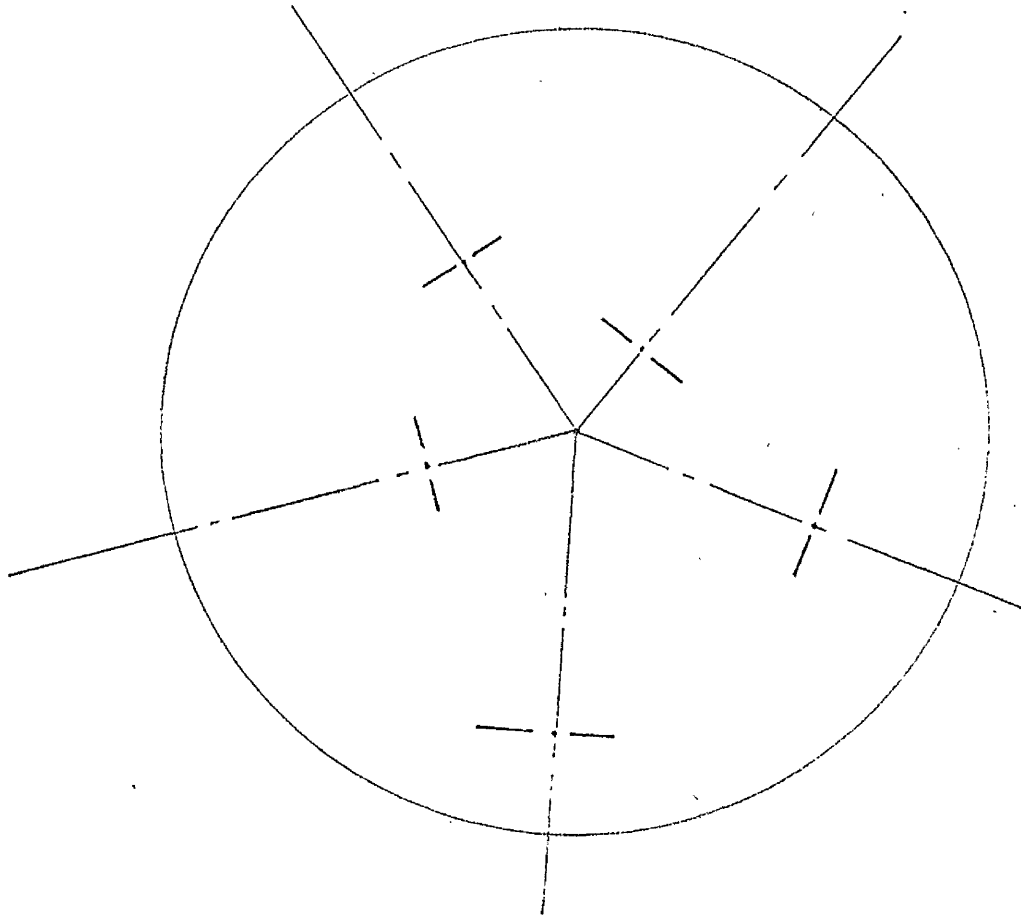


Fig. 5.15.

Location of pressure cells.

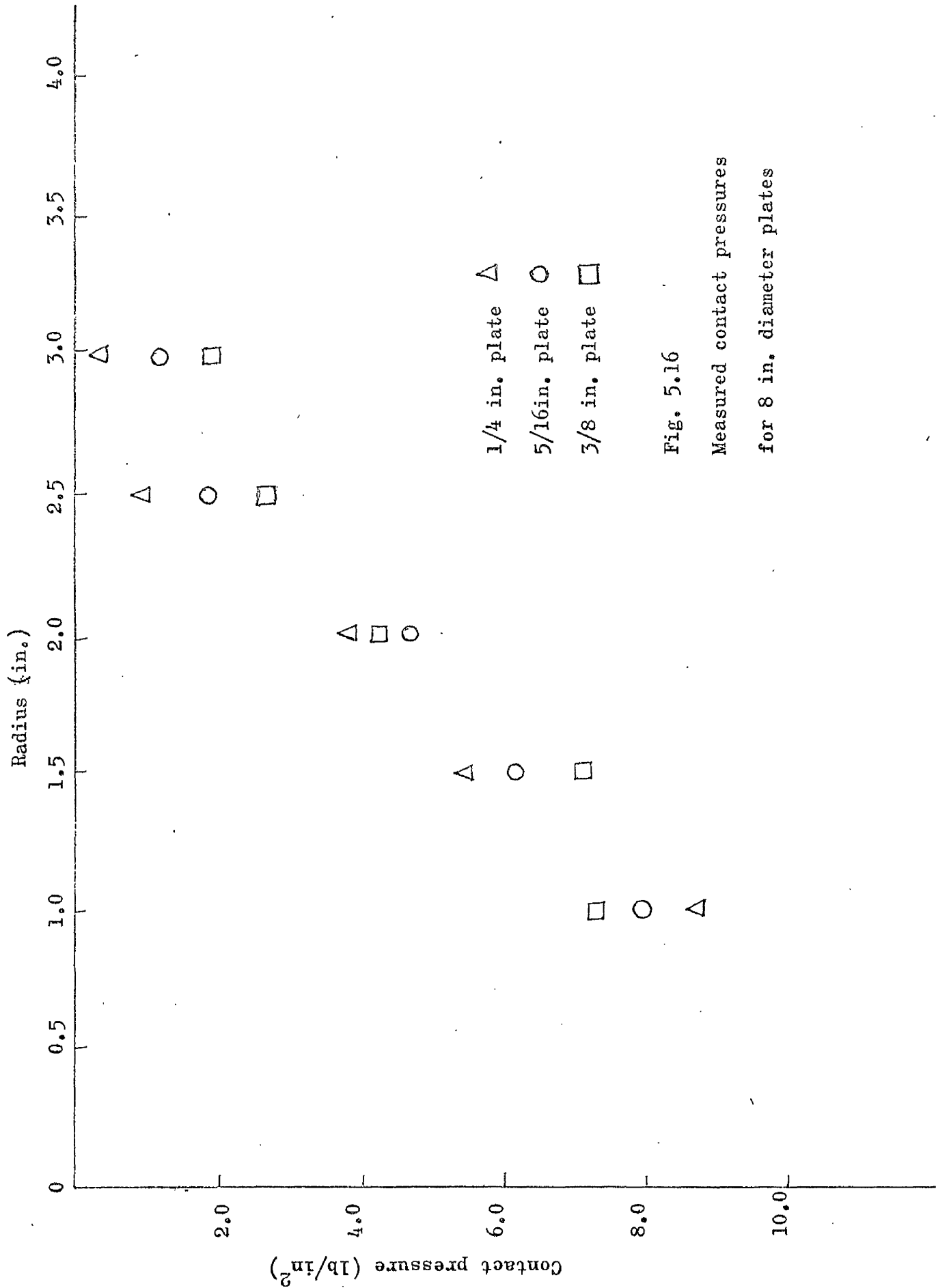


Fig. 5.16

Measured contact pressures

for 8 in. diameter plates

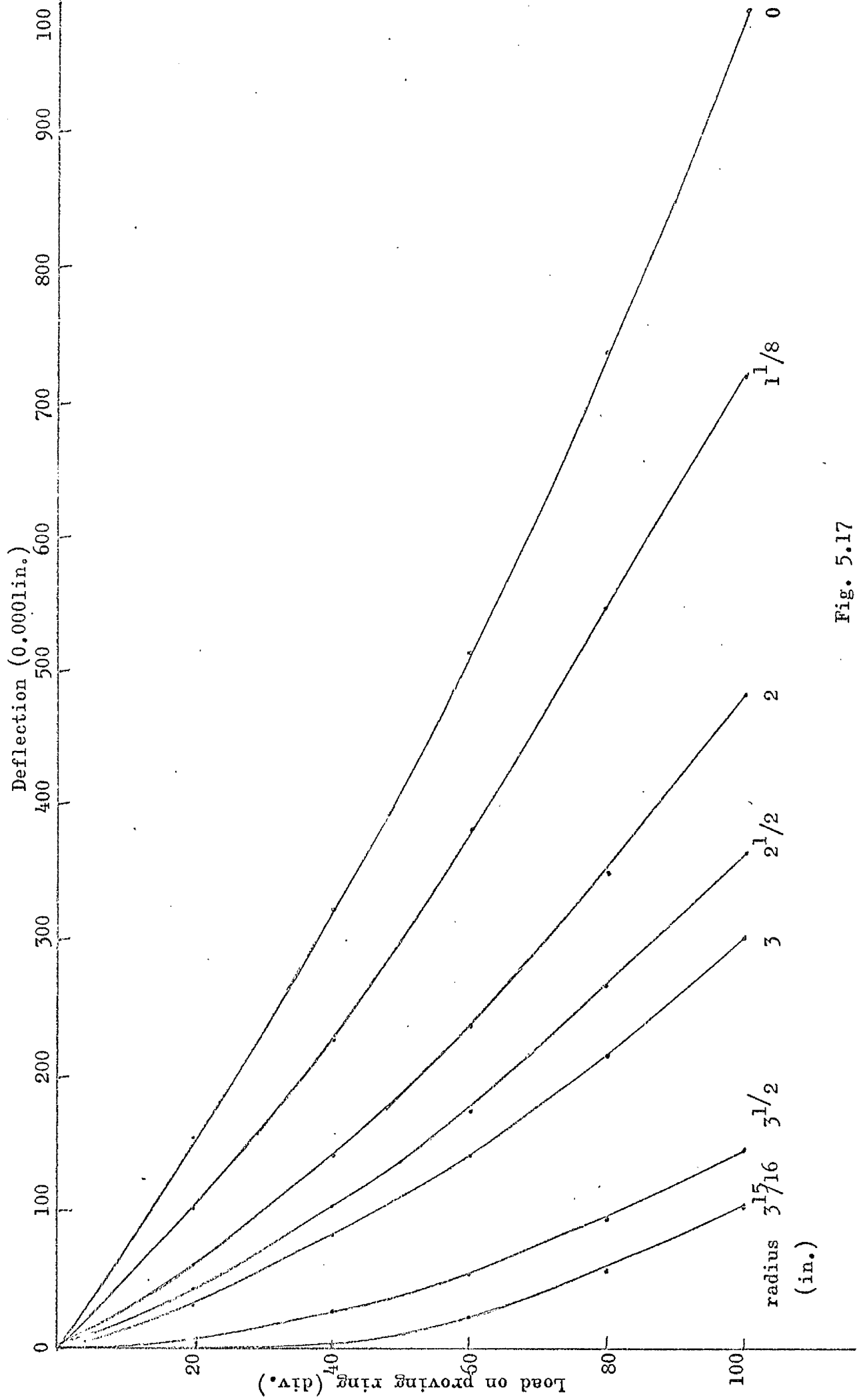


Fig. 5.17

Load-deflection curves for 1/4 in. thick 8 in. diameter plate.

In the first series of tests, only the deflected forms of the 9 plates were measured for loads of 32.76, 65.52, 98.28, 131.04, 163.80 lb (corresponding to convenient proving ring readings). The determination of these deflected forms usually required about 5 independent tests on each plate, such was the scatter of the experimental results. The container was refilled before every test, so that all results refer to first loading of the sand only. The effects of repeated loading were not investigated. The tests on any plate were continued until three sets of results differing by less than 10% were obtained. The averages of these sets are plotted in Figs.5.12-5.14 for a load of 163.8 lb.

In the second series of tests, involving three 8 inch diameter plates only, pressure cells were incorporated in the plates at the positions shown in Fig.5.15. In this test series, it was only necessary to check the deflections at a few points to ensure that they agreed with the measurements from the first series. The measured contact pressures for a load of 163.8 lb. are plotted in Fig.5.16.

To determine the magnitudes of the curvatures of the three plates at the positions of the pressure cells, a third series of tests was conducted using the original 8 inch diameter plates. Foil electrical resistance strain gauges, gauge length $\frac{1}{4}$ inch and resistance 50 ohms, were cemented to the upper surfaces of the plates using Eastman 910 cement. The radial strains recorded by these gauges at full load were nowhere in excess of 400 micro-inches per inch. A similar order of curvature is produced in a $\frac{1}{4}$ inch thick perspex plate, clamped in the test chamber described in Section 5.3, at radii of $\frac{15}{32}$ inch and $\frac{45}{32}$ inch under a pressure of about 7 lb/in². By clamping a plate containing a pressure cell in the calibration chamber it was therefore possible to assess the effect of curvatures of the order of those developed in the main tests on the performance of the pressure cells. This was found to be negligible, and no corrections to the pressure cell readings to allow for curvature of the plates were necessary.

5.10 Analysis and Discussion of the Experimental Results

In the chapters of this thesis devoted to theoretical analysis of circular plates bearing on elastic foundations, two types of analysis were developed. In Section 2.9 the method of analysing a circular plate bearing on a Winkler-type foundation whose stiffness varied with radius was described. The type of variation allowed across an annulus with inner and outer radii b and a was $k(r) = k_b + \frac{(k_a - k_b)(r-b)}{a-b}$, that is a linear variation.

The results shown in Figs.5.12-5.14 were analysed using a computer program embodying the above assumption. By trial and error, the distribution of k was varied across each of the nine plates until the deflections obtained from the computer program were within 3% of the measured deflections. This did however prove impossible in the case of the 10 inch diameter, $\frac{1}{2}$ inch thick plate where the deflections at the centre of the plate, and at a radius of $\frac{1}{2}$ inch could not be fitted closer than 8% below the measured deflections. This was attributed to the presence of significant shear deformations in this the thickest of the plates tested, which were not included in the theoretical analysis. The calculated distributions of k values are shown in Figs.5.18-5.20.

Then on the basis of the Winkler hypothesis that the contact pressure $p = k \times$ the deflection of every point on the plate, the theoretical Winkler contact pressures could be calculated and are shown in Figs.5.21-5.23. These contact pressures are most interesting in that, apart from the thinnest (8 inch diameter, $\frac{1}{4}$ inch thick) plate, they show the "inverse parabolic" pressure distribution characteristic of plates bearing on semi-infinite elastic media. The infinite edge stresses predicted by the theory of the elastic medium are physically inadmissible in sands and it can be seen that all of the pressure distributions reduce to zero at the edges of the plates.

Other trends exhibited by the results are that the maximum contact pressure on any plate was found to decrease with increasing plate stiffness and with increasing plate size, and that the location of this maximum pressure was about $1\frac{1}{2}$ in. from the centre of the plate for all of the plates involved. It can be inferred

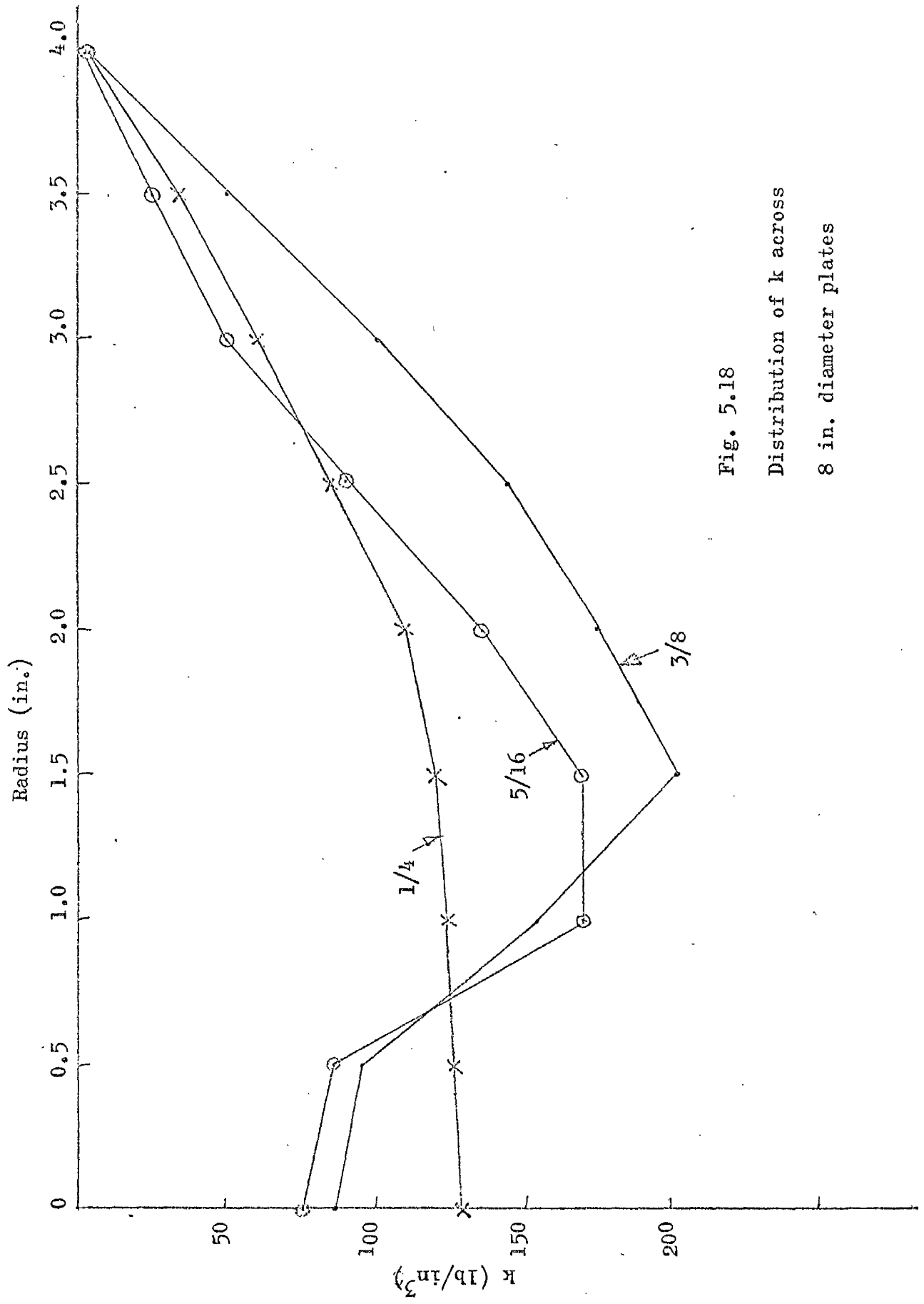


Fig. 5.18
 Distribution of k across
 8 in. diameter plates.

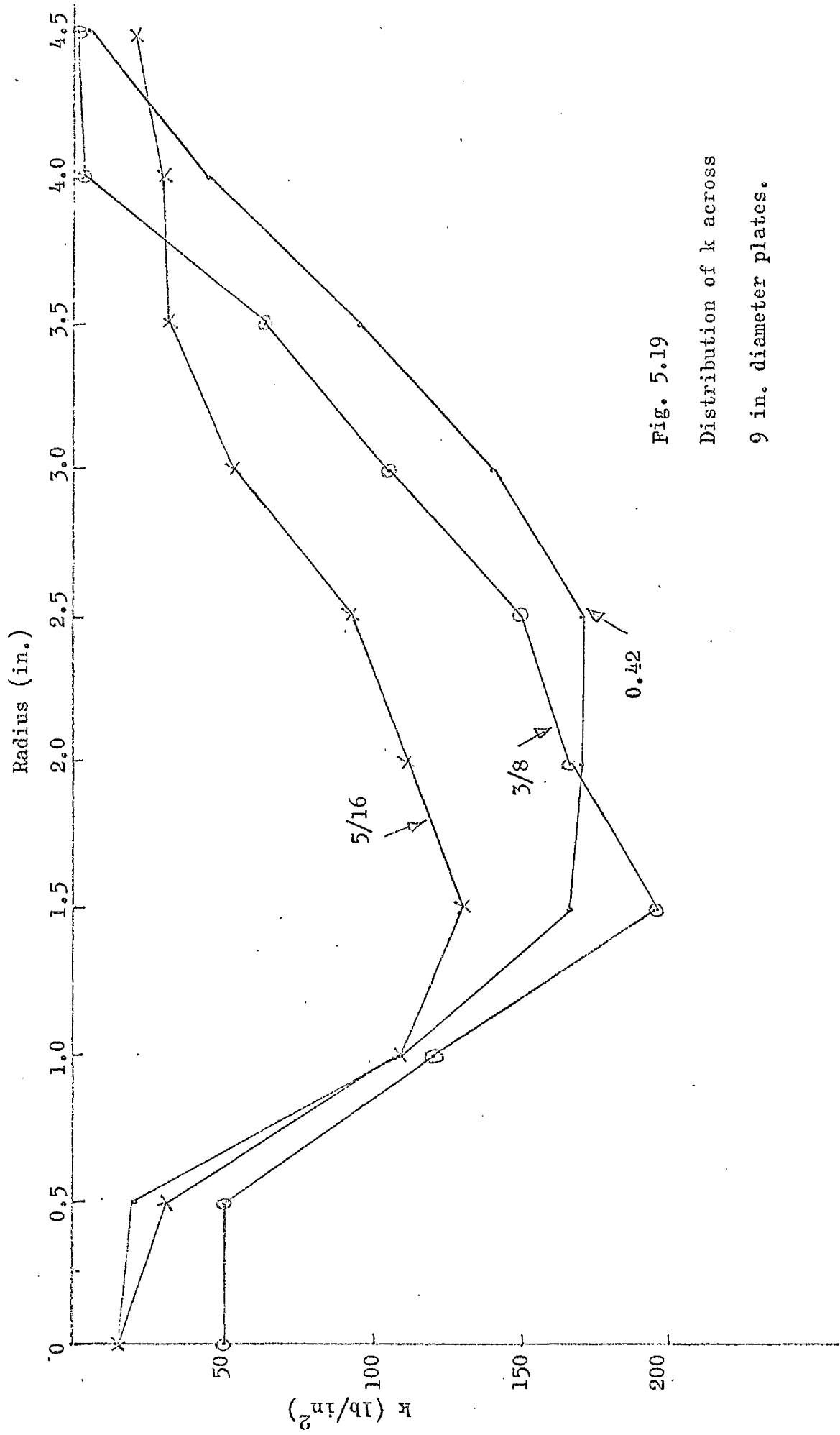


Fig. 5.19

Distribution of k across

9 in. diameter plates.

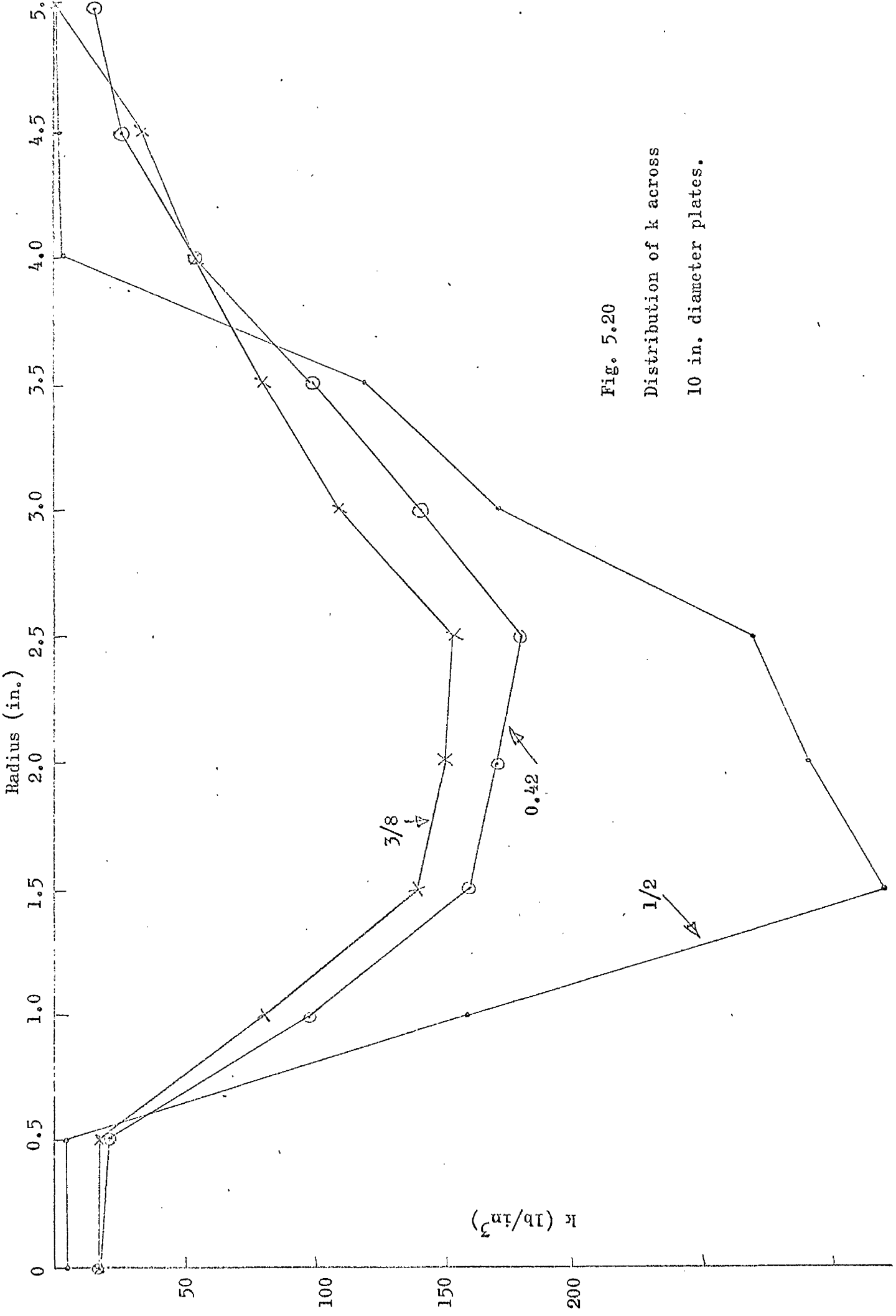


Fig. 5.20
 Distribution of k across
 10 in. diameter plates.

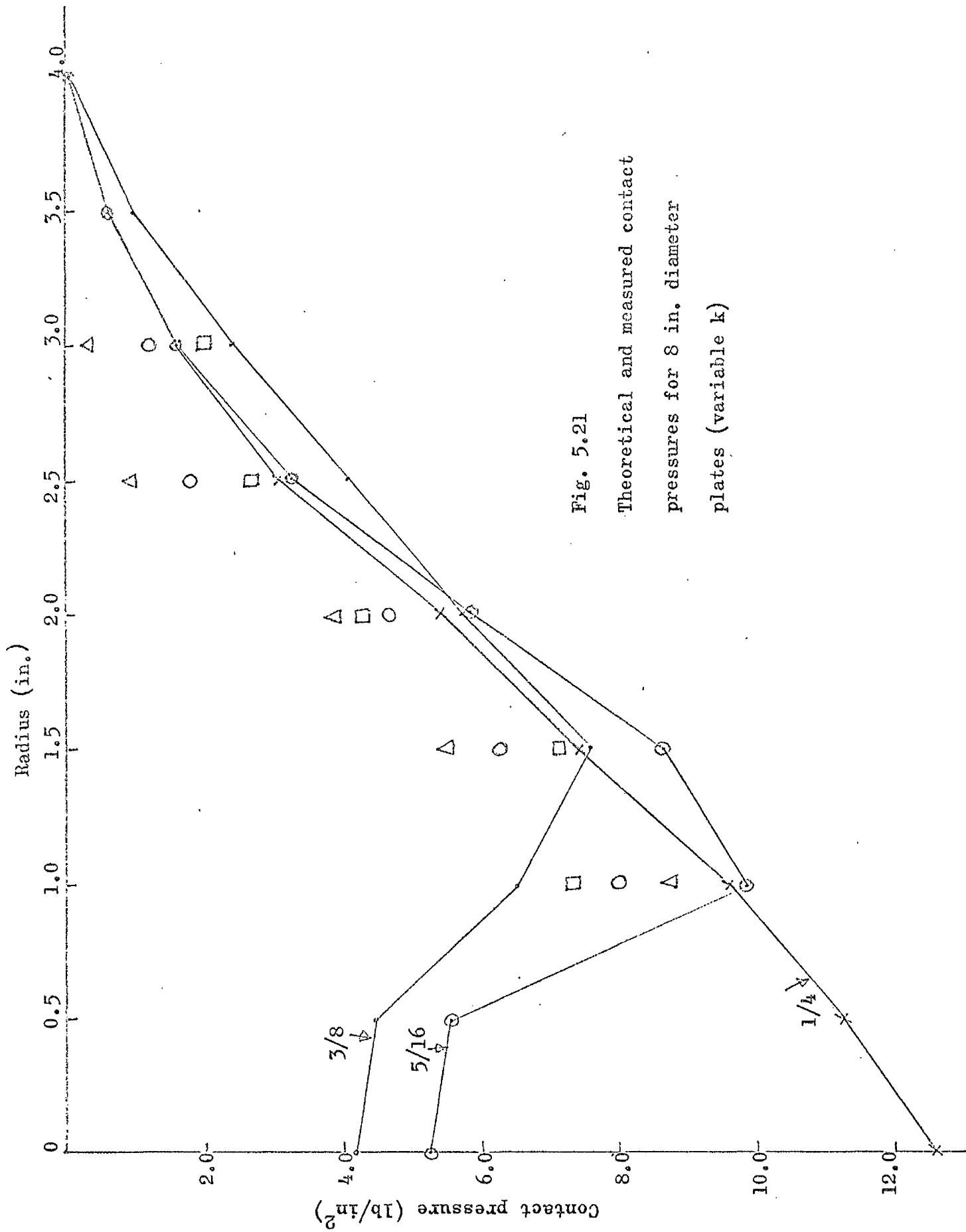


Fig. 5.21

Theoretical and measured contact pressures for 8 in. diameter plates (variable k)

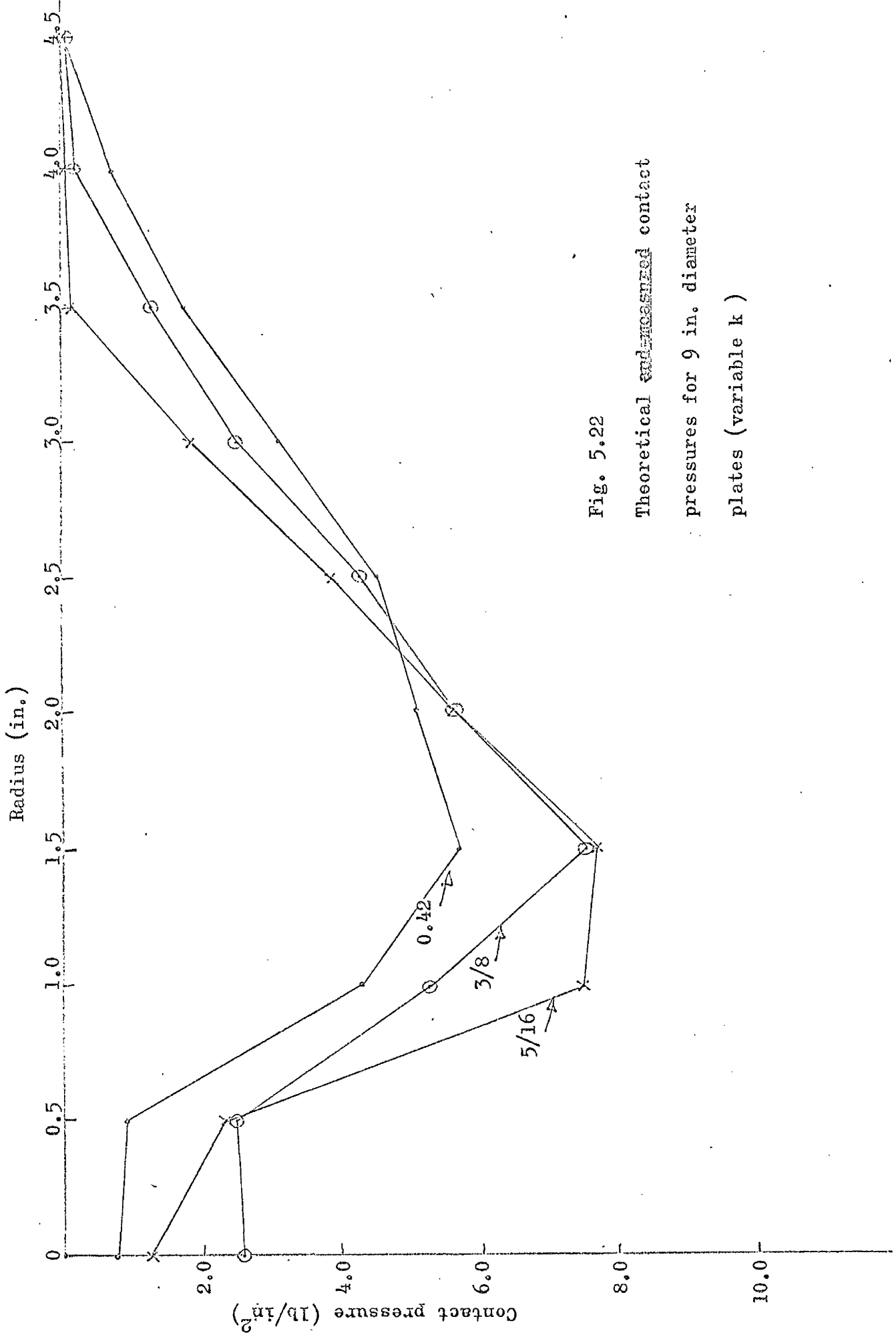


Fig. 5.22

Theoretical and measured contact pressures for 9 in. diameter plates (variable k)

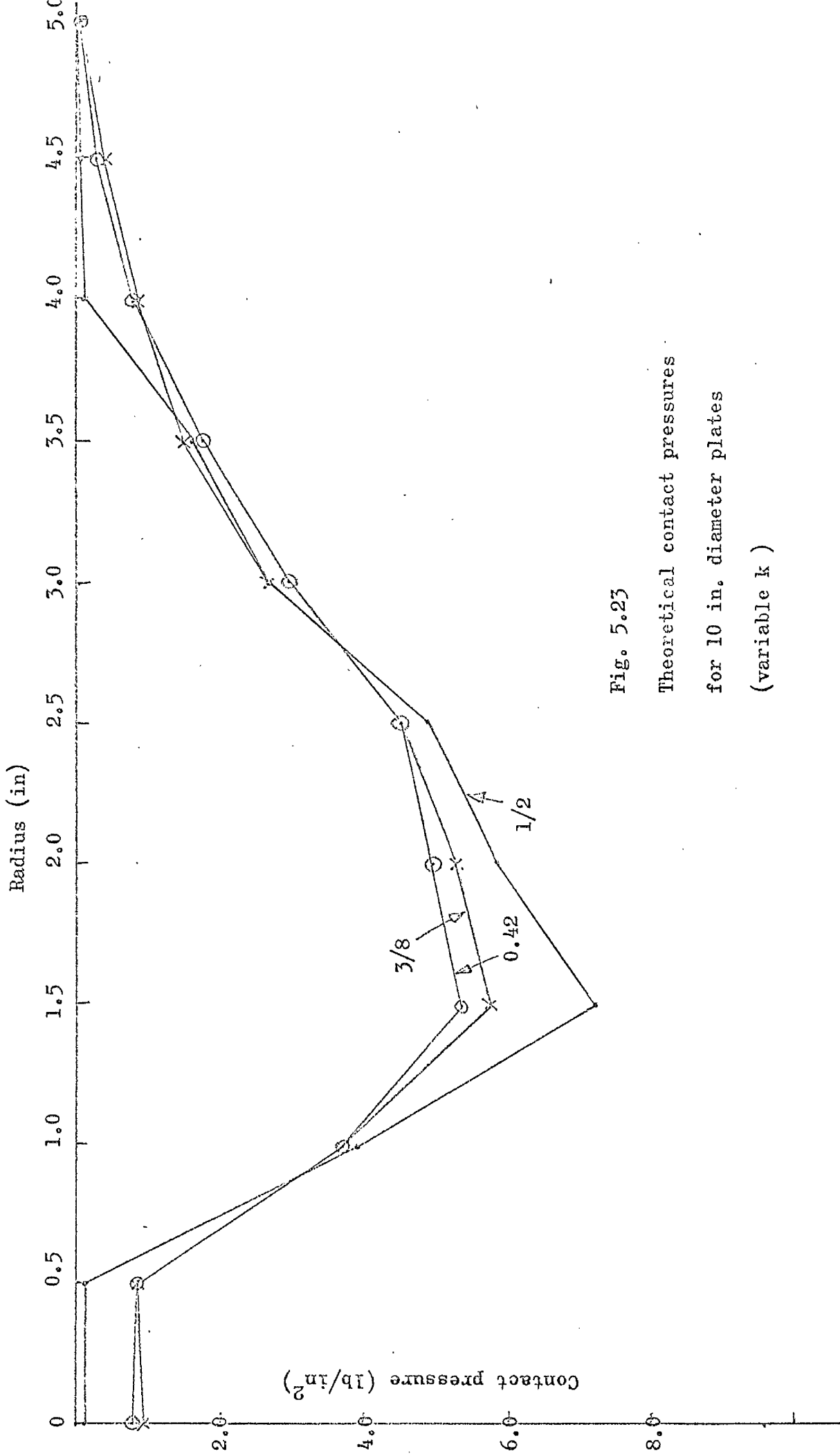


Fig. 5.23
 Theoretical contact pressures
 for 10 in. diameter plates
 (variable k)

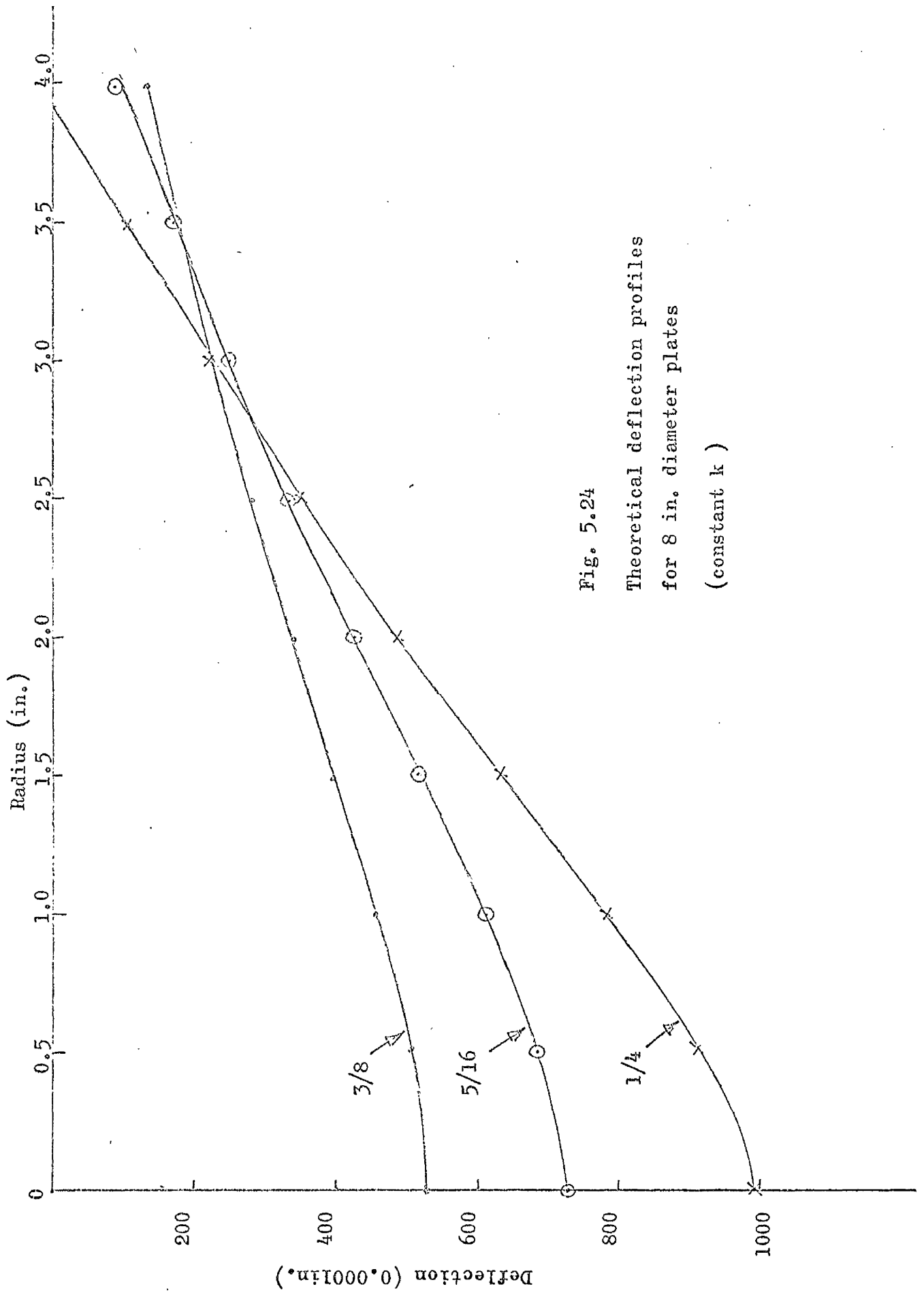


Fig. 5.24
 Theoretical deflection profiles
 for 8 in. diameter plates
 (constant k)

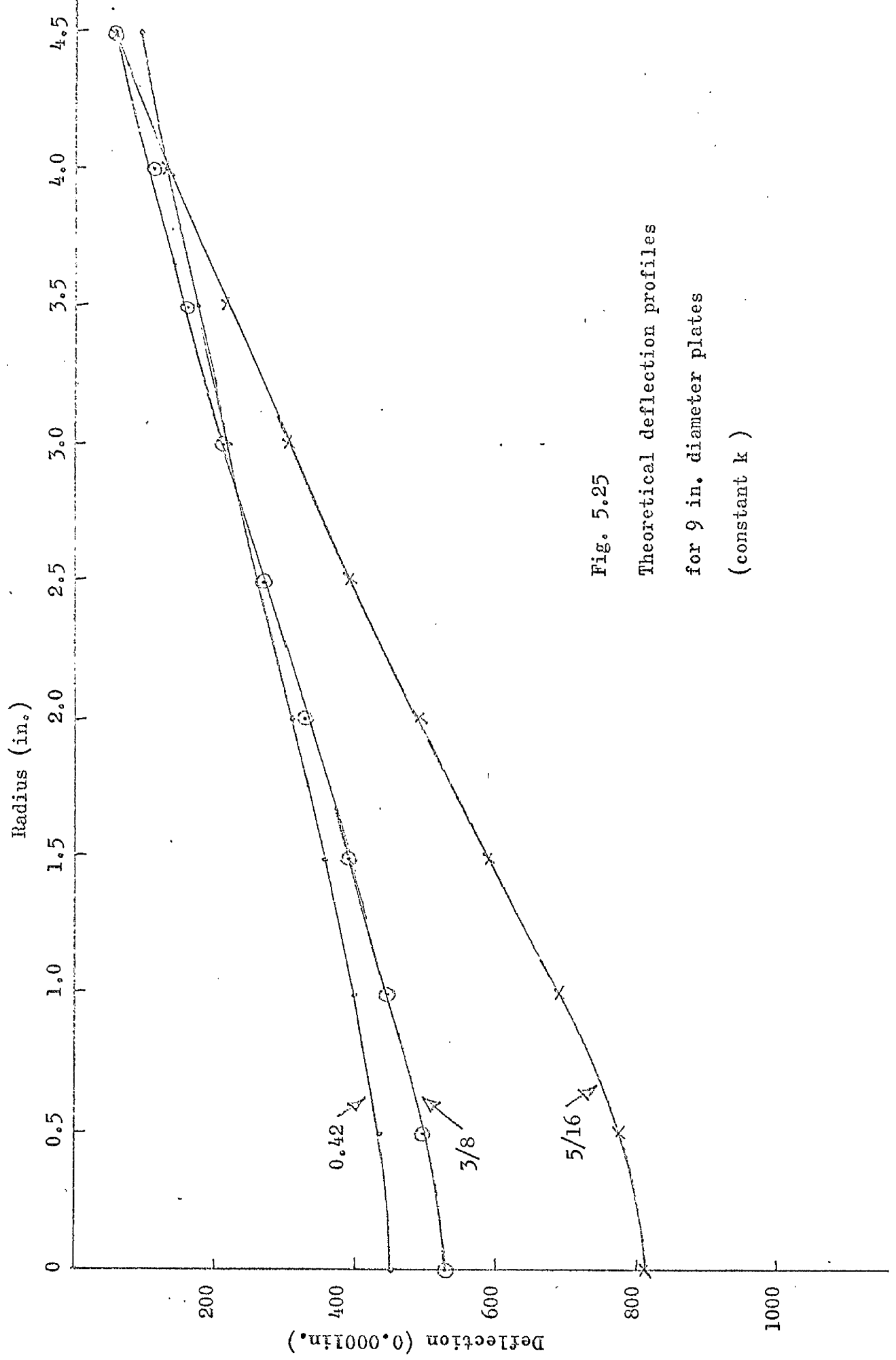


Fig. 5.25

Theoretical deflection profiles

for 9 in. diameter plates

(constant k)

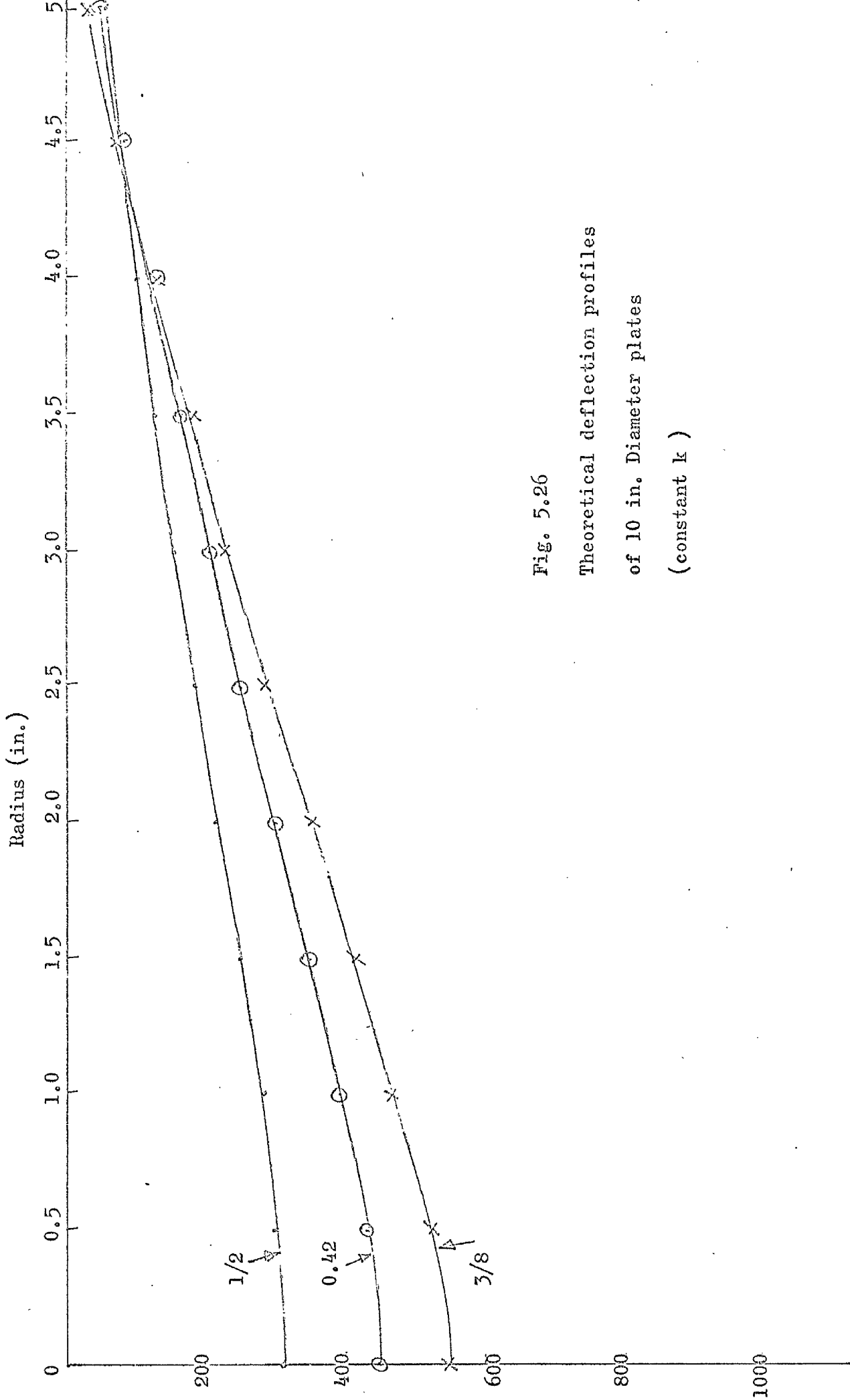


Fig. 5.26
 Theoretical deflection profiles
 of 10 in. Diameter plates
 (constant k)

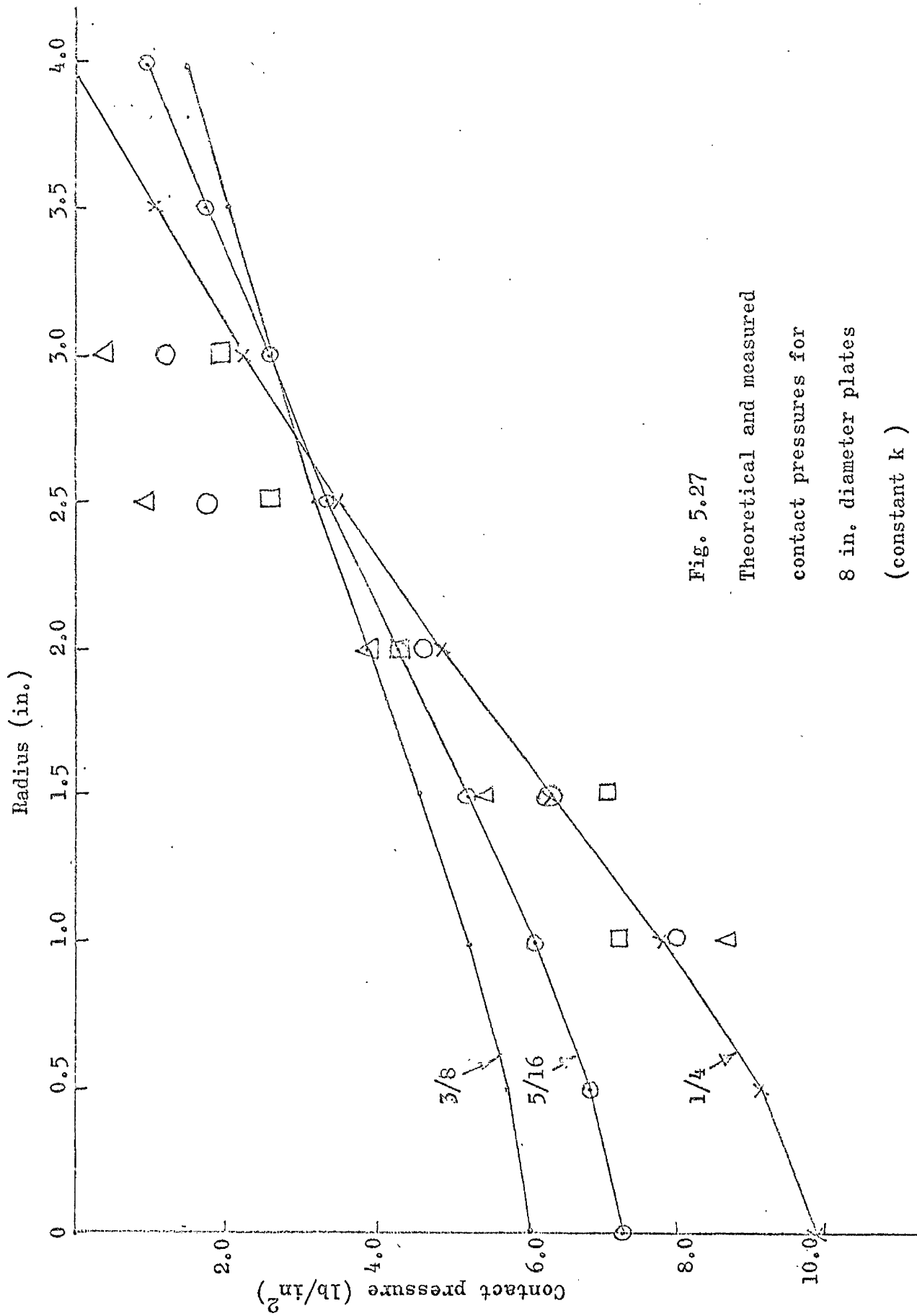


Fig. 5.27

Theoretical and measured
 contact pressures for
 8 in. diameter plates
 (constant k)

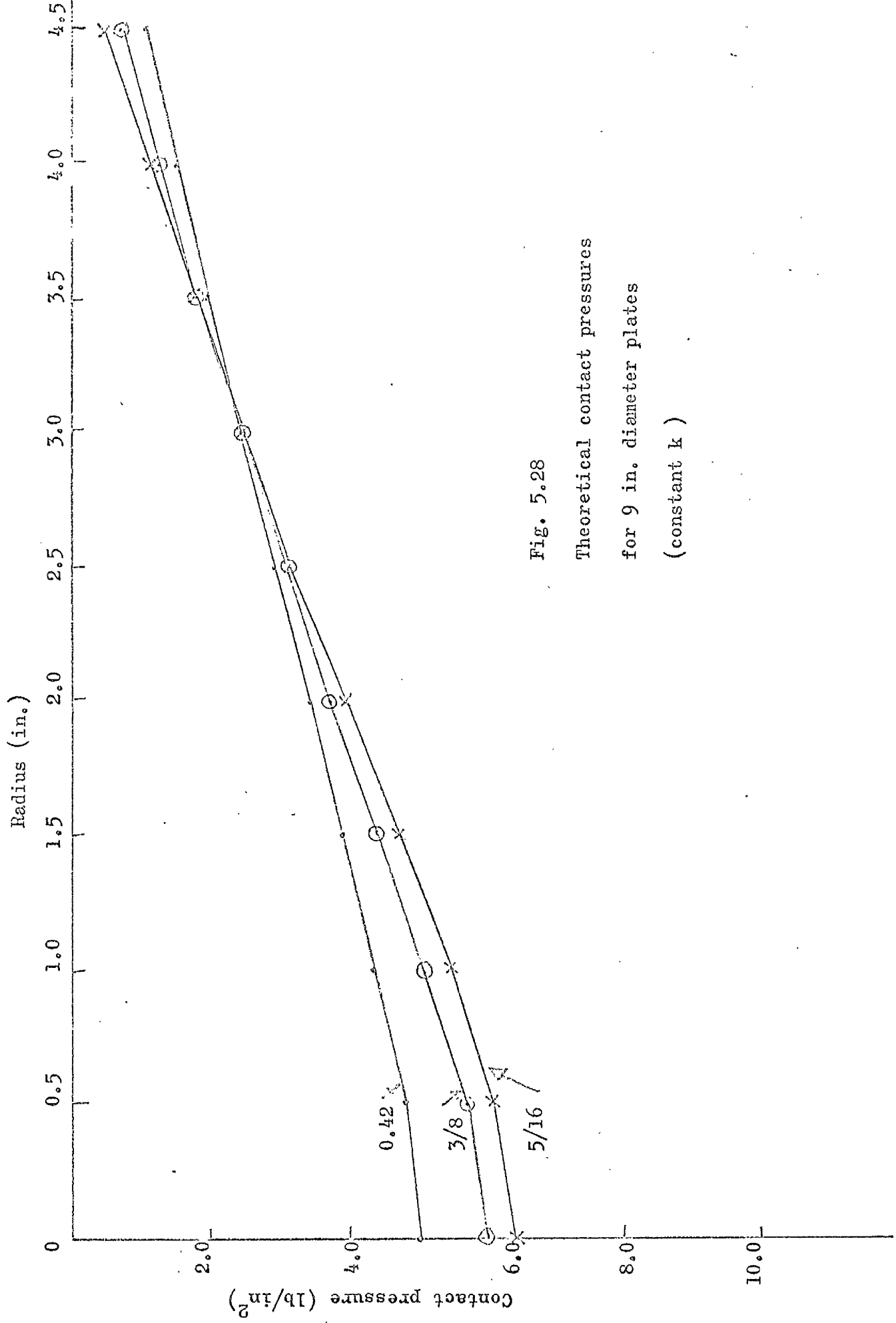


Fig. 5.28

Theoretical contact pressures
for 9 in. diameter plates
(constant k)

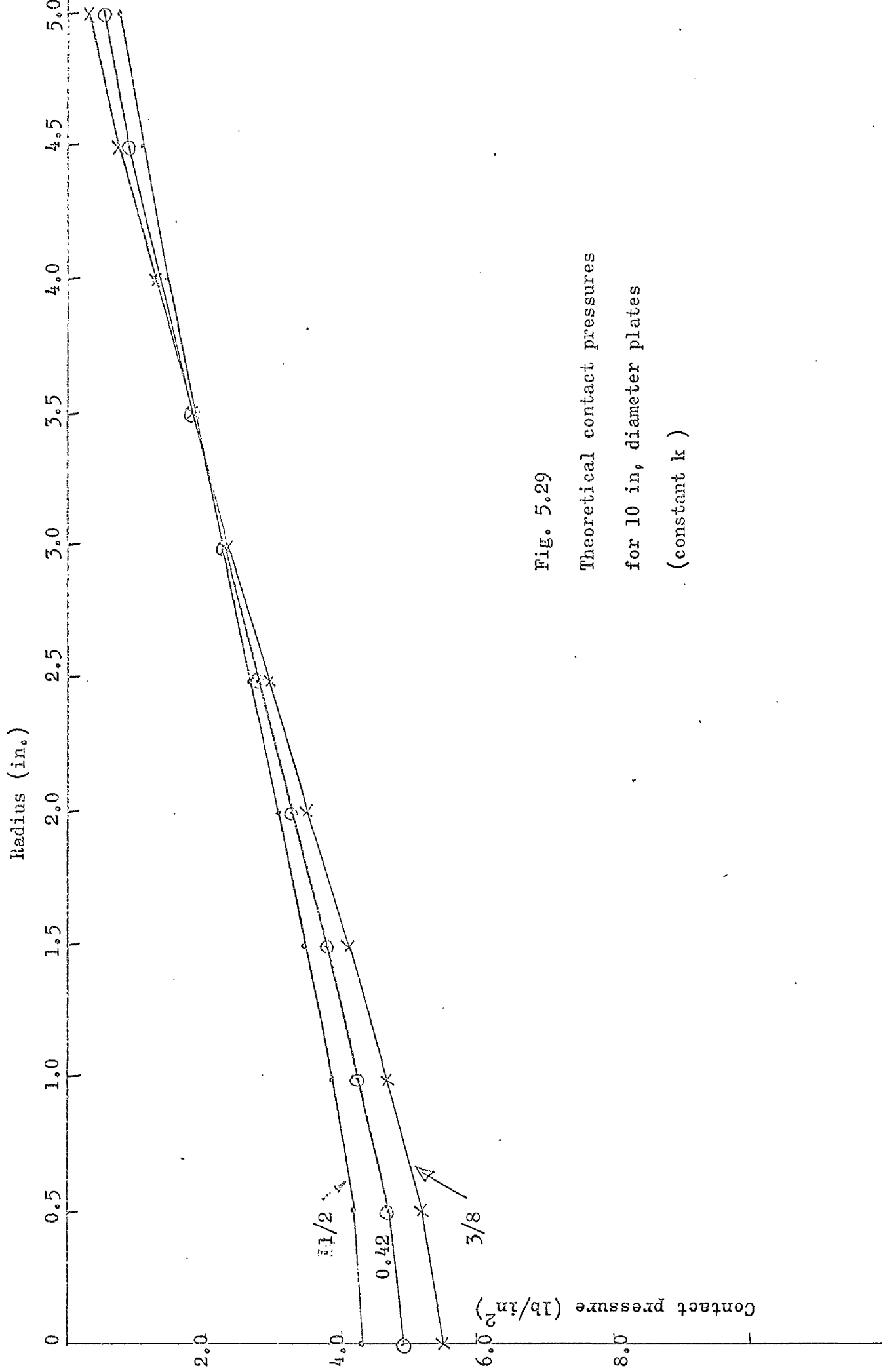


Fig. 5.29

Theoretical contact pressures
for 10 in. diameter plates
(constant k)

therefore that the pressure on a rigid punch would be a maximum at about the same position on the punch.

The measured contact pressures of Fig.5.16 have been superimposed on Fig.5.21 and can be seen to be in fairly good agreement with the predictions of the Winkler hypothesis. They are consistently below the predicted values, which could be due to the arching of the sand over the cells.

Since good agreement between experimental results and the predictions of theory using uniform Winkler media has been reported for beams (4), (25), this method was also examined. It was decided to fit the theoretical and experimental values of deflection at the centres of the plates, although other fits could be tried, for example a fit of average deflection. The deflected forms are shown in Figs.5.24-5.26 and should be compared with Figs.5.12-5.14. Superficially the results are quite good, especially near the centres of the plates, but towards the edges of the plates errors of 300% do occur.

The contact pressure distributions for the uniform Winkler assumptions are plotted in Figs.5.27-5.29 again with the measured values superimposed on Fig.5.27. In the range of radii containing the pressure cells there is not a great deal of difference between the uniform and non-uniform Winkler predictions, but the uniform theory predicts pressures which are too high at the edges and too low at the 1 inch and $1\frac{1}{2}$ inch positions. Unfortunately, due to the type of pressure cell used, no measurements could be taken near the centres of the plates, to check whether the reduced pressures predicted by the non-uniform Winkler theory actually occurred. However the high edge pressures predicted by the uniform Winkler theory are most unlikely in practice due to the very low strength of the unconfined sand. In addition, the measured contact pressures are in some cases greater than those predicted by the uniform Winkler theory. This implies cell action factors in excess of 1 which is unlikely.

Only preliminary results were obtained using the method of analysis described in Section 3.4, where the plate was coupled with a semi-infinite elastic medium in which inhomogeneity could be accounted for. Again by trial and error, the theoretical central deflection, treating the sand as a homogeneous semi-infinite elastic

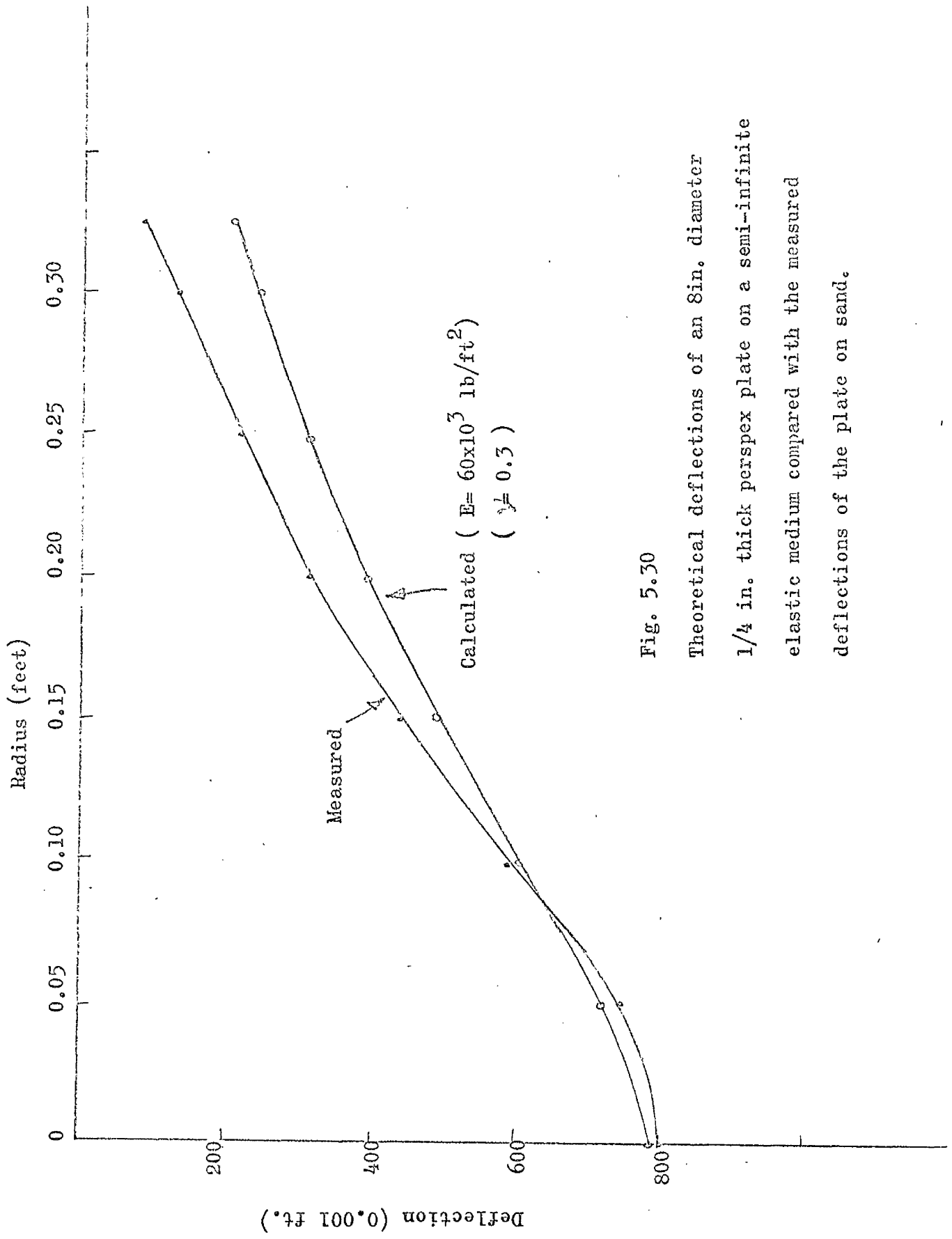


Fig. 5.30

Theoretical deflections of an 8in. diameter
1/4 in. thick perspex plate on a semi-infinite
elastic medium compared with the measured
deflections of the plate on sand.

medium with Poisson's Ratio of 0.3 was fitted to the measured central deflection. This gave an E value of 60,000 lb/ft² and the deflected form shown in Fig.5.30 together with the measured deflections. The theoretical deflections are too large at the edge of the plate and suggest a stiffening of the medium as the radius increases. However, due to the cumbersome nature of the computer program for this analysis, which was written at a time when only 14,300 words of store were available, and the slow turn-round time for programs due to the enlargement of the Glasgow computing installation, it was not feasible to pursue this analysis further. In any event, the contact pressure distributions would have the same form as those shown in Figs.5.21-5.23.

The only results directly comparable with those quoted above were obtained by Brand (88). In a limited series of tests on quite flexible plates, he obtained a set of parabolic pressure distributions similar to that obtained by the Author for the 8 inch diameter ¹/₄ inch thick plate. The tests on beams quoted in Section 5.1 can not readily be compared with tests on plates because a beam has negligible ability to spread load, and, when loaded by knife-edge loads across its full breadth merely attracts high pressures to the load points, as observed by Lenczner (87) and others.

Further experimental work on the behaviour of plates bearing on sand foundations should therefore be aimed at ascertaining whether the reduced contact pressures at the centres of all but the most flexible plates, predicted by the non-uniform Winkler theory, actually exist, and whether this is a feature of the density of the sand or the type of loading. Secondly, the method of analysis developed by the Author in Section 3.4 should be applied, using a more sophisticated computer program, to the analysis of experimental results, to determine the distribution of stiffness in a sand foundation assumed to be an inhomogeneous, elastic medium. As a reasonable starting point, the modulus of the sand could be increased with depth in proportion to the increase in standard penetration test values.

5.11 Conclusions

1. The rectangular finite element analyses for thin plates in bending, available in 1964, have been studied and some analyses which were thought to be different have been shown to be the same.
2. Three new rectangular finite element analyses for thin plates have been derived which have advantages over present methods. In particular, shear forces have been determined by the finite element method for the first time.
3. The finite element method, using rectangular elements, has been applied to problems of moderately thick plates for the first time.
4. An explicit stiffness matrix suitable for the analysis of circular plates in bending has been derived.
5. The possibility of applying the finite element method to problems of plates on elastic foundations where realistic account is taken of the inhomogeneity of soil deposits has been appreciated.
6. The finite difference method has been used for the solution of some plate problems which were previously thought to be difficult to solve by such methods.
7. The results of a series of tests involving flexible plates bearing on sand foundations have been analysed by theoretical methods, and the theoretical predictions have been partially confirmed, within the limitations of the apparatus used. The principal deduction, for a particular loading system and sand condition, is that the contact pressure distribution is of the form predicted by assuming the sand to be a semi-infinite elastic medium, rather than a pure Winkler medium.

REFERENCES.

1. Terzaghi, K. "Evaluation of Coefficients of Subgrade Reaction". Geotechnique, 5, 1955.
2. Hetenyi, M. "Beams on Elastic Foundations". University of Michigan Press, 1946.
3. Hetenyi, M. "Beams and Plates on Elastic Foundations and Related Problems". Applied Mechanics Reviews, 19, 1966.
4. Barden, L. Ph.D. Thesis, Liverpool University, 1962.
5. Hendry, A. "New Method for the Analysis of Beams on Elastic Foundations". Civil Engineering and Public Works Review, 53, 1958.
6. Timoshenko, S. and Woinowsky-Krieger, S. "Theory of Plates and Shells". McGraw-Hill, 1959.
7. Schleicher, F. "Kreisplatten auf elastischer Unterlage". Berlin, 1926.
8. Vint, J. and Elgood, W. "Deformation of a loaded Bloom Plate". Philosophical Magazine, 19, 1935.
9. Murphy, G. "Stress and Deflections in Loaded Rectangular Plates on Elastic Foundations". Iowa State College Eng. Expt. Sta. Bull. 135, 1937.
10. Pickett, G., Raville, M., Janes, W. and McCormick, F. "Deflections, Moments and Reactive Pressures for Concrete Pavements". Kansas State College Eng. Expt. Sta. Bull. 65, 1951.
11. Allen, D. and Severn, R. "The Stresses in Foundation Rafts". Proceedings of the Institution of Civil Engineers, 15, 1960: 20, 1961: 25, 1963.
12. Sawko, F. "Grid Frameworks with Normal Elastic Restraints at the Joints". Civil Engineering and Public Works Review, 58, 1963.
13. Kerr, A. "Elastic and Viscoelastic Foundation Models". Journal of Applied Mechanics, 31, 1964.
14. Severn, R. "The Solution of Foundation Mat Problems by Finite Element Methods". The Structural Engineer, 44, 1966.
15. Cheung, Y. and Zienkiewicz, O. "Plates and Tanks on Elastic Foundations - An Application of the Finite Element Method". International Journal of Solids and Structures, 1, 1965.
16. Holl, D. Proceedings of Fifth International Congress on Applied Mechanics, Cambridge, Mass., 1938.

17. Borowicka, H. "Druckverteilung unter Elastischen Platten". Ingenieur-Archiv, 10, 1939.
18. Gorbunov-Posadov, M. and Serebrjanyi, R. "Design of Structures on Elastic Foundations". Proceedings Fifth International Conference on Soil Mechanics and Foundation Engineering, Paris, 1961.
19. Habel, A. Bauingenieur, 18, 1937.
20. Pickett, G. and McCormick, F. "Circular and Rectangular Plates under Lateral Load and Supported by an Elastic Solid Foundation". Proc. First U.S. National Congress on Applied Mechanics, Chicago, 1951.
21. Barden, L. "Contact Pressures under Circular Slabs". The Structural Engineer, 43, 1965.
22. Barden, L. "Stress and Displacements in Cross-Anisotropic Soil". Geotechnique, 13, 1963.
23. Sommer, H. "A Method for Calculation of Settlements, Contact Pressures and Bending Moments in a Foundation, Including the Influence of Flexural Rigidity of the Superstructure". Proc. Sixth Int. Conf. Soil Mech. and Found. Eng. Montreal, 1965.
24. Tsyтовich, N. "General Report on Foundations of Structures". Proc. Fifth Int. Conf. Soil Mech. and Found. Eng. Paris, 1961.
25. Vesic, A. "Model Studies of Beams resting on a Silt Subgrade". Proc. A.S.C.E., Journal of the Soil Mechanics Division, February 1963.
26. Jakobsen, B. "Some Fundamental Properties of Sand". Proc. Fourth Int. Conf. Soil Mech. and Found. Eng. London, 1957.
27. Chaplin, T. "Compressibility of Sands and Settlements of Model Footings and Piles in Sand". Proc. Fifth Int. Conf. Soil Mech. and Found. Eng. Paris, 1961.
28. Schultze, E. and Moussa, A. "Factors affecting the Compressibility of a Sand". Proc. Fifth Int. Conf. Soil Mech. and Found. Eng. Paris, 1961.
29. Brinch Hansen, J. "Stress-Strain relationships for Sand". Danish Geotechnical Bulletin, 20, 1966.
30. Rowe, P. "The Stress-Dilatency Relation for Static Equilibrium of an Assembly of Particles in Contact". Proc. Royal Society, A269, 1962.
31. "Suggested Design Procedures for Combined Footings and Mats". Report of A.C.I. Committee No. 436. Journal of A.C.I. 63, 1966.

32. Baker, A. "Raft Foundations". Concrete Publications Ltd. 1957.
33. Baker, A. Proceedings of the Institution of Civil Engineers, 17, 1960.
34. Johansen, K. "Yield Line Theory". Cement and Concrete Association, 1962.
35. Wood, R. "Plastic and Elastic Design of Slabs and Plates". Thames and Hudson, 1961.
36. Davies, J. "Yield Line Theory applied to Edge Loaded Circular Foundation Slabs". Civil Engineering and Public Works Review, 57, 1962.
37. Southwell, R. "Relaxation Methods in Theoretical Physics". Vol. II. University Press, Oxford, 1956.
38. Hrennikoff, A. "Solution of Problems in Elasticity by the Framework Method". Journal of Applied Mechanics, 8, 1941.
39. McHenry, D. "A Lattice Analogy for the Solution of Plane Stress Problems". Journal of the Institution of Civil Engineers, 21, 1943-44.
40. Yettram, A. and Husain, H. "Grid Framework Method for Plates in Flexure". Proc. A.S.C.E., 91, E.M.3., 1965.
41. Hrennikoff, A. Proc. A.S.C.E., 92, E.M.3., 1966.
42. Argyris, J. "Energy Theorems and Structural Analysis". Butterworth's London, 1960.
43. Turner, M., Clough, R., Martin, H. and Topp, L. "Stiffness and Deflection Analysis of Complex Structures". Journal of the Aeronautical Sciences, 23, 1956.
44. Argyris, J. "On the Analysis of Complex Elastic Structures". Applied Mechanics Reviews, 11, 1958.
45. Gallagher, R. "A Correlation Study of Methods of Matrix Structural Analysis". Pergamon, 1964.
46. Fraeijs de Venbeke, B. "Matrix Methods of Structural Analysis". Pergamon, 1964.
47. Melosh, R. "Basis for Derivation of Matrices for the Direct Stiffness Method". A.I.A.A. Journal, 1, 1963.
48. Denke, P. "Matrix Methods of Structural Analysis". Pergamon, 1964.
49. Taig, I. "Structural Analysis by the Matrix Displacement Method". English Electric Report, S.O. 17. 1962.

50. Adini, A. M.S. Thesis. University of California at Berkeley, 1959.
51. Papenfuss, S. M.S. Thesis, University of Washington, 1959.
52. Dill, E and Ortega, M. "Derivation of a Stiffness Matrix for a Rectangular Plate Element in Bending". Boeing Report S.A.R.M. 13, 1960.
53. Melosh, R. "A Stiffness Matrix for the Analysis of Thin Plates in Bending". Journal of the Aerospace Sciences, 28, 1961.
54. Pearson, K. "On the Construction of Tables and on Interpolation". Tracts for Computers, II, Cambridge, 1919.
55. Zienkiewicz, O. and Cheung, Y. "The Finite Element Method for Analysis of Elastic Isotropic and Orthotropic Slabs". Proc. I.C.E. 28, 1964.
56. Tocher, J. and Kapur, K. Journal of A.I.A.A. (Technical Comment) 3, 1965.
57. Clough, R. and Tocher, J. "Finite Element Stiffness Matrices for Analysis of Plates in Bending". A.F.I.T. Conference, Ohio, 1965.
58. Schmit, L. "Energy Search Methods of Structural Analysis". A.F.I.T. Conference, Ohio, 1964.
59. Severn, R. and Taylor, P. "The Finite Element Method for Flexure of Slabs when Stress Distributions are Assumed". Proc. I.C.E.34, 1966.
60. Zienkiewicz, O., Mayer P. and Cheung, Y. Proc. A.S.C.E., 92, E.M.I. 1966.
61. Duncan, W. Ph.D. Thesis, Glasgow University. (Forthcoming).
62. Bogner, F., Fox, R., and Schmit, L. "The Generation of Interelement Compatible Stiffness and Mass Matrices by the Use of Interpolation Formulas". A.F.I.T. Conference, Ohio, 1965.
63. Hansteen, H. "Finite Element Displacement Analysis of Plate Bending Based on Rectangular Elements". Int. Conf. Use Computers in Civil Eng., Newcastle University, 1966.
64. Butlin, G. and Leckie, F. "A Study of Finite Elements Applied to Plate Flexure". Symposium on Numerical Methods in Vibration Problems, Institute of Sound and Vibration Research, Southampton University, 1966.
65. Gallagher R. "The Development and Evaluation of Matrix Methods for Thin Shell Structural Analysis". Bell Aerosystems Report 8500 - 902011, 1966

66. (a) Argyris, J. "Continua and Discontinua". A.F.I.T. Conference, Ohio, 1965.
(b) Argyris, J. "Matrix Displacement Analysis of Plates and Shells". Ingenieur - Archiv, 35, 1966.
67. Bazeley, G., Cheung, Y., Irons, B. and Zienkiewicz, O. "Triangular Elements in Plate Bending - Conforming and Non-Conforming Solutions". A.F.I.T. Conference, Ohio, 1965.
68. Jones, R. "A Generalization of the Direct-Stiffness Method of Structural Analysis". A.I.A.A. Journal, 2, 1964.
69. Pian, T. "Derivation of Element Stiffness Matrices by Assumed Stress Distributions". A.I.A.A. Journal (Technical Note) 2, 1964.
70. Pian, T. "Element Stiffness Matrices for Boundary Compatibility and for Prescribed Boundary Stresses". A.F.I.T. Conference, Ohio, 1965.
71. Gallagher, R. Comments on Reference 69, A.I.A.A. Journal (Technical Comments), 3, 1965.
72. Smith, I. Proceedings of the Institution of Civil Engineers, 35, 1966.
73. Reissner, E. "The Effect of Transverse Shear Deformation on the Bending of Elastic Plates". Journal of Applied Mechanics, 12, 1945.
74. Love, A. "The Mathematical Theory of Elasticity". Cambridge University Press, 1927.
75. Salerno, V. and Goldberg, M. "Effect of Shear Deformation on the Bending of Rectangular Plates". Journal of Applied Mechanics, 27, 1960.
76. Herrmann, L. "A Bending Analysis for Plates". A.F.I.T. Conference, Ohio, 1965.
77. Grafton, P. and Strome, D. "Analysis of Axisymmetric Shells by the Direct Stiffness Method". A.I.A.A. Journal 1, 1963.
78. Macleod, I. Ph.D. Thesis, Glasgow University, 1966.
79. Melosh, R. "Structural Analysis of Solids". Third A.S.C.E. Conference on Electronic Computation, Proc. A.S.C.E. 89, S.T.4., 1963.
80. Argyris, J. "Three-Dimensional Anisotropic and Inhomogeneous Elastic Media-Matrix Analysis for Small and Large Displacements". Ingenieur-Archiv, 34, 1965.
81. Argyris, J. "Tetrahedron Elements with Linearly varying Strain for the Matrix Displacement Method". Journal of the Royal Aeronautical Society, 69, 1965.

82. Clough, R. and Rashid, Y. "Finite Element Analysis of Axisymmetric Solids". Proc. A.S.C.E., 91, E.M.I. 1965.
83. Argyris, J. "The TRIAX 6 Element for Axisymmetric Analysis by the Matrix Displacement Method". Journal Royal Aero. Soc. 70, 1966.
84. Lee, S. and Ballerteros, P. "Uniformly Loaded Rectangular Plate supported at the Corners". International Journal of Mechanical Science, 2, 1960.
85. Haber, O. "Pressure Distribution under Bases and Stability of Foundations". Structural Engineer, 11, 1933.
86. Wright, W. Ph.D. Thesis, Aberdeen University, 1952.
87. Lenczner, D. Ph.D. Thesis, Nottingham University, 1962.
88. Brand, E. Ph.D. Thesis, Leeds University, 1963.
89. l'Herminier R., Bachelier, M. and Soeiro, F. "Investigation on the Foundation Raft for the First Atomic Reactor at Marcoule". Proc. Fourth Int. Conf. Soil Mech. and Found. Eng. London, 1957.
90. Neale, D. Ph.D. Thesis, Glasgow University, 1966.
91. Rowe, P. and Briggs, A. "Measurements on Model Strutted Sheet Pile Excavations". Proc. Fifth Int. Conf. Soil Mech. and Foundation Eng., Paris 1961.
92. Peaker, K. Ph.D. Thesis, Manchester University, 1963.
93. "Soil Pressure Cell Investigation". U.S. Waterways Experiment Station, Technical Memo. 210-1, 1944.
94. Trollope, D. and Lee, I. "The measurement of Soil Pressures". Proc. Fifth Int. Conf. Soil Mech. and Found. Eng., Paris, 1961.
95. Allwood, R. Ph.D. Thesis, Birmingham University, 1956.

APPENDIX 1

Fifth Order Stiffness Matrix

$$[K] = \begin{bmatrix} [A_1] & & & & \\ [B_1] & [A_2] & & & \\ [C_1] & [D_2] & [A_3] & & \\ [D_1] & [C_2] & [B_2] & [A_4] & \end{bmatrix}$$

Symmetrical

Submatrices denoted by the same letter contain identical terms but the signs of the terms are subject to change:

$$A_1 = \begin{bmatrix} K_{1,1} & & & & & \\ K_{2,1} & K_{2,2} & & & & \\ K_{3,1} & K_{3,2} & K_{3,3} & & & \\ K_{4,1} & K_{4,2} & K_{4,3} & K_{4,4} & & \\ K_{5,1} & K_{5,2} & K_{5,3} & K_{5,4} & K_{5,5} & \\ K_{6,1} & K_{6,2} & K_{6,3} & K_{6,4} & K_{6,5} & K_{6,6} \end{bmatrix}$$

Symmetrical

$$A_2 = \begin{bmatrix} K_{1,1} & & & & & \\ K_{2,1} & K_{2,2} & & & & \\ -K_{3,1} & -K_{3,2} & K_{3,3} & & & \\ K_{4,1} & K_{4,2} & -K_{4,3} & K_{4,4} & & \\ K_{5,1} & K_{5,2} & -K_{5,3} & K_{5,4} & K_{5,5} & \\ -K_{6,1} & -K_{6,2} & K_{6,3} & -K_{6,4} & -K_{6,5} & K_{6,6} \end{bmatrix}$$

Symmetrical

$$A_3 = \begin{bmatrix} K_{1,1} & & & & & \\ -K_{2,1} & K_{2,2} & & & & \\ -K_{3,1} & K_{3,2} & K_{3,3} & & & \\ K_{4,1} & -K_{4,2} & -K_{4,3} & K_{4,4} & & \\ K_{5,1} & -K_{5,2} & -K_{5,3} & K_{5,4} & K_{5,5} & \\ K_{6,1} & -K_{6,2} & -K_{6,3} & K_{6,4} & K_{6,5} & K_{6,6} \end{bmatrix}$$

Symmetrical

$$A_4 = \begin{bmatrix} K_{1,1} & & & & & \\ -K_{2,1} & K_{2,2} & & & & \\ K_{3,1} & -K_{3,2} & K_{3,3} & & & \\ K_{4,1} & -K_{4,2} & K_{4,3} & K_{4,4} & & \\ K_{5,1} & -K_{5,2} & K_{5,3} & K_{5,4} & K_{5,5} & \\ -K_{6,1} & K_{6,2} & -K_{6,3} & -K_{6,4} & -K_{6,5} & K_{6,6} \end{bmatrix}$$

Symmetrical

$$B_1 = \begin{bmatrix} K_{7,1} & K_{7,2} & K_{7,3} & K_{7,4} & K_{7,5} & -K_{12,1} \\ K_{8,1} & K_{8,2} & -K_{12,1} & K_{10,2} & K_{11,2} & -K_{12,2} \\ K_{9,1} & K_{9,2} & K_{9,3} & K_{10,3} & -K_{11,3} & K_{12,3} \\ K_{10,1} & K_{10,2} & K_{10,3} & K_{10,4} & K_{10,5} & K_{10,6} \\ K_{11,1} & K_{11,2} & K_{11,3} & K_{11,4} & K_{11,5} & K_{11,6} \\ K_{12,1} & K_{12,2} & K_{12,3} & K_{12,4} & K_{12,5} & K_{12,6} \end{bmatrix}$$

$$B_2 = \begin{bmatrix} K_{7,1} & -K_{7,2} & -K_{7,3} & K_{7,4} & K_{7,5} & K_{7,6} \\ -K_{8,1} & K_{8,2} & K_{8,3} & -K_{8,4} & -K_{8,5} & -K_{8,6} \\ -K_{9,1} & K_{9,2} & K_{9,3} & -K_{9,4} & -K_{9,5} & -K_{9,6} \\ K_{10,1} & -K_{10,2} & -K_{10,3} & K_{10,4} & K_{10,5} & K_{10,6} \\ K_{11,1} & -K_{11,2} & -K_{11,3} & K_{11,4} & K_{11,5} & K_{11,6} \\ K_{12,1} & -K_{12,2} & -K_{12,3} & K_{12,4} & K_{12,5} & K_{12,6} \end{bmatrix}$$

$$C_1 = \begin{bmatrix} K_{13,1} & K_{13,2} & K_{13,3} & K_{13,4} & K_{13,5} & K_{18,1} \\ K_{14,1} & K_{14,2} & -K_{18,1} & -K_{16,2} & -K_{17,2} & -K_{18,2} \\ K_{15,1} & -K_{18,1} & K_{15,3} & -K_{16,3} & -K_{18,3} & -K_{18,3} \\ K_{16,1} & K_{16,2} & K_{16,3} & K_{16,4} & K_{16,5} & K_{16,6} \\ K_{17,1} & K_{17,2} & K_{17,3} & K_{17,4} & K_{17,5} & K_{17,6} \\ K_{18,1} & K_{18,2} & K_{18,3} & K_{18,4} & K_{18,5} & K_{18,6} \end{bmatrix}$$

$$C_2 = \begin{bmatrix} K_{13,1} & K_{13,2} & -K_{13,3} & K_{13,4} & K_{13,5} & -K_{13,6} \\ K_{14,1} & K_{14,2} & -K_{14,3} & K_{14,4} & K_{14,5} & -K_{14,6} \\ -K_{15,1} & -K_{15,2} & K_{15,3} & -K_{15,4} & -K_{15,5} & K_{15,6} \\ K_{16,1} & K_{16,2} & -K_{16,3} & K_{16,4} & K_{16,5} & -K_{16,6} \\ K_{17,1} & K_{17,2} & -K_{17,3} & K_{17,4} & K_{17,5} & -K_{17,6} \\ -K_{18,1} & -K_{18,2} & K_{18,3} & -K_{18,4} & -K_{18,5} & K_{18,6} \end{bmatrix}$$

$$D_1 = \begin{bmatrix} K_{19,1} & K_{19,2} & K_{19,3} & K_{19,4} & K_{19,5} & -K_{24,1} \\ K_{20,1} & K_{20,2} & K_{24,1} & -K_{22,2} & -K_{23,2} & K_{24,2} \\ K_{21,1} & -K_{24,1} & K_{21,3} & K_{22,3} & K_{23,3} & -K_{24,3} \\ K_{22,1} & K_{22,2} & K_{22,3} & K_{22,4} & K_{22,5} & K_{22,6} \\ K_{23,1} & K_{23,2} & K_{23,3} & K_{23,4} & K_{23,5} & K_{23,6} \\ K_{24,1} & K_{24,2} & K_{24,3} & K_{24,4} & K_{24,5} & K_{24,6} \end{bmatrix}$$

$$D_2 = \begin{bmatrix} K_{19,1} & K_{19,2} & -K_{19,3} & K_{19,4} & K_{19,5} & -K_{19,6} \\ K_{20,1} & K_{20,2} & -K_{20,3} & K_{20,4} & K_{20,5} & -K_{20,6} \\ -K_{21,1} & -K_{22,2} & K_{21,3} & -K_{21,4} & -K_{21,5} & K_{21,6} \\ K_{22,1} & K_{22,2} & -K_{22,3} & K_{22,4} & K_{22,5} & -K_{22,6} \\ K_{23,1} & K_{23,2} & -K_{23,3} & K_{23,4} & K_{23,5} & -K_{23,6} \\ -K_{24,1} & -K_{24,2} & K_{24,3} & -K_{24,4} & -K_{24,5} & K_{24,6} \end{bmatrix}$$

Algebraically for example:

$$K_{1,1} = 3600 \left[\frac{181}{210.462} \frac{b}{a^3} A_{11} + \frac{2}{42.42} \frac{1}{ab} A_{21} \right. \\ \left. + \frac{181}{210.462} \frac{a}{b^3} A_{22} + \frac{900}{630.630} \frac{1}{ab} A_{33} \right]$$

where A_{11} etc. are the coefficients in the generalised moment-curvature relationship:

$$\begin{Bmatrix} M_{xx} \\ M_{yy} \\ M_{xy} \end{Bmatrix} = \begin{bmatrix} A_{11} & A_{21} & 0 \\ A_{21} & A_{22} & 0 \\ 0 & 0 & A_{33} \end{bmatrix} \begin{Bmatrix} \frac{\partial^2 w}{\partial x^2} \\ \frac{\partial^2 w}{\partial y^2} \\ \frac{\partial^2 w}{\partial x \partial y} \end{Bmatrix}$$

In practice it is easier to obtain the terms of K from the computer program given in Appendix 4.

The numerical values of the terms of K for a square element of side one unit and flexural rigidity $D =$ one unit ($\nu = 0.3$) are given on the next page.

Numerical values of the first 6 columns of K :

+1.7514 _n +1	+5.5529 _n +0	+5.5529 _n +0	+2.8881 _n -1	+2.8881 _n -1	+1.3744 _n +0
+5.5529 _n +0	+3.0595 _n +0	+1.6744 _n +0	+1.9208 _n -1	+8.0968 _n -2	+6.6444 _n -1
+5.5529 _n +0	+1.6744 _n +0	+3.0595 _n +0	+8.0968 _n -2	+1.9208 _n -1	+6.6444 _n -1
+2.8881 _n -1	+1.9208 _n -1	+8.0968 _n -2	+4.0055 _n -2	+4.6279 _n -3	+4.3967 _n -2
+2.8881 _n -1	+8.0968 _n -2	+1.9208 _n -1	+4.6279 _n -3	+4.0055 _n -2	+4.3967 _n -2
+1.3744 _n +0	+6.6444 _n -1	+6.6444 _n -1	+4.3967 _n -2	+4.3967 _n -2	+2.6914 _n -1
-8.9425 _n +0	-1.2672 _n +0	-3.4100 _n +0	-7.4521 _n -2	-1.4595 _n -1	-4.5297 _n -1
-1.2672 _n +0	-3.1664 _n -1	-4.5297 _n -1	-3.4941 _n -2	-9.5393 _n -3	-4.7297 _n -2
+3.4100 _n +0	+4.5297 _n -1	+1.0036 _n +0	+3.4539 _n -2	+1.5090 _n -2	+1.1506 _n -1
-7.4521 _n -2	-3.4941 _n -2	-3.4539 _n -2	-2.8021 _n -3	-1.0565 _n -3	-7.5387 _n -3
-1.4595 _n -1	-9.5393 _n -3	-1.5090 _n -2	-1.0565 _n -3	+9.4104 _n -3	+3.8157 _n -3
+4.5297 _n -1	+4.7297 _n -2	+1.1506 _n -1	+7.5387 _n -3	-3.8157 _n -3	-1.2863 _n -2
+3.7106 _n -1	-8.7570 _n -1	-8.7570 _n -1	-6.8336 _n -2	-6.8336 _n -2	-4.6846 _n -1
+8.7570 _n -1	+5.3927 _n -1	+4.6846 _n -1	+4.2053 _n -2	+3.6889 _n -2	+1.8923 _n -1
+8.7570 _n -1	+4.6846 _n -1	+5.3927 _n -1	+3.6889 _n -2	+4.2053 _n -2	+1.8923 _n -1
-6.8336 _n -2	-4.2053 _n -2	-3.6889 _n -2	-2.2676 _n -3	-2.5149 _n -3	-1.3816 _n -2
-6.8336 _n -2	-3.6889 _n -2	-4.2053 _n -2	-2.5149 _n -3	-2.2676 _n -3	-1.3816 _n -2
-4.6846 _n -1	-1.8923 _n -1	-1.8923 _n -1	-1.3816 _n -2	-1.3816 _n -2	-5.8813 _n -2
-8.9425 _n +0	-3.4100 _n +0	-1.2672 _n +0	-1.4595 _n -1	-7.4521 _n -2	-4.5297 _n -1
+3.4100 _n +0	+1.0036 _n +0	+4.5297 _n -1	+1.5090 _n -2	+3.4539 _n -2	+1.1506 _n -1
-1.2672 _n +0	-4.5297 _n -1	-3.1664 _n -1	-9.5393 _n -3	-3.4941 _n -2	-4.7297 _n -2
-1.4595 _n -1	-1.5090 _n -2	-9.5393 _n -3	+9.4104 _n -3	-1.0565 _n -3	+3.8157 _n -3
-7.4521 _n -2	-3.4539 _n -2	-3.4941 _n -2	-1.0565 _n -3	+2.8021 _n -3	-7.5387 _n -3
+4.5297 _n -1	+1.1506 _n -1	+4.7297 _n -2	-3.8157 _n -3	+7.5387 _n -3	-1.2863 _n -2

APPENDIX 2

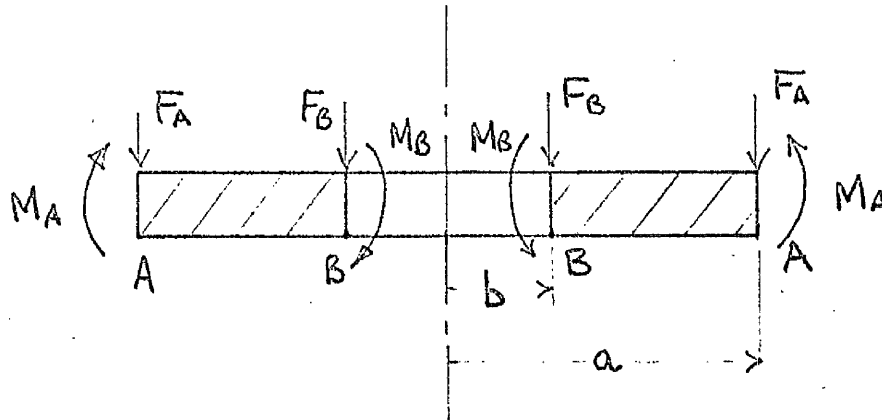
Seventh Order Stiffness Matrix

Numerical values of the terms of submatrix A_1 (notation of Appendix 1)

for a square element of side one unit and flexural rigidity one unit.

2.593 ₁₀ +1	8.592 ₁₀ +0	8.592 ₁₀ +0	7.717 ₁₀ -1	7.717 ₁₀ -1	2.309 ₁₀ +0	3.059 ₁₀ -2	3.059 ₁₀ -2	2.132 ₁₀ -1	2.132 ₁₀ -1	2.132 ₁₀ -1
8.592 ₁₀ +0	4.599 ₁₀ +0	2.609 ₁₀ +0	4.843 ₁₀ -1	2.132 ₁₀ -1	1.100 ₁₀ +0	2.109 ₁₀ -2	8.842 ₁₀ -3	1.165 ₁₀ -1	1.165 ₁₀ -1	9.752 ₁₀ -2
8.592 ₁₀ +0	2.609 ₁₀ +0	4.599 ₁₀ +0	2.132 ₁₀ -1	4.843 ₁₀ -1	1.100 ₁₀ +0	8.842 ₁₀ -3	2.109 ₁₀ -2	9.752 ₁₀ -2	1.165 ₁₀ -1	1.165 ₁₀ -1
7.717 ₁₀ -1	4.843 ₁₀ -1	2.132 ₁₀ -1	1.069 ₁₀ -1	1.987 ₁₀ -2	1.165 ₁₀ -1	5.065 ₁₀ -3	8.271 ₁₀ -4	2.314 ₁₀ -2	1.036 ₁₀ -2	1.036 ₁₀ -2
7.717 ₁₀ -1	2.132 ₁₀ -1	4.843 ₁₀ -1	1.967 ₁₀ -2	1.069 ₁₀ -1	1.165 ₁₀ -1	8.271 ₁₀ -4	5.065 ₁₀ -3	1.036 ₁₀ -2	2.314 ₁₀ -2	2.314 ₁₀ -2
2.309 ₁₀ +0	1.100 ₁₀ +0	1.100 ₁₀ +0	1.165 ₁₀ -1	1.165 ₁₀ -1	4.651 ₁₀ -1	5.176 ₁₀ -3	5.176 ₁₀ -3	4.933 ₁₀ -2	4.933 ₁₀ -2	4.933 ₁₀ -2
3.059 ₁₀ -2	2.109 ₁₀ -2	8.842 ₁₀ -3	5.065 ₁₀ -3	8.271 ₁₀ -4	5.176 ₁₀ -3	2.856 ₁₀ -4	3.409 ₁₀ -5	1.106 ₁₀ -3	1.106 ₁₀ -3	4.588 ₁₀ -4
3.059 ₁₀ -2	8.842 ₁₀ -3	2.109 ₁₀ -2	8.271 ₁₀ -4	5.065 ₁₀ -3	5.176 ₁₀ -3	3.409 ₁₀ -5	2.856 ₁₀ -4	4.588 ₁₀ -4	1.106 ₁₀ -3	1.106 ₁₀ -3
2.132 ₁₀ -1	1.165 ₁₀ -1	9.752 ₁₀ -2	2.314 ₁₀ -2	1.036 ₁₀ -2	4.933 ₁₀ -2	1.106 ₁₀ -3	4.588 ₁₀ -4	8.252 ₁₀ -3	5.234 ₁₀ -3	5.234 ₁₀ -3
2.132 ₁₀ -1	9.752 ₁₀ -2	1.165 ₁₀ -1	1.036 ₁₀ -2	2.314 ₁₀ -2	4.933 ₁₀ -2	4.588 ₁₀ -4	1.106 ₁₀ -3	5.234 ₁₀ -3	8.252 ₁₀ -3	8.252 ₁₀ -3

A Stiffness Matrix for Axisymmetrically Loaded Circular Plates



Annular Plate Element

$$\begin{Bmatrix} M_B \\ F_B \\ M_A \\ F_A \end{Bmatrix} = \begin{bmatrix} KP_{11} & & & \\ KP_{21} & KP_{22} & & \\ KP_{31} & KP_{32} & KP_{33} & \\ KP_{41} & KP_{42} & KP_{43} & KP_{44} \end{bmatrix} \begin{Bmatrix} \theta_B \\ \Delta_B \\ \theta_A \\ \Delta_A \end{Bmatrix}$$

$$\begin{aligned} KP_{11} &= K_5 / (K_1 K_5 - K_3 K_4) \\ KP_{21} &= K_3 / (K_1 K_5 - K_3 K_4) \\ KP_{22} &= K_1 / (K_1 K_5 - K_3 K_4) \\ KP_{31} &= (K_3 K_6 - K_2 K_5) / (K_1 K_5 - K_3 K_4) \\ KP_{32} &= (K_1 K_6 - K_2 K_4) / (K_1 K_5 - K_3 K_4) \\ KP_{33} &= V_5 / (V_3 V_5 - V_2 V_4) \\ KP_{41} &= -b K_3 / a (K_1 K_5 - K_3 K_4) \\ KP_{42} &= -b K_1 / a (K_1 K_5 - K_3 K_4) \\ KP_{43} &= -V_2 / (V_3 V_5 - V_2 V_4) \\ KP_{44} &= -V_3 / (V_3 V_5 - V_2 V_4) \end{aligned}$$

where

$$K_2 = \frac{2b^2}{b^2(1+\nu) + a^2(1-\nu)}$$

$$K_1 = \left[\frac{a^2}{b} - b \right] \left[\frac{a^2 K_2 - b^2}{(1+\nu) D (a^2 - b^2)} \right]$$

$$K_3 = \left[\frac{a^2 - b^2}{2} + a^2 \log \frac{b}{a} \right] \left[\frac{a^2 K_2 - b^2}{(1+\nu) D (a^2 - b^2)} \right]$$

$$K_4 = \left[\frac{b^2}{4D} (2 \log \frac{b}{a} - 1) - \frac{c_1 b}{2} - \frac{c_2}{b} \right]$$

$$K_5 = \left[\frac{b^3}{4D} (\log \frac{b}{a} - 1) - \frac{c_1 b^2}{4} - c_2 \log \frac{b}{a} + c_3 \right]$$

$$K_6 = \left[-\frac{b}{4} (1-\nu) + \frac{c_1 D}{2} (1+\nu) - \frac{c_2 D}{a^2} (1-\nu) \right].$$

$$C_2 = \frac{(1+\nu) \left[\frac{ab}{2D} \log \frac{b}{a} + \frac{ab}{4D} \right] + (1-\nu) \left(\frac{ab}{4D} \right)}{\left[-\frac{(1+\nu)}{a} - \frac{(1-\nu)a}{b^2} \right]}$$

$$C_1 = -\frac{2C_2}{a^2} - \frac{b}{2D}$$

$$C_3 = \frac{c_1 a^2}{4} + \frac{ba^2}{4D}.$$

$$V_1 = \frac{2a^2}{a^2(1+\nu) + b^2(1-\nu)}$$

$$V_2 = \left[\frac{b^2 - a^2}{2} + b^2 \log \frac{a}{b} \right] \left[\frac{a^2 - b^2 V_1}{(1+\nu) D (a^2 - b^2)} \right]$$

$$V_3 = \left[\frac{b^2}{a} - a \right] \left[\frac{a^2 - b^2 V_1}{(1+\nu) D (a^2 - b^2)} \right]$$

$$W_2 = \frac{\frac{a}{D} \log \frac{a}{b} + \frac{a}{2D} \frac{(1-\nu)}{(1+\nu)} + \frac{a}{2D}}{\left[-\frac{2}{b^2} - \frac{2}{a^2} \frac{(1-\nu)}{(1+\nu)} \right]}$$

$$W_1 = -\frac{2W_2}{b^2} - \frac{a}{2D}$$

$$W_3 = \frac{W_1 b^2}{4} + \frac{a b^2}{4D}$$

$$V_4 = \left[\frac{a^2}{4D} \left(2 \log \frac{a}{b} - 1 \right) - \frac{W_1 a}{2} - \frac{W_2}{a} \right]$$

$$V_5 = \left[\frac{a^3}{4D} \left(\log \frac{a}{b} - 1 \right) - \frac{W_1 a^2}{4} - W_2 \log \frac{a}{b} + W_3 \right]$$

APPENDIX 4

->ESTABLISH DBG003SOOKP4;
 SEVENTH ORDER SOLUTION;
 O/P 8;->

begin library A0,A6,A7,A8;

comment A program for a finite element solution to the
 problem of transverse flexure of a thin plate
 on an elastic foundation : 7th order displacement
 function;

real E,E11,E22,E21,G,v,iso,h,nxe,nye,a,b,
 A11,A21,A22,A33,c,loads,X,Y,Z;

integer i,j,r,s,t,lc,Nn,R,N,w,k,l,ak,al,am,an,I;

array KM[1:40,1:40];

open(20);open(70); find(110,[DG100006]);

I:=read(20);

skip(110,I);

read binary(110,KM,[KM000000]);

write text(70,[IAN*M*SMITH*CIVIL*ENGINEERING[2c]]);

lc:=read(20);

for Y:=1 step 1 until lc do

begin nye:=read(20);Nn:=read(20);N:=read(20); R:=read(20);

nxe:=read(20); loads:=read(20); w:=read(20);

iso:=read(20); h:=read(20); a:=read(20); b:=read(20);

begin array KB[1:N,1:w+1],NF[1:Nn,1:10],g[1:40];

for i:=1 step 1 until N do

for j:=1 step 1 until w+1 do

KB[i,j]:=0.0;

if iso=0 then

begin E11:=read(20); E22:=read(20); E21:=read(20);

G:=read(20);

end else

begin E:=read(20); v:=read(20);

E11:=E22:=E/(1-v²);

E21:=vxE11; G:=E/(2*(1+v));

end;

A11:=E11*xh³/12;

A22:=E22*xh³/12;

A21:=E21*xh³/12;

A33:=G*xh³/12;

```

P: for i:=1 step 1 until Nn do
for j:=1 step 1 until 10 do
NF[i,j]:=1;
for s:=1 step 1 until R do
begin r:=read(20);
for j:=1 step 1 until 10 do
begin if read(20)=0 then goto L1;
NF[r,j]:=0;
L1: end;
end;
r:=1;
for i:=1 step 1 until Nn do
for j:= 1 step 1 until 10 do
begin if NF[i,j]=0 then goto L2;
NF[i,j]:=r;
r:=r+1;
L2: end;
for s:=1 step 1 until nye do
for t:=1 step 1 until nxe do
begin ak:=(t-1)×(nye+1)+s;
a1:=ak+1;
am:=t×(nye+1)+s;
an:=am+1;
for i:=1 step 1 until 10 do
begin g[i]:=NF[ak,i]; g[i+10]:=NF[a1,i];
g[i+20]:=NF[an,i]; g[i+30]:=NF[am,i];
end;
for i:=1 step 1 until 40 do
begin if g[i]=0 then goto S2;
for j:=1 step 1 until 40 do
begin if g[j]=0 then goto S1;
c:=g[j]-g[i]+w+1;
if c>w+1 then goto S1;
KB[g[i],c]:=KB[g[i],c]+KM[i,j];
S1: end;
S2:end;
end;

```

```

SOLVE: begin array p[1:N],d[0:N]; d[0]:=0;
for i := 1 step 1 until N do
begin X:= 0;
for j:=1 step 1 until w do X:= X+KB[i,j]2;
KB[i,w+1] := sqrt(KB[i,w+1] - X);
for k:=1 step 1 until w do
begin X := 0;
if i+k>N then goto R2 else
if k = w then goto R1 else
for l := w-k step -1 until 1 do
X:= X+KB[i+k,l]×KB[i,l+k];
R1:a :=i+k; b := w-k+1;
KB[a,b] := (KB[a,b]-X)/KB[i,w+1];
R2: end;
end;

```

```

for i:= 1 step 1 until N do p[i]:=0.0;
for i:= 1 step 1 until loads do p[read(20)]:=read(20);

      p[1]:= p[1]/KB[1,w+1];
      for i := 2 step 1 until N do
      begin X :=0;
            for j:= if i< w+1 then w-i+2
            else 1 step 1 until w do
            X := X+ KB[i,j]Xp[i+j-w-1];
            p[i] := (p[i]-X) / KB[i,w+1];
      end;

      d[N]:= p[N]/KB[N,w+1];
      for i:= N-1 step -1 until 1 do
      begin X:= 0; l:= if i> N-w then N else i+w;
            for j:= i+1 step 1 until l do
            X:=X+KB[j,w+1-j+1]Xd[j];
            d[i]:= (p[i]-X)/KB[i,w+1];
      end;

write text(70,[LOAD*CASE[2s]]);
write(70,format([nd]),Y); write text(70,[[c]]);
write text(70,[NODE[4s]DEFLECTION[8s]MMT
*ABOUT*OY[5s]MMT*ABOUT*OX[5s]MOMT*ABOUT*
XY[5s]SHEAR******QX[5s]SHEAR******QY[2c]]);
Z:=format([+d.ddd[s]ddd[10]+nd]);

begin for i:=1 step 1 until Nn do
begin write(70,format([ndd]),i);
write text(70,[[3s]]);
write(70,Z,d[NF[i,1]]);
write text(70,[[2s]]);
write(70,Z,A11Xd[NF[i,4]]+A21Xd[NF[i,5]]);
write text(70,[[2s]]);
write(70,Z,A22Xd[NF[i,5]]+A21Xd[NF[i,4]]);
write text(70,[[2s]]);
write (70,Z,A33Xd[NF[i,6]]);
write text(70,[[2s]]);
write(70,Z,A11X(d[NF[i,7]]+d[NF[i,10]]));
write text(70,[[2s]]);
write(70,Z,A22X(d[NF[i,8]]+d[NF[i,9]]));
write text(70,[[2c]]);
end;
end;
end;
close(20); close(70);
close(110);
end->

```

→ESTABLISH DEB003TOOKP4;
 TO DEGREES OF FREEDOM TRANSVERSE SHEAR INCLUDED;
 O/P 8;→

```

begin comment Generation of dimensionless vector A
  from coefficients of polynomials;
  library AO,A6,A7,A8,A9;
  integer FLN,NF,F,u,v,n,I;
  open(20);open(70); I:=read(20);
  find(110,[DG100006]); skip(110,I); interchange(110);
  write text(70,[IAN*M*SMITH*CIVIL*ENGINEERING[2c]]);
  FLN:=read(20); NF:=read(20); v:=read(20); u:=read(20);
  n:=read(20);
  F:=FLN×NF;
  begin real C,D,nu,h;
    integer c,d,e,i,j,k,l,p,q,r,s,p1,p2,q1,q2;
    array w[1:F,1:2],E[1:12,1:2],DERF[1:v,0:4,1:u],
      ARR1[1:2,1:4],ARR2[1:2],
      ARR3[1:144],A[1:144,1:n],KM[1:F,1:F],
      MK[1:F,1:F,1:n];
    for i:= 1 step 1 until 144 do
    for e:= 1 step 1 until n do A[i,e]:=0.0;

    for e:= 1 step 1 until n do
    begin D:= read (20); nu:= read (20); h:= read (20);
    A[1,e]:=A[14,e]:=D;
    A[2,e]:= A[13,e]:= nu×D;
    A[27,e]:= 2×(1-nu)×D;
    A[8,e]:=A[21,e]:=A[85,e]:=A[98,e]:= Dxh↑2×(2-nu)
    /10/(1-nu);
    A[9,e]:=A[20,e]:=A[86,e]:=A[97,e]:=
    Dxh↑2×nu/10/(1-nu);
    A[10,e]:=A[22,e]:=A[109,e]:=A[110,e]:=
    2×Dxh↑2/10/(1-nu);
    A[35,e]:= A[36,e]:= A[123,e]:= A[135,e]:=
    2×Dxh↑2/5;
    A[40,e]:= A[43,e]:= A[53,e]:= A[54,e]:= A[65,e]:=
    A[66,e]:= A[76,e]:= A[79,e]:= Dxh↑2/5/(1-nu);
    A[92,e]:= A[105,e]:=
    Dxh↑4×(4-2×nu↑2)/100/(1-nu↑2)/(1-nu);

    A[93,e]:= A[104,e]:= Dxh↑4×nu↑2/50/(1-nu↑2)/(1-nu);
    A[94,e]:= A[106,e]:= A[116,e]:= A[117,e]:=
    Dxh↑4/25/(1-nu↑2)/(1-nu);
    A[118,e]:= 2×A[94,e];
    A[131,e]:= A[132,e]:= A[143,e]:= A[144,e]:=
    2×Dxh↑4/25/(1-nu);
    end;
  
```

```

for i:= 1 step 1 until F do
for j:= 1 step 1 until 2 do w[i,j]:= read (20);

```

```

E[1,1]:= E[2,2]:= E[6,1]:= E[7,2]:= E[10,1]:=
E[10,2]:= 2;
E[1,2]:= E[2,1]:= E[4,2]:= E[5,1]:= E[8,2]:=
E[9,1]:= 0;
E[3,1]:= E[3,2]:= E[6,2]:=E[7,1]:= E[11,2]:=
E[12,1]:= 1;
E[8,1]:= E[9,2]:= 4;
E[4,1]:= E[5,2]:= E[11,1]:= E[12,2]:= 3;
for i:= 1 step 1 until v do
for j:= 1 step 1 until u do
DERF[1,0,j]:=read(20);

```

```

for p:= 1 step 1 until v do
for q:= 1 step 1 until 4 do
for r:= 1 step 1 until u do
begin DERF[p,q,r]:=0.0;
if DERF[p,q-1,r]=0 then goto L1 else
if r+q< u then DERF[p,q,r]:=DERF[p,q-1,r]
x(u+1-q-r) else
if r+q >u then DERF[p,q,r]:=0.0;
L1: end;

```

```

for c:= 1 step 1 until F do
for d:= 1 step 1 until c do
begin for i:= 1 step 1 until 12 do
for j:= 1 step 1 until 12 do
begin l:=(i-1)x12+j;
if A[l,1]=0 then goto L2;
ARR1[1,1]:=w[c,1]; ARR1[2,1]:=w[c,2];
ARR1[1,2]:=E[1,1]; ARR1[2,2]:=E[1,2];
ARR1[1,3]:=w[d,1]; ARR1[2,3]:=w[d,2];
ARR1[1,4]:=E[j,1]; ARR1[2,4]:=E[j,2];
for k:= 1,2 do
begin p1=ARR1[k,1]; q1:=ARR1[k,2];
p2:=ARR1[k,3]; q2:=ARR1[k,4];

```

```

C:=0.0;
q:=2Xu-q1-q2;
for r:= 1 step 1 until u do
for s:= 1 step 1 until u do
begin C:=C+(if DERF[p1,q1,r]=0
or DERF[p2,q2,s]=0 then 0.0
else DERF[p1,q1,r]X
DERF[p2,q2,s]/(q-r-s+1));
end;
ARR2[k]:=C;
end;
ARR3[1]:=ARR2[1]XARR2[2];
L2:end;
for e:= 1 step 1 until n do
begin C:=0.0;
for l:= 1 step 1 until 144 do
C:=C+ARR3[l]XA[l,e];
MK[c,d,e]:=C;
end;
end;
write binary(110,ARR3,[ARR30000]);
for e:= 1 step 1 until n do
for i:= 1 step 1 until F do
for j:= i+1 step 1 until F do
MK[i,j,e]:=MK[j,i,e];

for e:= 1 step 1 until n do
begin for i:= 1 step 1 until F do
for j:= 1 step 1 until F do
KM[i,j]:=MK[i,j,e];
write binary(110,KM,[KM000000]);
end;
begin integer f1,f2;
f1:=format([-d.ddd10+nd;]);
f2:=format([-d.ddd10+nd;ccc]);
for e:= 1 step 1 until n do
for i:= 1 step 1 until F do
begin for j:= 1 step 1 until F-1
do write(70,f1,MK[i,j,e]);
write(70,f2,MK[i,F,e]);
end;
end;
end;
end;
close(20); close(70); close(110);
end->

```